

17th | SOLEIL USERS' MEETING

JANUARY 18th - 20th, 2023

Synchrotron SOLEIL (Saint-Aubin)



SCIENTIFIC COMMITTEE

Pierre ASSELIN (De la Molécule aux Nano-objets : Réactivité, Interactions et Spectroscopies - Paris)

Amélie BORDAGE (Inst. de Chimie Moléculaire et des Matériaux d'Orsay - Orsay)

Florent CARN (Lab. de Matière et Systèmes Complexes - Paris)

Fabien CHEYNIS (Centre Interdisciplinaire de Nanoscience de Marseille - Marseille)

Héloïse DOSSMANN (Inst. Parisien de Chimie Moléculaire - Paris)

Emmanouil FRANTZESKAKIS (Univ.Paris Sud - Orsay)

Rozenn LE HIR (Inst. Jean-Pierre Bourgin - Versailles)

Rémi MARSAC (Géosciences Rennes - Rennes)

Benoît MASQUIDA (Génétique Moléculaire Génomique Microbiologie - Strasbourg)

Debora PIERUCCI (Centre de Nanosciences et de Nanotechnologies - Palaiseau)

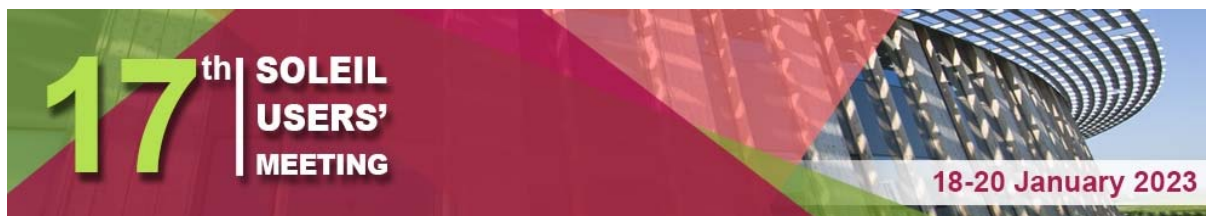
Simona RANERI (National Research Council - Institute of Chemistry of Organometallic Compounds – Sesto Fiorentino)

Asma TOUGERTI (Unité de Catalyse et de Chimie du Solide – Villeneuve d'Ascq)



Information and registration:
www.synchrotron-soleil.fr/en/events/sum-2023





SOLEIL Users' Meeting

January 18th - 20th, 2023

Synchrotron SOLEIL, Saint-Aubin - France

Summary

SUM2023

- Welcome
- Programme
- Plenary Session
- Parallel Sessions
 - Dynamic, Reactivity & Chemical analysis (Diluted Matter & Chemistry)
 - Life & Earth Sciences (Biology / Cultural heritage / Health & Environment / Geoscience)
 - New Materials (Structure / Electronic Properties / Surfaces & Interfaces)
- Posters Session
 - List of Student Posters
 - List of Other Posters

Tutorials

- 1/ Use of FASTOSH for XAS data treatment – Part I
- 2/ Use of FASTOSH for XAS data treatment – Part II
- 3/ Using μ -Focused X-rays for Cryo-Crystallography and Plate Screening

- Companies Advertisements

Welcome

The 17th SOLEIL Users' Meeting takes place on Wednesday 18th to Friday 20th, January 2023, on site.

Two plenary lectures will deal with different aspects related to Synchrotron sources use, in the following scientific fields:

- Biology and Health,
- Surfaces/Interfaces/Electronic properties

Scientific communications will be presented during parallel sessions, selected from submitted abstracts.

Three tutorials are organised.

- Use of FASTOSH for XAS data treatment

- The first tutorial, on Wednesday 18th, 2023 (14:00 - 17:00), is dedicated to the basic functions of the FASTOSH software and concerns the users who want to discover XAS data treatment and / or the new software developed by the SAMBA beamline - Part I.
- The second tutorial, on Friday 20th, 2023 (14:00 - 17:00), presents the advanced functionalities of the software (Chemometry, PCA, ...)
- Part II.

- Tricks and Tips in using Micro-beams for Crystallography Experiments

- The third tutorial on Friday 20th, 2023 (14:00 - 17:00), presents Tricks and Tips in using Micro-beams for Crystallography Experiments (PROXIMA 2A).

A round table takes place on Friday 20th at SOLEIL about "Data Analysis Management".

This invaluable forum for the synchrotron radiation users' community provides the opportunity to exchange and learn about the evolution of the machine and the beamlines. It is also the occasion to share scientific, technical and practical issues about the Synchrotron radiation use.

Bienvenue

Le 17^{ème} Colloque des Utilisateurs de SOLEIL se tiend du mercredi 18 au vendredi 20 janvier 2023 sur le site de SOLEIL.

Deux conférences plénières traitent de différents aspects liés à l'utilisation des sources Synchrotron, dans les domaines scientifiques suivants :

- Biologie et santé,
- Surfaces/interfaces/propriétés électroniques

Des communications scientifiques sont présentées lors de sessions parallèles, sélectionnées parmi les résumés soumis.

Trois tutoriels sont proposés :

- Utilisation du logiciel FASTOSH pour traitement de données XAS

- Le premier tutoriel a lieu le mercredi 18 janvier 2023 (14:00 - 17:00), et est dédié aux fonctions de base du logiciel FASTOSH. Il concerne les utilisateurs qui veulent découvrir le traitement des données "XAS et / ou le nouveau logiciel développé par la SAMBA beamline - Part I".
- Le second tutoriel se déroule le vendredi 20 janvier 2023 (14:00 - 17:00), et présente les fonctionnalités avancées du logiciel FASTOSH (Chimométrie, PCA, ...) Part II.

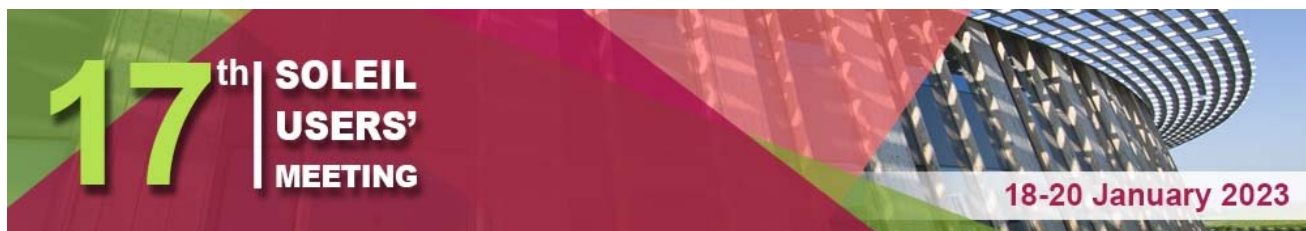
- Astuces pour utiliser les microfaisceaux en cristallographie

- Le troisième tutoriel se tiendra le vendredi 20 janvier 2023 (14:00 - 17:00), et présentera les Astuces dans l'utilisation des Micro-faisceaux en Cristallographie (PROXIMA 2A).

Une table ronde a lieu le vendredi 20 janvier 2023 à SOLEIL : « Gestion de l'analyse des données »

Ce rendez-vous incontournable pour la communauté des utilisateurs du rayonnement synchrotron qu'est le Colloque des Utilisateurs est l'occasion d'échanges et de restitutions sur l'évolution de la machine et des lignes de lumière.

Il est aussi le lieu pour échanger sur les aspects scientifiques, techniques et pratiques de l'utilisation du rayonnement Synchrotron.



Programme

Wednesday, January 18th, 2023

SOLEIL Auditorium - Main Building

Tutorial:

14:00 - 17:00 Use of the Fastosh software for the XAS data treatment—Part. I
Gautier Landrot – SAMBA Beamline

Thursday, January 19th, 2023

SOLEIL Auditorium - Main Building

09:00 - 10:00 *Registration & coffee*

10:00 - 10:10 Welcome / Introduction, ORGUES Chair – **Rozenn Le Hir**

10:10 - 10:20 The word of SOLEIL General Director – **Jean Dailant**

10:20 - 11:05 **Surfaces/Interfaces**

Itinerant-to-localized transmutation of electrons across the metal-to-insulator transition
Andrès F. Santander Syro - *Institut des Sciences Moléculaires d'Orsay, France*

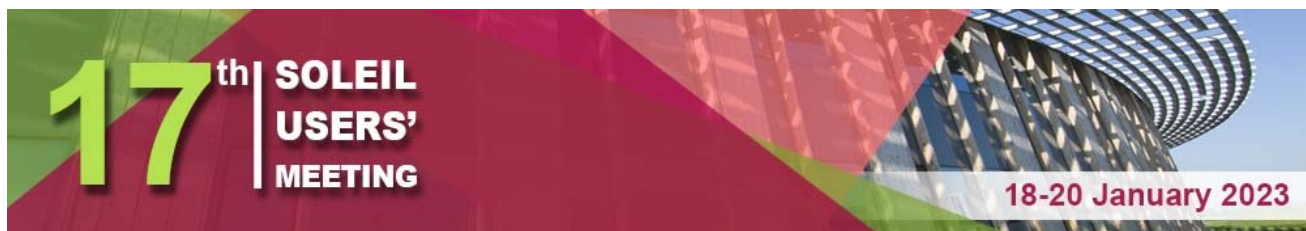
11:05 - 11:50 **Biology/Health**

Functional consequences of a bacterial amyloid interaction with single stranded DNA
Véronique Arluison - *Laboratoire Léon Brillouin, Gif-sur-Yvette, France*

11:50 - 12:10 Peer Review Committee 5 (Biology/Health) – **Thibaud Crépin**
Peer Review Committee 6 (New Materials) – **Emmanuelle Montarges-Pelletier**
Questions 10mn

12:10 - 12:30 Projection vidéo HELIOBIO (Tatiana Isabet / Frédéric Jamme / Aurélien Thureau)

12:30 - 13:45 *Lunch*



Parallel sessions – 3 different auditoriums (see the detailed programme below)

- 14:00 - 16:00
- Dynamic, Reactivity & Chemical analysis (Diluted Matter & Chemistry)
 - Life & Earth Sciences (Biology / Cultural heritage / Health & Environment / Geoscience)
 - New Materials (Structure / Electronic Properties / Surfaces & Interfaces)

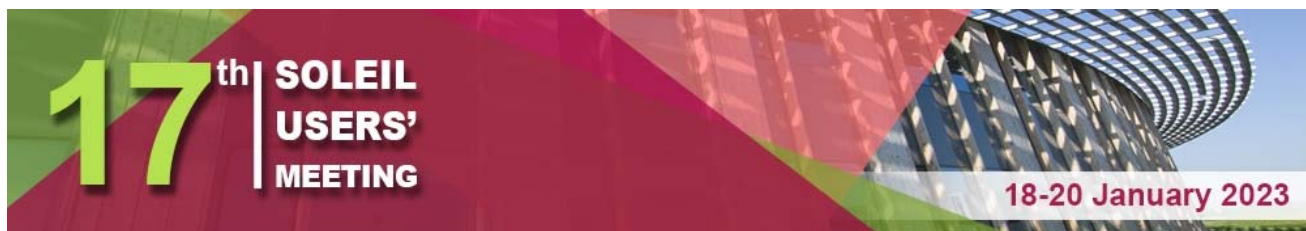
16:00 - 16:30 *Coffee break*

Parallel sessions – 3 different auditoriums (see the detailed programme below)

- 16:30 - 18:00
- Dynamic, Reactivity & Chemical analysis (Diluted Matter & Chemistry)
 - Life & Earth Sciences (Biology / Cultural heritage / Health & Environment / Geoscience)
 - New Materials (Structure / Electronic Properties / Surfaces & Interfaces)

18:00 - 20:00 Posters session
Visit of 3 Beamlines (LUCIA / METROLOGY / PROXIMA-2A)

20:00 - 21:30 Award of the best student poster / *Dinner*



Programme

Friday, January 20th, 2023

Parallel sessions – 3 different auditoriums (see the detailed programme below)

- 09:00 -10:45
- Dynamic, Reactivity & Chemical analysis (Diluted Matter & Chemistry)
 - Life & Earth Sciences (Biology / Cultural heritage / Health & Environment / Geoscience)
 - New Materials (Structure / Electronic Properties /Surfaces & Interfaces)

10:45 - 11:15 *Coffee break* – Cafeteria Space near [SOLEIL Auditorium - Main Building](#)

Round Table - [SOLEIL Auditorium - Main Building](#)

Data analysis management (Brigitte Gagey / Emmanuel Farhi / Majid Ounsy / Ana Valcarel Orti / Andy Goetz):

11:15 - 12:30

- Open science tools
- Data service
- E-learning / training

12:30 - 13:45 *Lunch*

[SOLEIL Auditorium - Main Building](#)

Use of the Fastosh software for the XAS data treatment–Part. II

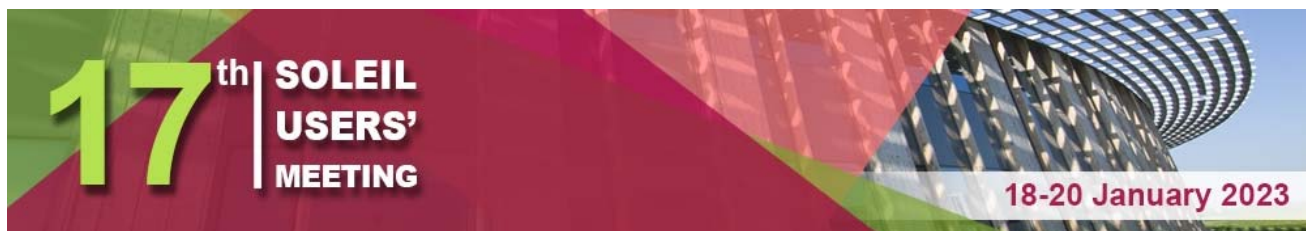
Gautier Landrot - SAMBA Beamline

14:00 - 17:00

[Libra & Phenix Rooms –SOLEIL Main Building](#)

PROXIMA 2A Training Tutorial: Using μ -Focused X-rays for Cryo-Crystallography and Plate Screening

William Shepard – PROXIMA-2A Beamline



Parallel Session Schedule

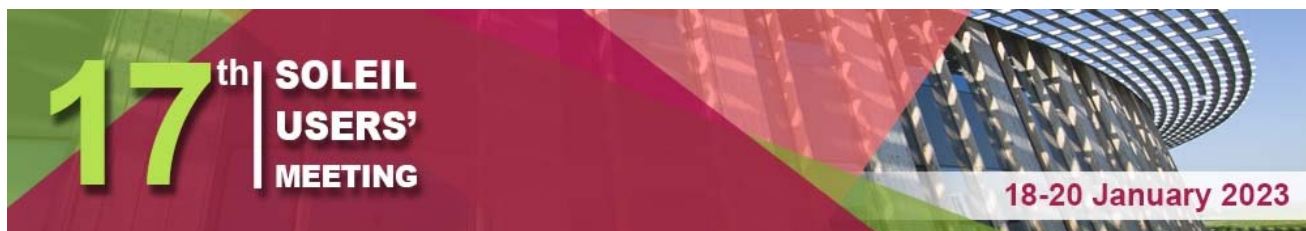
Dynamic, reactivity and Chemical analysis (Diluted Matter & Chemistry)

Chairpersons: A. Tougeri, P. Asselin, F. Carn, H. Dossmann

*SOLEIL - Reception Building Auditoriums
Ground Floor & PA.1.12 Rooms*

Thursday, January 19th, 2023

- 14:00 - 14:30
(25'+5') Precision UV spectroscopy for astronomy and search of new physics
Edcel Salumbides - *Vrije Universiteit, Amsterdam, The Netherlands*
- 14:30 - 14:55
(20'+5') Catalytic properties at the nanoscale probed by surface X-ray diffraction and coherent diffraction imaging
David Simonne - *Synchrotron SOLEIL, Gif-sur-Yvette and CEA Grenoble, Grenoble, France*
- 14:55 - 15:20
(20'+5') Study of post collision interaction effect following K shell photoionization of solvated ions
Bastien Lutet-Toti - *LCPMR, Paris, France*
- 15:20 - 15:45
(20'+5') Green synthesis of IrO₂ nanocages for the production of hydrogen: A contribution of in situ QUICK X-ray absorption spectroscopy
Marion Giraud - *ITODYS, Paris, France*
- 15:45 - 16:15 *Coffee break*
- 16:15 - 16:45
(25'+5') Shaping plasmonic supercrystals by nesting shapes
Cyril Hamon - *Laboratoire de Physique des Solides, Orsay, France*
- 16:45 - 17:10
(20'+5') The SOLEIL view on and astronomical detection of the ¹³C isotopic species of ethyl cyanide in vibrational excitation
Christian P. Endres - *Max-Planck-Institut für extraterrestrische Physik, Garching Germany*
- 17:10 - 17:35
(20'+5') Evolution of active species in homogenous Ru-based catalyst in liquid phase under high pressures and temperatures
Elizaveta Kozyr - *Department of Chemistry, University of Turin, Italy*
- 17:35 - 18:00
(20'+5') Reactivity of the HCO⁺/HOC⁺ isomers as a function of photon and collision energy for astrochemistry
Nicolas Solem - *Institut de Chimie-Physique, Orsay, France*



Parallel Session Schedule

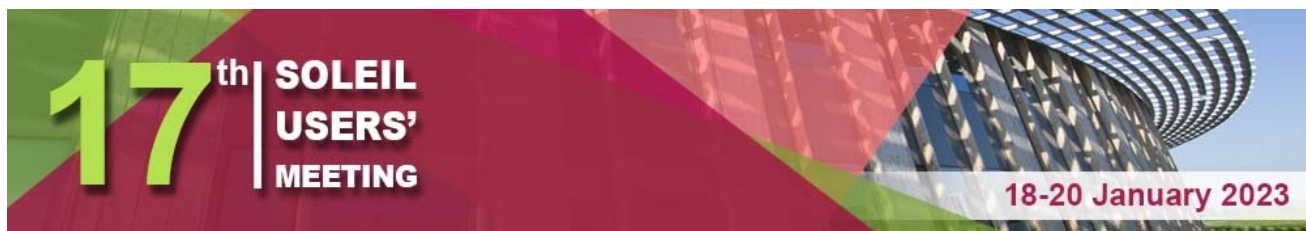
Dynamic, reactivity and Chemical analysis
(Diluted Matter & Chemistry)

Chairpersons: A. Tougerti, P. Asselin, F. Carn, H. Dossmann

*SOLEIL - Reception Building Auditoriums
Ground Floor & PA.1.12 Rooms*

Friday, January 20th, 2022

- 09:00 - 09:30
(25'+5') Microfluidic analysis at the Paris-Saclay Institute of Physical Chemistry
Antoine Pallandre - *Institut de Chimie Physique, Orsay, France*
- 09:30 - 09:55
(20'+5') Phthalocyanines in the gas-phase from Valence to core-shell electron spectroscopy
Gildas Goldsztejn - *Institut des Sciences Moléculaires d'Orsay, Orsay, France*
- 09:55 - 10:20
(20'+5') Study chemical & structural evolution of Mn and Ti in disordered rocksalt $\text{Li}_2\text{Mn}_{1-x}\text{Ti}_x\text{O}_2\text{F}$
cathode materials through operando XAFS
Yang Hu - *Helmholtz-Institute Ulm, Ulm, Germany*
- 10:20 - 10:45
(20'+5') Probing the photodynamics of cyano-PAHs in the vacuum-ultraviolet range
Madhusree Roy Chowdhury - *Synchrotron SOLEIL, Gif-sur-Yvette, France*
- 10:45 - 11:15 *Coffee break*



Parallel Session Schedule

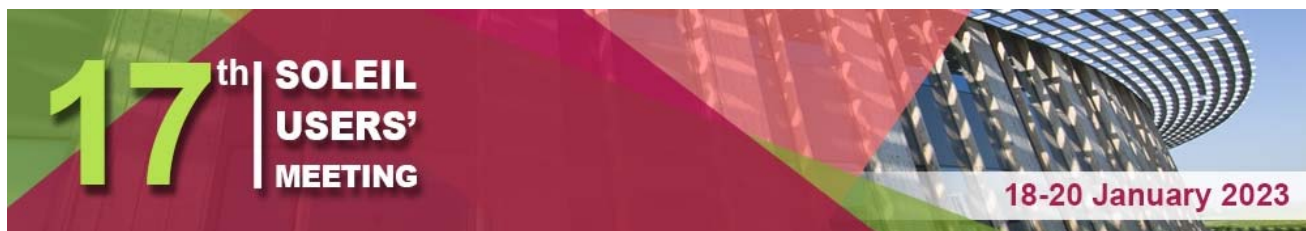
Life & Earth Sciences
(Biology / Cultural heritage / Health & Environment / Geoscience)

Chairpersons: B. Masquida, R. Le Hir, R. Marsac, S. Raneri

SOLEIL Auditorium - Main Building

Thursday, January 19th, 2023

- 14:00 - 14:30
(25'+5')
- The interactions between metal(loid)s and environmental plastics: Chromium and arsenic examples
Charlotte Catrouillet - *Institute de physique du globe de Paris, France*
- 14:30 - 14:55
(20'+5')
- Lanthanide distribution in Daphnia magna via micro and nano S-XRF imaging
Marion Revel - *Hamburg University of Applied Science, Hamburg, Germany*
- 14:55 - 15:20
(20'+5')
- Probing chromium and manganese speciation in Chinese RED Soils
Xiaoquan Qin - *Institut de Physique du Globe de Paris, France*
- 15:20 - 15:45
(20'+5')
- Unravelling the pathways of cadmium in cacao
Géraldine Sarret - *ISTERRE, Grenoble, France*
- 15:45 - 16:15
- Coffee Break
- 16:15 - 16:45
(25'+5')
- Synchrotron-based X-ray imaging of pigments and secondary products in Cimabue's ceiling paintings of the upper basilica of Assisi
Ermanno Avranovich Clerici - *Antwerpen University, Belgium*
- 16:45 - 17:10
(20'+5')
- Synchrotron μ -XRF imaging and μ -XANES spectroscopy at the cultural heritage dedicated PUMA beamline at SOLEIL
Alessandra Gianoncelli - *Elettra Sincrotrone, Trieste, Italy*
- 17:10 - 17:35
(20'+5')
- Chemical imaging at PUMA, SOLEIL, of samples of polychrome cave art from Font-de-Gaume cave to validate in-situ results
José Tapia - *IRCP Chimie ParisTech., Paris, France*
- 17:35 - 18:00
(20'+5')
- Synchrotron X-ray spectro-imaging clarifies the anatomy and taphonomy of amphibians from the Montceau-les-Mines lagerstätte
Pierre Gueriau - *IPANEMA, Saint-Aubin, France*



Parallel Session Schedule

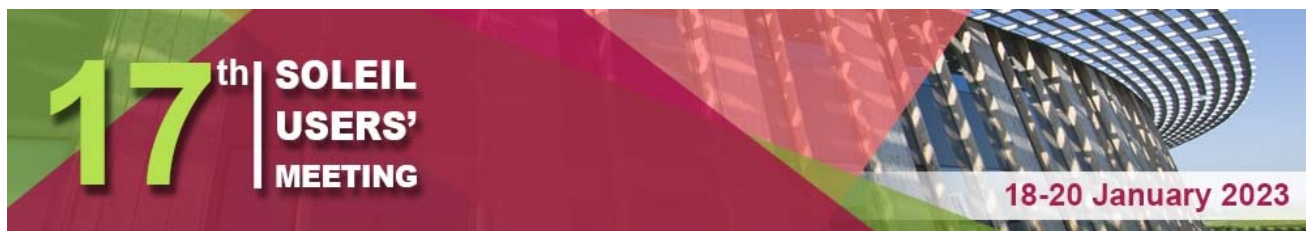
Life & Earth Sciences
(Biology / Cultural heritage / Health & Environment / Geoscience)

Chairpersons: B. Masquida, R. Le Hir, R. Marsac, S. Raneri

SOLEIL Auditorium - Main Building

Friday, January 20th, 2023

- 09:00 - 09:30
(25'+5') Structural studies of antibody antigen complexes
Félix Rey - Institut Pasteur, Paris, France
- 09:30 - 09:55
(20'+5') Why do we see Amyloid- β plaques in phase-contrast imaging?
Mathieu Chourrout - Lyon Neuroscience Research Center, Bron, France
- 09:55 - 10:20
(20'+5') Synchrotron based X-ray microtomography reveals cellular morphological features of developing wheat grain
David Legland - INRAE, Nantes, France
- 10:20 - 10:45
(20'+5') Multimetal methyl transferase making methanogenesis
Cameron Fyfe - MICALIS Institut, Jouy en Josas, France
- 10:45 - 11:15 Coffee Break



Parallel Session Schedule

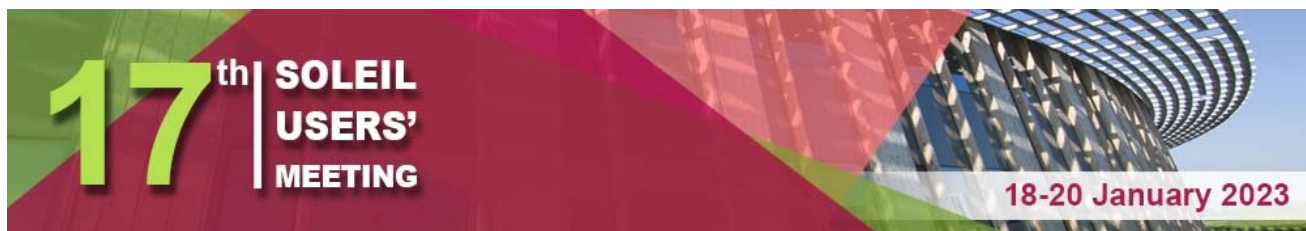
New Materials (Structure / Electronic Properties / Surfaces & Interfaces)

Chairpersons: E. Frantzeskakis, A. Bordage, D. Pierucci, F. Cheynis

SOLEIL - Main Building
Libra, Phénix, Pixys & Colomba Rooms

Thursday, January 19th, 2023

- 14:00 - 14:30 (25'+5') From multiferroicity to superconductivity: 1D Fe spin ladder under pressure
Victor Balédent - *Laboratoire de Physique des Solides, Orsay, France*
- 14:30 - 14:55 (20'+5') Operando XAS investigation of bimetallic iron–molybdenum sulfide electrocatalysts for the hydrogen evolution reaction in proton exchange membrane electrolyzers
Anastassiya Khan - *Synchrotron SOLEIL, Gif-sur-Yvette, France*
- 14:55 - 15:20 (20'+5') UV and X-ray stability of CsPbBr₃ perovskite nanocrystals
Azmat Ali - *Institut des NanoSciences de Paris, France*
- 15:20 - 15:45 (20'+5') The effect of side chain structure on self-organization properties and the electronic structure of low band gap polymers
David Batchelor - *Karlsruher Institut für Technologie, Eggenstein-Leopoldshafen, Germany*
- 15:45 - 16:15 *Coffee Break*
- 16 :15 - 16 :45 (25'+5') Multi beamlines investigation of HgTe nanocrystals electronic structure
Emmanuel Lhuillier - *Institut des NanoSciences de Paris, France*
- 16:45 - 17:10 (20'+5') In situ XPS Synchrotron study of solid-liquid interphase in lithium-ion batteries
Federico Giovanni Capone - *PHENIX, Paris and Synchrotron SOLEIL, Gif-sur-Yvette, France*
- 17:10 - 17:35 (20'+5') Resonant Auger spectroscopy on adsorbed xenon on gold, silver and copper substrates
Fredrik O.L. Johansson - *Uppsala University, Uppsala, Sweden*
- 17:35 - 18:00 (20'+5') Self-assembled monolayers of functionalised spin crossover complexes
Patrick Rosa - *Université de Bordeaux, Pessac, France*



Parallel Session Schedule

New Materials (Structure / Electronic Properties / Surfaces & Interfaces)

Chairpersons: E. Frantzeskakis, A. Bordage, D. Pierucci, F. Cheynis

SOLEIL - Main Building
Libra, Phénix, Pixys & Colomba Rooms

Friday, January 20th, 2023

- 09:00 - 09:30
(25'+5')
- Fundamental mechanisms of stress-build-up during thin films formation: multimethod real time Synchrotron experiments
Bärbel Krause - *Karlsruher Institut für Technologie, Germany*
- 09:30 - 09:55
(20'+5')
- Probing the chemical and electronic structure of BaTiO₃ ultrathin films using X-ray spectroscopy
Sara Gonzalez - *Institut des Nanotechnologies de Lyon, Villeurbanne, France*
- 09:55 - 10:20
(20'+5')
- Carbon-based defects in pristine α boron
Yeonsoo Cho - *Laboratoire des Solides Irradiés, Palaiseau, France*
- 10:20 - 10:45
(20'+5')
- Band structure and Rashba effect of ferroelectric α -GeTe as function of the thickness
Alexandre Lopez - *CINaM, Marseille, France*
- 10:45 - 11:15 *Coffee break*

PLENARY SESSION

PLENARY SESSION

Rozenn LE HIR, Chairperson

SOLEIL Auditorium - Main Building

Thursday, January 19th, 2023

- 10:00 – 10:10 **Welcome / Introduction, ORGUES Chair – Rozenn Le Hir**
- 10:10 – 10:20 The word of SOLEIL General Director – **Jean Daillant**
- 10:20 – 11:05 **Surfaces/Interfaces**
Itinerant-to-localized transmutation of electrons across the metal-to-insulator transition
Andrès Santander Syro - *Institut des Sciences Moléculaires d'Orsay, France*
- 11:05 – 11:50 **Biology/Health**
Functional consequences of a bacterial amyloid interaction with single stranded DNA
Véronique Arluison - *Laboratoire Léon Brillouin, Gif-sur-Yvette, France*
- 11:50 – 12:10 Peer Review Committee 5 (Biology/Health) – **Thibaud Crépin**
Peer Review Committee 6 (New Materials) – **Emmanuelle Montarges-Pelletier**
Questions 10mn
- 12:10 - 12:30 Projection vidéo HELIOBIO (**Tatiana Isabet / Frédéric Jamme / Aurélien Thureau**)

Itinerant-to-localized Transmutation of Electrons across the Metal-to-insulator Transition

A. F. Santander-Syro

Institut des Sciences Moléculaires d'Orsay, Université Paris-Saclay, Orsay, France

ABSTRACT

The most familiar physical property of a material is its ability to conduct (metals) or not (insulators) electric current. The conductivity of metals increases when the temperature decreases. Thus, copper conducts over ten times better the current at -200°C than at 400°C. But for V_2O_3 , a metal at room temperature, the conductivity drops sharply by a factor of a million or more when the temperature falls below -113°C. It becomes a so-called “Mott insulator” at low temperatures! How to explain this astonishing transition?

In this talk, I will discuss our recent experimental studies of the metal-to-insulator transition in V_2O_3 [1]. We experimentally imaged for the first time how the itinerant, wave-like electrons in the metallic phase of V_2O_3 localize across the Mott metal-insulator transition. We used angle-resolved photoemission spectroscopy (ARPES), a technique that directly measures the quantum-mechanical electronic energies of a solid. I will show how the changes observed in those microscopic electronic states are related to the macroscopic changes in conductivity across the metal-to-insulator transition.

REFERENCES

- [1] M. Thees *et al.*, *Science Advances* **7**, eabj1164 (2021).

Functional Consequences of a Bacterial Amyloid Interaction with Single Stranded DNA

V. Arluison

*Laboratoire Léon Brillouin, UMR 12 CEA/CNRS, 91191 Gif-sur-Yvette, France
& Université Paris Cité, 75006 Paris, France*

ABSTRACT

Interactions between proteins and single stranded DNA (ssDNA) are crucial for many fundamental biological processes, including DNA replication and genetic recombination. Thus, understanding detailed mechanisms of these interactions is necessary to uncover regulatory rules occurring in all living cells. The RNA-binding Hfq is a pleiotropic bacterial regulator that mediates many aspects of nucleic acids metabolism. The protein notably mediates RNA-based regulations and helps to compact double stranded DNA. Here, we focused on the action of Hfq on ssDNA. A combination of experimental methodologies, including spectroscopy (SRCD, FTIR...) and molecular imaging (fluorescence, TEM...), have been used to probe the interactions of Hfq with ssDNA. Our analysis reveals that Hfq binds to ssDNA and drastically changes the structure and helical parameters of ssDNA, a property mainly due to Hfq amyloid-like domain. The formation of the nucleoprotein complex between Hfq and ssDNA unveil important implications for DNA replication and recombination processes.

PARALLEL SESSIONS

PARALLEL SESSION

Dynamic, Reactivity & Chemical analysis (Diluted Matter & Chemistry)

*SOLEIL - Reception Building Auditoriums
Ground Floor & PA.1.12 Rooms*

Thursday, January 19th

Chairpersons:

A. Tougerti, P. Asselin, F. Carn, H. Dossmann

- IT-01 Precision UV spectroscopy for astronomy and search of new physics
E. Salumbides
- OC-01 Catalytic properties at the nanoscale probed by surface X-ray diffraction and coherent diffraction imaging
D. Simonne
- OC-02 Study of post collision interaction effect following K shell photoionization of solvated ions
B. Lutet-Toti
- OC-03 Green synthesis of IrO₂ nanocages for the production of hydrogen: A contribution of in situ QUICK X-ray absorption spectroscopy
M. Giraud
- IT-02 Microfluidic analysis at the Paris-Saclay Institute of Physical Chemistry
A. Pallandre
- OC-04 The SOLEIL view on and astronomical detection of the ¹³C isotopic species of ethyl cyanide in vibrational excitation
C.P. Endres
- OC-05 Evolution of active species in homogenous Ru-based catalyst in liquid phase under high pressures and temperatures
E. Kozyr
- OC-06 Reactivity of the HCO⁺/HOC⁺ isomers as a function of photon and collision energy for astrochemistry
N. Solem

PARALLEL SESSION

Dynamic, Reactivity & Chemical analysis (Diluted Matter & Chemistry)

*SOLEIL - Reception Building Auditoriums
Ground Floor & PA.1.12 Rooms*

Friday, January 20th

Chairpersons:

A. Tougerti, P. Asselin, F. Carn, H. Dossmann

- IT-03 Shaping plasmonic supercrystals by nesting shapes
C. Hamon
- OC-07 Phthalocyanines in the gas-phase from Valence to core-shell electron
spectroscopy
G. Goldsztejn
- OC-08 Study chemical & structural evolution of Mn and Ti in disordered rocksalt
 $\text{Li}_2\text{Mn}_{1-x}\text{Ti}_x\text{O}_2\text{F}$ cathode materials through operando XAFS
Y. Hu
- OC-09 Probing the photodynamics of cyano-PAHs in the vacuum-ultraviolet range
M. Roy-Chowdhury

Precision UV Spectroscopy for Astronomy and Search of New Physics

E. Salumbides

Vrije Universiteit, Amsterdam, The Netherlands

ABSTRACT

The laboratory measurements of accurate ultraviolet spectra of atoms and molecules provide necessary reference data for the highest resolution astronomical observations of high redshift objects. The accurate comparison of the lab and astronomical data is a very sensitive probe of any time- and space-dependent deviation by virtue of the billions of lightyears separation. The observation of such discrepancies would point to new physical phenomena beyond the Standard Model. Our precision laser spectroscopic investigations combined with with UV Fourier Transform measurements on atomic and molecular systems at the DESIRS beamline of Soleil Synchrotron were used in studies to probe the possible variation of fundamental constants, such as the proton-to-electron mass ratio, at a cosmological timescale. At present the data points to a null result and provides the tightest constraints for extensions to the Standard Model.

Catalytic Properties at the Nanoscale Probed by Surface X-ray Diffraction and Coherent Diffraction Imaging

D. Simonne^{1,2}, A. Resta¹, A. Coati¹, A. Vlad¹, B. Voisin¹, Y. Garreau¹, C. Chatelier^{2,3}, M. Dupraz^{2,3}, and M-I. Richard^{2,3}

¹*Synchrotron SOLEIL, L'Orme des Merisiers, Saint-Aubin*

²*Univ. Grenoble Alpes, CEA Grenoble, 17 Av. des Martyrs 38000 Grenoble*

³*European Synchrotron Research Facility, 71 Av. des Martyrs, 38000 Grenoble*

ABSTRACT

We aim at investigating in situ and operando the catalytic structure-activity relationships to understand and optimise the working route of Platinum catalysts. We focus on the ammonia (NH₃) oxidation of Pt model catalysts, i.e. nanoparticles and monocrystals.

The gas flow reactor (XCAT) at the SixS beamline allows us to perform near ambient pressure measurements under variant gas flows. A graphite layer below the sample's surface is used as a heater by tuning the input current. The multi-environment diffractometer (MED), has recently been updated for Coherent Diffraction Imaging (CDI) via a new set of coherence optics and used for Bragg CDI experiments (Li et al. 2020).

On one hand, we explore the surface evolution of Pt monocrystals using Surface X-Ray Diffraction (SXRD), for specific gas and temperature conditions linked to product selectivity. The analysis of Crystal Truncation Rods (CTRs) and low incident angle reflectivity allows one to have a precise idea of the evolution of the surface (roughness, thickness, density, formation of new layers). Reciprocal space maps are collected simultaneously and then projected onto a plane perpendicular to the sample surface for details about the surface evolution for given NH₃/O₂ ratios and temperature (Resta et al. 2020).

On the other hand we perform in-situ and operando Bragg Coherent Diffraction Imaging (BCDI) measurements of isolated Pt nanoparticles during the oxidation of Ammonia, for the same gas and temperature conditions. By following the evolution of multiple parameters in 3D (size, strain, shape, re-faceting) of the reconstructed nanoparticle, we gain important insight (Kim et al. 2019) into the structure dependence of the catalytic properties of the nanoparticle which provides information on the catalytically active facets and on the deactivation process of the particles.

During both experiments, the evolution of the reaction is followed by mass spectroscopy with a direct link from the chamber to a residual gas analyser (RGA), allowing us to connect the dynamical structural changes of Pt model catalysts to their catalytic activity (Wang et al. 2016). Finally, we performed near-ambient pressure X-ray Photoelectron Spectroscopy experiments during the oxidation of Ammonia to establish a connection between selectivity and surface moieties, preserving the same ammonia to oxygen ratios.

REFERENCES

1. Li, Ni et al. (2020).
2. Resta, Andrea et al. (2020).
3. Kim, Dongjin et al. (2019).
4. Wang, Haotian et al. (2016).

Study of Post Collision Interaction Effect Following K shell Photoionization of Solvated Ions

B. Lutet-Toti¹, J. Palaudoux¹, F. Penent¹, P. Lablanquie¹,
S. Sheinerman², L. Gerchikov³, T. Saisopa⁴,
Y. Rattanachai⁴ and D. Céolin⁵

¹ LCPMR, Sorbonne Université – UMR 7614, 75231 Paris Cedex 05, France

² Department of Physics, St. Petersburg State Maritime Technical University,
198262 St. Petersburg, Russia

³ Department of experimental Physics, Polytechnical University, 195251 St Petersburg, Russia

⁴ Department of Applied Physics, Faculty of Sciences and Liberal Arts, Rajamangala University
of Technology Isan, Nakhon Ratchasima 30000, Thailand

⁵ Synchrotron SOLEIL, 91190 Saint Aubin Cedex, France

ABSTRACT

After inner-shell photoionization of an atom, a photoelectron is emitted, and a highly excited ionic state with a short lifetime is created. This core-ionized ion can then relax to a doubly charged ion by emitting a second electron in the Auger decay process. The Coulombic interaction between those two electrons and the ion allows energy exchange between the two electrons. In a simplistic description, close to the 1s threshold, the photoelectron is slow and will be overtaken by the (fast) Auger electron: the two electrons will see the ion charge varying from 1 to 2 for the photoelectron, that will be slowed down, and from 2 to 1 for the Auger electron that is hence accelerated. This effect is called post-collision interaction (PCI) and leads to an energy shift and a distortion of the electron's peaks in the vicinity of the inner-shell ionization threshold. This effect was studied on the main Auger KLL peak of Argon¹, in gas phase. A maximum energy shift of 0.8eV at threshold was observed that decreases with increasing photon energy. Furthermore, according to literature in solid state², this energy shift varies with the effective charge of the residual ion (screening effect).

To verify this effect in liquid phase, we chose to study, by Auger spectroscopy, the PCI effect for different Argon isoelectronic ions: Cl⁻, K⁺ and Ca²⁺, in water. Moreover, to evaluate the influence of the solvent, we also studied the PCI for Cl⁻ in ethanol and methanol. The experiments were conducted on the GALAXIES³ beam line with a liquid micro-jet under vacuum coupled to the HAXPES⁴ photoemission end station. To evaluate the PCI shift, we focused our study on the position of the maximum of the ¹D KLL Auger peak depending on the incident photon energy. We have compared our results to the atomic Argon case and to a theoretical model⁵ taking into account the scattering of the photoelectron in water and the screened Coulomb interaction. A greater energy shift than in gas phase was observed that extends farther above threshold, while non-significant charge and solvent effects could be detected.

REFERENCES

- 1 R. Guillemin et al, Phys.Rev A, **92**, 012503 (2015)
- 2 T. Miller and T.-C. Chiang, Phys Rev B, **29**, 1121-1124, (1994)
- 3 J.-P. Rueff et al, J. Synch.Rad, **22**, 175-179 (2015)
- 4 J.-P Rueff et al, J. Synch.Rad, **31**, 4-9, (2018)
- 5 GB. Armen et al, Phys.Rev. A,**36**,12(1987)

Green Synthesis of IrO₂ Nanocages for the Production of Hydrogen: A Contribution of *in situ* QUICK X-ray Absorption Spectroscopy

M. Elmaalouf,^a A. Da Silva,^a S. Duran,^b C. Tard,^b M. Comesaña-Hermo,^a
S. Gam-Derouich,^a V. Briois,^c D. Alloyeau,^d J-Y. Piquemal,^a
J. Peron^a and M.Giraud^a

^a Université Paris Cité, CNRS, ITODYS, F-75013 Paris, France.

^b Laboratoire de Chimie Moléculaire (LCM), CNRS, École Polytechnique de Paris,
91120 Palaiseau, France

^c SOLEIL Synchrotron, UR1-CNRS, L'Orme des Merisiers, BP48, 91192 Gif-sur-Yvette,

^d Université Paris Cité, Laboratoire Matériaux et Phénomènes Quantiques (MPQ),
F-75013 Paris, France.

ABSTRACT

IrO₂ is the only active electrocatalyst being sufficiently stable to sustain the drastic oxidative and acidic conditions at the anode of proton exchange membrane water electrolyzers.¹ Highly porous iridium oxide structures are particularly well-suited for the preparation of porous catalyst layers needed in such devices. In this contribution, we report the formation of iridium oxide nanostructured cages,² via a water-based process performed at room temperature, using cheap Cu₂O cubes as the template. In this synthetic approach, based on Pearson's hard and soft acid–base theory, the replacement of the Cu₂O core by an iridium shell is permitted by the difference in hardness/softness of cations and anions of the two reactants Cu₂O and IrCl₃. Calcination followed by acid leaching allow the removal of residual copper oxide cores and leave IrO₂ hierarchical porous structures with outstanding activity toward the oxygen evolution reaction. Fundamental understanding of the reaction steps and identification of the intermediates are permitted by coupling a set of ex situ and in situ techniques including *in situ* Quick-X-ray absorption spectroscopy during the synthesis.³

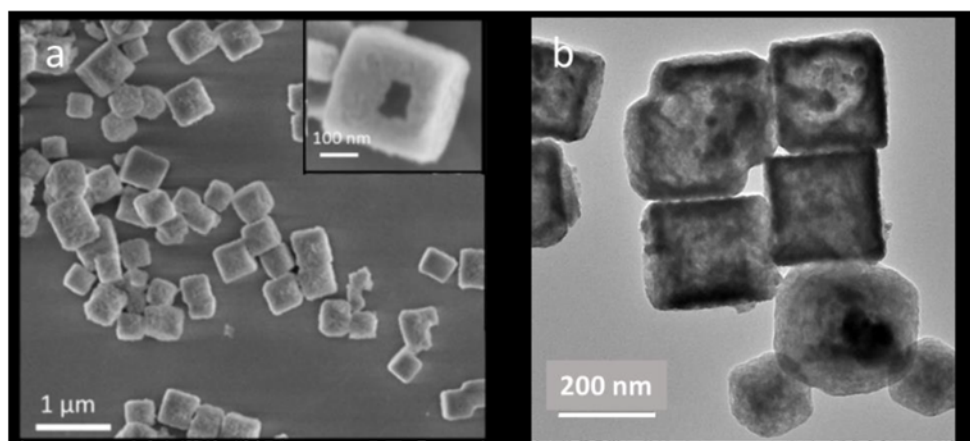


Figure 1: (a) SEM and (b) TEM images of the particles recovered after the replacement step of the synthesis.

REFERENCES

1. Chatenet, M., *et al.*, *Chem. Soc. Rev.*, **2022**, 51, 4583–4762. doi: 10.1039/D0CS01079K.
2. Elmaalouf, M., *et al.*, *Chemical Science*, **2022**, 13, 11807–11816. doi: 10.1039/D2SC03640A.
3. Briois, V., *et al.*, *Journal of Physics: Conference Series*, **2016**, 712, 012149. doi: 10.1088/1742-6596/712/1/012149.

Microfluidic Analysis at the Paris-Saclay Institute of Physical Chemistry

A. Pallandre, A. Boulghobra, F-D. Delapierre, A-M. Haghiri,
F. Moussa, M. Bonose

Institut de Chimie Physique, Orsay, France

ABSTRACT

After a brief introduction showing the microfluidic facilities at Institut de Chimie Physique. We will focus on specific diagnosis of metabolites from the cerebrospinal fluid and propose a comparison between conventional chromatographic techniques and the miniaturized ones.

Dopamine and serotonin are important neurotransmitters in mood and movement regulation in the central nervous system. Inborn errors of dopamine and serotonin metabolism correspond to mutations on the genes coding for enzymes involved in these metabolic pathways or for neurotransmitter transporters. To diagnose these orphan diseases, biomarkers have been identified and validated in cerebrospinal fluid (CSF). Among these biomarkers, there are five metabolites of dopamine and serotonin, namely 5-hydroxy-tryptophan, 5-hydroxy-indol-acetic acid, 3-*ortho*-methyl-DOPA, homovanillic acid and 3-methoxy-4-hydroxyphenylglycol. Currently, the diagnosis of inborn errors of dopamine and serotonin metabolites is based on biomarkers quantification by ultrahigh performance liquid chromatography (UHPLC) with electrochemical detection. Recently we found that the fluorescence in the UV range was an alternative detection method to identify and quantify those biomarkers with microfluidic and conventional instruments.

The SOLEIL View on and Astronomical Detection of the ^{13}C Isotopic Species of Ethyl Cyanide in Vibrational Excitation

C.P. Endres,¹ M.A. Martin-Drumel,² O. Pirali,^{2,3} L. Bonah,⁴
O. Zingsheim,⁴ J-C. Guillemin,⁵ A. Belloche,⁶ M.C. McCarthy,⁷
P. Caselli,¹ S. Schlemmer⁴ and S. Thorwirth⁴

1. Center for Astrochemical Studies, Max-Planck-Institut für extraterrestrische Physik, Garching Germany
2. Institut des Sciences Moléculaires d'Orsay, Université Paris-Saclay, CNRS, Orsay, France
3. AILES beamline Synchrotron SOLEIL, l'Orme des Merisiers 91190 Saint Aubin, France
4. I. Physikalisches Institut, Universität zu Köln, Köln Germany
5. Univ Rennes, Ecole Nationale Supérieure de Chimie de Rennes, CNRS, ISCR-UMR 6226, F-35000 Rennes, France
6. Max-Planck-Institut für Radioastronomie, Bonn, Germany
7. Center for Astrophysics, Harvard & Smithsonian, Cambridge, MA, U.S.A.

ABSTRACT

High-resolution FTIR spectroscopy may provide information of great importance for the interpretation of astronomical spectra, in particular those of vibrationally excited molecules. We recently have recorded vibrational spectra of the three singly substituted ^{13}C isotopic species of ethyl cyanide ($\text{CH}_3\text{CH}_2\text{CN}$) at the AILES beamline of SOLEIL. The measurements covered the wavenumber range up to 700 cm^{-1} and the fundamental vibrational modes ν_{13} (CCN in-plane bending), ν_{21} (methyl torsion), ν_{20} (CCN out-of-plane bending) as well as ν_{12} (CCC in-plane bending). Spectroscopic analysis was performed using the well-established *Automated Spectral Assignment Procedure* (ASAP, Martin-Drumel et al. 2015), to derive accurate excited-state rotational energy levels. Subsequently, the measurements were complemented further by measurements of the vibrational satellites pattern in the millimeter-wave regime using spectrometers at Garching, Orsay and Cologne.

Based on the present analysis, strong vibrational satellites of the three species were readily detected in the ReMoCA millimeter-wave survey obtained with the Atacama Large Millimeter Array, ALMA (Belloche et al. 2019).

REFERENCES

1. Martin-Drumel, Endres, Zingsheim et al., *J. Mol. Spectrosc.* **315**, 72 (2015).
2. Belloche, Garrod, Müller et al., *Astron. Astrophys.* **628**, A10 (2019).

Evolution of Active Species in Homogenous Ru-based Catalyst in Liquid Phase under High Pressures and Temperatures

A. Bugaev¹, K. Janssens², E. Kozyr³, O. Usoltsev⁴, A. Guda⁴,
V. Lemmens², A. Soldatov⁴, D. De Vos²

¹ Paul Scherrer Institute, Villigen, Switzerland

² KU Leuven, Leuven, Belgium

³ Department of Chemistry, University of Turin, Italy

⁴ Southern Federal University, Rostov-on-Don, Russia

ABSTRACT

In situ and *operando* spectroscopy is a powerful tool for studying catalytic materials under relevant working conditions. However, due to the technical complexity of experiments, homogenous catalysts are significantly less investigated in comparison with their heterogeneous counterparts. In this work, we investigate the formation of active species and their evolution under reaction condition, in a homogenous catalytic system for selective hydrodeoxygenation of ketones to alkenes based on of highly diluted ruthenium sites in ionic liquid (IL) under high H₂ and CO pressures by *in situ* X-ray absorption spectroscopy (XAS). Experimental studies were performed at SAMBA beamline of SOLEIL synchrotron (proposal 20210394) using a specially designed *in situ* cell for fluorescence XAS measurements [1], which was successfully tested for homogenous reactions at temperatures up to 220 °C and pressures up to 200 bar. The typical catalytic system was made by dissolving 0.01 mmol RuBr₃ (or RuCl₃) in 1.7 mmol of IL: Bu₄PBr, which results in Ru:Br ratio of 1:170. Acetone and 1-propanol were added as model substrate. Variable H₂/CO/He mixtures were applied under the total pressure of up to 40 bar. XAS data were collected *in situ* in continuous scanning mode and analyzed with FASTOSH program including also the MCR-ALS routine [2].

XAS data revealed the formation of several types of Ru-species. First, irrespective of the used precursor, RuBr_x species were formed due to interaction with the IL. High CO pressures or addition of formaldehyde as a CO source, pushed the system towards Ru bromide carbonyls (Ru(CO)₃Br₂) which were shown to be the main active species responsible for C=O bond hydrogenation. In the absence of CO but in presence of H₂, formation of Ru(0) was identified accompanied with the loss of selectivity towards C=O hydrogenation and increase of the undesired C=C hydrogenation. All *in situ* data were confirmed by high-quality XAS acquisition for “frozen states” of the catalytic system solidified in the IL and by density functional theory (DFT) calculations of the intermediate and transition states along the reaction pathway.

These results give a complete understanding of the evolution of the active species in the industrially relevant catalyst used for the valorization of biobased polyols to olefins in ionic liquids, identifying the undesired deactivation routes as well as the possibilities for the catalysts' reactivation.

REFERENCES

1. Shvets, et al. *Catalysts*, **2022**, 12, 1264
2. Jaumot, Gargallo, de Juan and Tauler, *Chemom. Intell. Lab. Syst.*, **2005**, 76, 101-110
3. Janssens, Bugaev, Kozyr, et al., *Chem. Sci.*, **2022**, 13, 10251-10259. 25-30.

Reactivity of the HCO⁺/HOC⁺ Isomers as a Function of Photon and Collision Energy for Astrochemistry

N. Solem^(a), C. Alcaraz^{(a)(b)}, D. Ascenzi^(c), V. Richardson^(d),
M. Sockath^(a), R. Thissen^{(a)(b)}, C. Romanzin^{(a)(b)}

^(a)Université Paris-Saclay, CNRS, Institut de Chimie-Physique, UMR8000, 91405 Orsay, France

^(b)Synchrotron SOLEIL, L'Orme des Merisiers, F-92292 Saint-Aubin, Gif-sur-Yvette, France

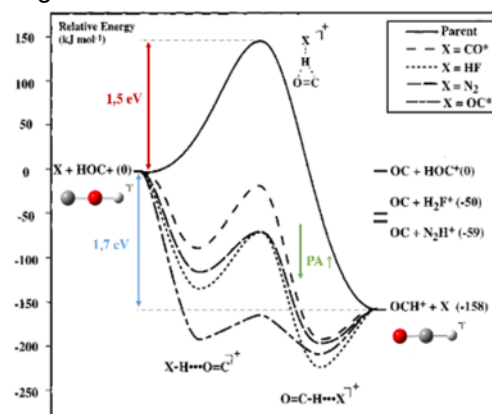
^(c)Department of Physics, University of Trento, Via Sommarive 14, 38123, Italy

^(d)Department of Physics, University of Liverpool, Oliver Lodge Laboratory, Oxford Street Liverpool, L69 7ZE, UK

ABSTRACT

HCO⁺ and HOC⁺ are two isomers that have been detected in Photon Dominated Regions¹, diffuse clouds², and Mars atmosphere^{3,4}. They correspond to the protonation of carbon monoxide on either the carbon or oxygen atom and are important intermediates in the formation of complex molecules as HCO⁺ is the most abundant ion in molecular clouds. We have differing reactivity of the two isomers and the potential for isomerization when energy is provided. The isomers have a difference of energy of 1.7 eV⁵ (HCO⁺ being the more stable) and are separated by an isomerization barrier of 1.5 eV⁵ (from HOC⁺). Previous studies of their reactivity have mostly been produced by electronic ionization^{6,7} which does not allow a precise determination of the internal energy of the ions and leads to a mixture of isomers. Moreover, studying pure isomers of HCO⁺/HOC⁺ reactivity is difficult because the isomerization barrier can be reduced in the presence of a second body, acting as a catalyzer with height increasing with the proton affinity⁵ of the neutral target.

The CERISES⁸ instrument connected on the branch B of the DESIRS beamline was used to produce the two isomers by dissociative photoionization of two precursors: HCO⁺ from formaldehyde (H₂CO) and HOC⁺ from deuterated methanol (CD₃OH). We have studied the reactivity of the two ions with 13 neutral targets chosen for two goals: (i) characterization of the ionic purity and internal energy content through the study of simple reactivity channels: proton transfer (PT) and charge transfer, and (ii) the study of more complex reactivity (with a potential for an increase in chemical complexity) with molecular targets of astrochemical interest such as methanol, benzonitrile, acetaldehyde, formamide, methyl formate, and acrylonitrile



Potential surface of HOC⁺/HCO⁺ isomer pair and illustration of the evolution of the isomerisation barrier for different collision partner, from Chalk and Radom⁵

From the extensive data set, we have determined isomeric purity, evolution of internal energy as a function of photon energy, and that the reactivity of both isomers with methanol is dominated by PT and dissociative PT. The collision-mediated isomerization has been evaluated through an innovative method that combines time-of-flight spectrometry with simulation.

REFERENCES

- (1) Fuente, A et al. *A&A* **2003**, 406 (3), 899–913. <https://doi.org/10.1051/0004-6361:20030712>.
- (2) Liszt, H. et al. *A&A* **2004**, 428 (1), 117–120. <https://doi.org/10.1051/0004-6361:20041649>.
- (3) Fox, J. L. *Icarus* **2015**, 252, 366–392. <https://doi.org/10.1016/j.icarus.2015.01.010>.
- (4) Matta, M. et al. *J. Geophys. Res. Space Physics* **2013**, 118 (5), 2681–2693. <https://doi.org/10.1002/jgra.50104>.
- (5) Chalk, A. J.; Radom, L. *J. Am. Chem. Soc.* **1997**, 119 (32), 7573–7578. <https://doi.org/10.1021/ja971055c>.
- (6) Illies, A. J. et al. *J. Am. Chem. Soc.* **1983**, 105 (9), 2562–2565. <https://doi.org/10.1021/ja00347a008>.
- (7) Wagner-Redeker, W. et al. *The Journal of Chemical Physics* **1985**, 83 (3), 1121–1131. <https://doi.org/10.1063/1.449474>.
- (8) Cunha de Miranda, B. et al. *J. Phys. Chem. A* **2015**, 119 (23), 6082–6098. <https://doi.org/10.1021/jp512846v>

Shaping Plasmonic Supercrystals by Nesting Shapes

W. Chaâbani,¹ J. Lyu,¹ T. Bizien,² C. Goldmann,¹ F. Smallenburg,¹
M. Impéror-Clerc,¹ D. Constantin,³ C. Hamon¹

1 Université Paris-Saclay CNRS, Laboratoire de Physique des Solides, Orsay 91405, France

2 SWING beamline, SOLEIL Synchrotron Gif-sur-Yvette 911190, France

3 Institut Charles Sadron, CNRS and Université de Strasbourg Strasbourg 67034, France

ABSTRACT

Nature has long inspired scientists with its ability to synthesize complex inorganic nanostructures by consistently exploiting the self-assembly in confinement of (often complex) building blocks. This level of complexity has not yet been reached synthetically with colloidal crystals, because most nanoparticles (NPs) are highly symmetric objects and because their self-assembly is unconstrained. Here, we aim at designing periodic plasmonic structures (supercrystals) of low symmetry by self-assembling in confinement nanoparticles (Au, Ag). Synergistic or antagonistic effects during the evaporation of the nanoparticle suspension within a mold are expected such as symmetry breaking and the formation of plasmonic topological defects. The originality of the design of the material consists in the self-assembly of anisotropic NPs under controlled confinement conditions within a mold made by soft-lithography.

First, NPs whose packing have not been studied yet but which shows interesting features in this respect have been used as building blocks. For instance, nanoparticles with a pentagonal cross section (rods, decahedra, bipyramids) are non-centrosymmetric and do not tile space in the plane that lead to a rich phase diagram. For instance, we successfully assembled pentagonal bipyramids into a triclinic periodic arrangement, which is the lowest lattice symmetry reported to date for a supercrystal.¹

Second, the NPs have been confined in microcavities and we investigated how the shapes of the mold and of the supercrystal nest together upon evaporation of the solvent, in order to break the symmetry of the nanostructures. The method combines the synthetic convenience of colloidal chemistry with the tunable confinement provided by the template. We aim at understanding how the shape of the mold can control the topology of the orientational defects. The resulting nanostructured materials are investigated using a multiscale approach to address the characteristic length of the interparticle distance (nm), of the supercrystals (μm) and the array of supercrystals (mm). To tackle this issue, a multiscale characterization strategy have been used by combining electron microscopy with small angle X-ray scattering (SAXS). We used a state of the art microbeam SAXS (μSAXS) synchrotron technique to study the 3D structuration of individual supercrystals with statistical significance.

REFERENCES

1. Lyu, J.; Chaabani, W.; Modin, E.; Chuvilin, A.; Bizien, T.; Smallenburg, F.; Imperor-Clerc, M.; Constantin, D.; Hamon, C., Double-Lattice Packing of Pentagonal Gold Bipyramids in Supercrystals with Triclinic Symmetry. *Adv Mater* **2022**, *34* (21), e2200883.

Phthalocyanines in the Gas-phase from Valence to Core-shell Electron Spectroscopy

J. Laurent^a, N. Shafizadeh^a, P. Çarçabal^a, D. Cubaynes^a, B. Soep^a,
M. Briant^b, M. Simon^c, R. Püttner^d and G. Goldsztejn^a

a) Université Paris-Saclay, Institut des Sciences Moléculaires d'Orsay ISMO, UMR CNRS 8214, F-91405 Orsay, France

b) CEA, IRAMIS, UMR 3685 NIMBE, F91191 Gif-sur-Yvette, France

c) Sorbonne Université, CNRS, Laboratoire de Chimie Physique-Matière et Rayonnement, LCPMR, F-75005 Paris Cedex 05, France

d) Fachbereich Physik, Freie Universität Berlin, Arnimallee 14, D-14195 Berlin, Germany

ABSTRACT

The importance of characterizing Metallophthalocyanines' (MPc) electronic ground state is twofold. First, the arrangement of the *d* electrons within the centered-metal atom influences greatly its ligation. This has been recently reviewed for heme, a closely-related molecule, in the gas-phase¹ through the joint experimental and theoretical study of binding energies with various ligands. Second, it is important for potential applications (such as in catalysis², optoelectronics³, spintronics⁴ or photodynamic therapy⁵) where the spin states of the metal and the substrate can couple (see e.g. Ref⁶). Although crucial for these possible applications, the determination of GS of transition metal MPc remains nowadays subject to controversy, as discussed in our recent publication⁷ with the showcase of FePc.

The MPc are aromatic macrocycle molecules that resemble to porphyrins, except for substitution of aza-bridge nitrogen atoms in place or carbon atoms. Thus leading to two different types of N atoms (see Fig.1). The ones surrounding the centered-metal atom, that are directly involved in the chemical bonds with it, and the peripheric "aza-bridge" N atoms. MPc is represented in Fig.1 where the orange sphere represents the metal, blue spheres are the N atoms, grey spheres the C atoms and white ones are H atoms.

We present our work on several phthalocyanines evaporated and interrogated with the soft X-ray radiation coming from the PLEIADES' beamline. These combined experimental and theoretical studies shed light on i) the electronic configuration within the metal, ii) the coupling between its *d* orbitals and the π orbitals in which the surrounding N atoms are involved and iii) on an unexpected interatomic Coulombic decay between M and N atoms after core-excitation at the N 1s edge.

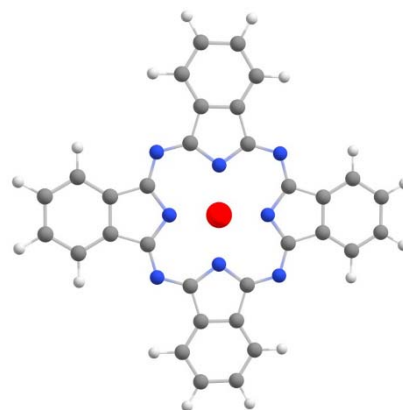


Figure 1: Representation of a MPc molecule, which is composed of a porphyrin-like aromatic macrocycle where « aza-bridge » N atoms replaced carbons. The macrocycle is surrounded by four aromatic rings and a Fe atom is located in its center.

REFERENCES

1. N. Shafizadeh, et al., *International Reviews in Physical Chemistry*, 2021, **40**, 365-404.
2. C. C. Leznoff et al., *Phthalocyanines, Properties and Applications*, VCH, New York, 1989, vol.4.
3. K. Walzer, et al., *Chem. Rev.*, 2007, **107**, 1233-1271.
4. N. Domingo, et al., *Chem. Soc. Rev.*, 2012, **41**, 258–302.
5. E. Reddi, et al., *Br J Cancer.*, 1987, **56**, 597–600.
6. S. Stepanow et al., *Phys. Rev. B : Condens. Matter Mater. Phys.*, 2011, **83**, 220401.
7. J. Laurent, et al., *Phys. Chem. Chem. Phys.*, 2022, **24**, 2656.

Study Chemical & Structural Evolution of Mn and Ti in Disordered Rocksalt $\text{Li}_2\text{Mn}_{1-x}\text{Ti}_x\text{O}_2\text{F}$ Cathode Materials through *Operando* XAFS

Y. Hu^{a,*}, Y.S. Moghadam^a, A. El Kharbachi^a, S. Belin^b,
T. Diemant^a, M. Fichtner^{a,c}

^a Helmholtz-Institute Ulm (HIU), Helmholtzstr. 11, 89081 Ulm, Germany

^b SOLEIL Synchrotron, F-91192 Gif-sur-Yvette, France

^c Institute of Nanotechnology, Karlsruhe Institute of Technology (KIT), P.O. Box 3640,
76021 Karlsruhe, Germany

ABSTRACT

Mn-based Li-rich disordered rocksalt (DRS) oxyfluorides have demonstrated promising electrochemical properties as cobalt-free cathode materials for high-energy Li-ion batteries, in addition to their low cost, eco-friendliness and nature abundance¹. However, the limited cycle life due to capacity degradation and the unclear cation and anion redox mechanisms hindered the further usage of high-performance DRS materials. We have investigated a Mn-based Li-rich DRS system $\text{Li}_2\text{Mn}_{1-x}\text{Ti}_x\text{O}_2\text{F}$ ($0 \leq x \leq 2/3$) – LMTOF². The substitution of high-valent $3d^0$ Ti^{4+} stabilises the DRS structure, and the lower-valent F^- sets up the charge balance to favour the incorporation of Mn as Mn^{2+} in the structure, allowing $\text{Mn}^{4+}/\text{Mn}^{2+}$ double-redox reaction. After the initial charge, the optimal composition with 33% Ti delivered a discharge capacity comparable to the Li-rich layered LNMCO (200-220 mAh/g) and greater than the conventional LCO or LFP (170 mAh/g). With extended cycles, a capacity retention of 190 mAh/g (~ 650 Wh/kg) after 100 cycles and 136 mAh/g (~ 460 Wh/kg) after 200 cycles was obtained. To further improve the capacity retention, a deep understanding of materials evolution and their redox chemistry remains incomplete³.

In order to track the chemical and structural evolution in LMTOF materials and to comprehend their redox mechanisms, Ti and Mn K-edge *Operando* XAFS were carried out at SOLEIL ROCK beamline. XANES and EXAFS results demonstrated an evolution of Mn oxidation states upon charge and discharge, and showed that Mn was the predominant redox-active TM with lower Ti substitution. Linear combination fit was used to monitor the Mn evolution during cycling, and shell fitting was performed to gain insights on the “average” local coordination environment for Mn and Ti. Fresh electrode was compared with pre-cycled ones to evaluate the degradation in extended cycles. *Operando* results were also compared with *ex-situ* data obtained from pre-cycled electrodes with different cycle numbers and cycling rate.

REFERENCES

1. J. Lee *et al.*, Reversible $\text{Mn}^{2+}/\text{Mn}^{4+}$ double redox in lithium-excess cathode materials, *Nature*, 556, 185-190 (2018)
2. Y. Shirazi Moghadam *et al.*, Toward Better Stability and Reversibility of the $\text{Mn}^{4+}/\text{Mn}^{2+}$ Double Redox Activity in Disordered Rocksalt Oxyfluoride Cathode Materials, *Chem. Mater.*, 33, 8235-8247 (2021)
3. Sharpe *et al.*, Redox Chemistry and the Role of Trapped Molecular O_2 in Li-Rich Disordered Rocksalt Oxyfluoride Cathodes, *J. Am. Chem. Soc.*, 142, 21799-21809 (2020)

Probing the Photodynamics of Cyano-PAHs in the Vacuum-ultraviolet Range

M.R. Chowdhury¹, G.A. Garcia¹, H.R. Hrodmarsson²,
J-C. Loison³ and L. Nahon¹

¹*Synchrotron SOLEIL, L'Orme des Merisiers, Départementale 128, 91190 Saint Aubin, France*

²*Laboratory for Astrophysics, Leiden Observatory, Leiden University,
NL-2300 RA Leiden, The Netherlands*

³*Université Bordeaux, CNRS, Bordeaux INP, ISM, UMR 5255, Talence F-33400, France*

ABSTRACT

Polycyclic aromatic hydrocarbons (PAHs) are postulated to be present abundantly in the interstellar medium (ISM) and they constitute a major source of carbon. The presence of the PAHs is widely acknowledged through the observation of the aromatic infrared emission bands (AIBs) in the 3-20 μm spectral range, however, the individual detection of them remains a challenge for interstellar chemistry owing to their highly symmetric molecular structures. Thus, the attention is shifted to detect the less symmetric ones, like the substituted PAHs. Recently, the two nitrile (or cyanide) group functionalized PAHs, i.e., 1- and 2-cyanonaphthalenes and cyanobenzene have been detected in the cold Taurus molecular cloud (TMC-1) [1,2]. Cyanides are easily detected in the ISM due to their large abundances and the recent detection indirectly confirms the presence of naphthalene and benzene.

The detection of these molecular species has driven further interest in studying the photodynamics of these molecules in vacuum ultraviolet (VUV) region, especially in terms of photoionization and cation fragmentation processes. We have performed the experimental investigations at the VUV DESIRS beamline at Synchrotron SOLEIL to study the photoelectron spectroscopy of the two cyano-PAHs and cyanobenzene on a molecular beam chamber available at the SAPHIRS permanent endstation coupled to a double imaging photoelectron-photoion coincidence (ⁱ²PEPICO) spectrometer, DELICIOUS 3 [3]. We have obtained the high resolution threshold photoelectron spectrum (TPES) over an extended binding energy range which is further compared with *ab initio* calculations. An overall good agreement is observed between the predicted and observed bands. The state selected fragmentation over a wide photon energy range have been obtained which when compared with the case of unsubstituted PAHs unravels the effect of cyano-substitution in terms of photostability. Theoretical investigations predict that PAHs contribute abundantly to the photoelectric heating of the ISM by thermalization of the emitted electrons [4]. The present measurements provide the photoelectron kinetic energy distributions as a function of the photon energy which can be employed to model the photoelectric heating for any incoming photon spectral distribution.

REFERENCES

1. B. A. McGuire *et. al. Science* **359**, 202-205 (2018).
2. B. A. McGuire *et. al. Science* **371**, 1265-1269 (2021).
3. G. A. Garcia *et. al. Rev. Sci. Inst.* **84**, 053112 (2013).
4. E. L. O Bakes and A. G. G. M Tielens *Astrophys. J* **427**, 822-838 (1994).

PARALLEL SESSION

Life & Earth Sciences

(Biology / Cultural heritage / Health & Environment / Geoscience)

SOLEIL Auditorium - Main Building

Thursday, January 19th

Chairpersons:

B. Masquida, R. Le Hir, R. Marsac, S. Raneri

- IT-04 The interactions between metal(loid)s and environmental plastics:
Chromium and arsenic examples
C. Catrouillet
- OC-10 Lanthanide distribution in *Daphnia magna* via micro and nano S-XRF
imaging
M. Revel
- OC-11 Probing chromium and manganese speciation in Chinese RED Soils
X. Qin
- OC-12 Unravelling the pathways of cadmium in cacao
G. Sarret
- IT-05 Synchrotron-based X-ray imaging of pigments and secondary products in
Cimabue's ceiling paintings of the upper basilica of Assisi
E. Avranovitch Clerici
- OC-13 Synchrotron μ -XRF imaging and μ -XANES spectroscopy at the cultural
heritage dedicated PUMA beamline at SOLEIL
A. Gianoncelli
- OC-14 Chemical imaging at PUMA, SOLEIL, of samples of polychrome cave art
from Font-de-Gaume cave to validate in-situ results
J. Tapia
- OC-15 Synchrotron X-ray spectro-imaging clarifies the anatomy and taphonomy of
amphibians from the Montceau-les-Mines lagerstätte
P. Gueriau

PARALLEL SESSION

Life & Earth Sciences

(Biology / Cultural heritage / Health & Environment / Geoscience)

SOLEIL Auditorium - Main Building

Friday, January 20th

Chairpersons:

B. Masquida, R. Le Hir, R. Marsac, S. Raneri

- | | |
|-------|--|
| IT-06 | Structural studies of antibody antigen complexes
<i>F. Rey</i> |
| OC-16 | Why do we see amyloid- β plaques in phase-contrast imaging?
<i>M. Chourrout</i> |
| OC-17 | Synchrotron based X-ray microtomography reveals cellular morphological features of developing wheat grain
<i>D. Legland</i> |
| OC-18 | Multimetal methyl transferase making methanogenesis
<i>C. Fyfe</i> |

The Interactions Between Metal(loid)s and Environmental Plastics: Chromium and Arsenic Examples

C. Catrouillet^{1,2}, M. Davranche¹, D. Vantelon³, I. Khatib,
C. Rivard^{3,4}, R. Tucoulou⁵, J. Gigault⁶

¹*Géosciences Rennes, UMR 6118, University of Rennes 1, Campus de Beaulieu, 35042 Rennes Cedex, France*

²*Université Paris Cité, Institut de physique du globe de Paris, CNRS, F-75005 Paris, France*
(email contact: charlotte.catrouillet@ipgp.fr)

³*Synchrotron SOLEIL, L'orme des merisiers, Saint Aubin BP48, 91192 Gif-sur-Yvette Cedex, France*

⁴*INRAE, Institut National de Recherche Pour L'agriculture, L'alimentation et L'environnement, BIA, TRANSFORM, 44316 Nantes, France*

⁵*ESRF, The European Synchrotron, 71, Avenue des Martyrs, 38043, Grenoble, France*

⁶*TAKUVIK CNRS/Université Laval, IRL 3376, G1V 0A6 Québec, Canada*

ABSTRACT

Around 6.3 billion tons of plastic were released unintentionally into the environment, with various sizes (i.e., macro-, micro- and nano-plastics). Plastics are particularly persistent in the environment. When released in the environment, they represent a danger for the biota for two main reasons: 1) As objects, micro- and macroplastics (e.g., net) can strangulate animals (e.g., turtles, fishes). 2) "Environmental" microplastics also contain toxicants. It is well-known that macro- and micro plastics contain organic additives, which can be released over time. But, microplastics also contain organic and inorganic metals (e.g., Zn, Ba, Cu, Pb, Cd, Mn, Ni, V, Cr) and metalloids (e.g., As, Sb)², which can be toxic. They can either originate from the plastics formulation (additives) or from the adsorption of external toxic compounds, directly onto their surface, or indirectly onto mineral or biofilm formed and associated at their surface.

The chemical form of an element controls its bioavailability and toxicity, making the determination of their speciation of primary importance. Various "environmental" plastics have been collected from beaches and ocean gyres around the world. Some samples show concentrations of Cr and Pb that can reach a few mg g⁻¹ and of As a few µg g⁻¹. These three elements are classified by the WHO as among the most dangerous in the world because they are carcinogenic. In order to determine in which chemical forms these elements are present in environmental plastics, XAS (X-ray Absorption Spectroscopy) and µXRF (X-Ray Fluorescence) analyses have been performed at the SOLEIL (Cr speciation) and ESRF (As speciation) synchrotrons. The results obtained show that the redox forms of these elements vary from one sample to another, depending on the pigment used (i.e., Cr). While some samples show a stability of Cr forms within the sample, others show variations in speciation from one area analysed to another. Contrary to Cr, As was always detected at the surface of the plastics. It is present in various forms (organic and inorganic ones), but the speciation was similar in all samples analysed (originated from the same area). Plastics can therefore be considered as vectors of metals and metalloids, potentially present in toxic forms.

REFERENCES

1. https://www.plasticseurope.org/application/files/9715/7129/9584/FINAL_web_version_Plastics_the_facts2019_14102019.pdf
2. C. Catrouillet, M. Davranche, I. Khatib, C. Fauny, A. Wahl, J. Gigault, Environ. Sci.: Processes Impacts, **23**, 553-558 (2021)

Lanthanide Distribution in *Daphnia Magna* via Micro and Nano S-XRF Imaging

M. Revel¹, K. Medjoubi², C. Rivard^{2,3}, D. Vantelon²,
A. Hursthouse⁴, S. Heise¹

¹Life Sciences, Hamburg University of Applied Science, Ulmenliet 20, D-21033 Hamburg, Germany

²SOLEIL synchrotron, L'Orme des Merisiers, 91190 Saint-Aubin, France

³TRANSFORM, INRAE, 44316 Nantes, France

⁴University of the West of Scotland, Paisley, PA1 2BE, UK

E-mail contact: marion.revel@haw-hamburg.de

ABSTRACT

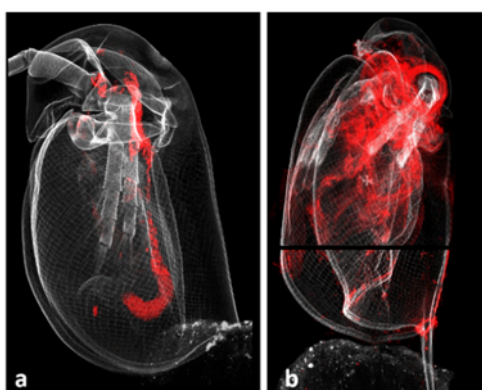


Figure 1: Lanthanide distribution (a. La b. Gd) in juvenile *Daphnia magna*.

Levels of Rare earth elements (REE) in aquatic systems have risen [1], and future research into their interactions with biological systems is becoming more crucial. According to experiments on daphnids (water fleas), the toxicity of lanthanum, for instance, may be comparable to that of copper [2]. Toxic effects require uptake and potentially accumulation of REEs into cells and tissues. But few data are available on the distribution of REE in organisms after exposure and on accumulated concentrations. In order to improve understanding of REE bioavailability, the accumulation of La and Gd in *Daphnia magna* has been studied via XRF imaging at the NANOSCOPIUM and LUCIA beamlines of SOLEIL. Neonates of less than 24h were

exposed to 15 mg/L of La or Gd for 48 and 72h. At the end of the test, the survival organisms were dehydrated through an acetone-water series and dried in HDMS (1,1,1,3,3,3-hexamethyldisilazane) in order to be analysed by XRF. The elemental distribution was mapped at both 17,02 and 7.25 keV to follow the distribution of heavy and light elements. Additionally, maps were performed with different resolutions (from 3 to 0.4 micron/pixel) to follow the elemental distribution in the entire animal and focus on the distribution in specific areas.

The results showed a difference of distribution between La and Gd in the organisms (figure 1). Gd was distributed on diffused manner in different tissues showing that it is assimilated by daphnid unlike La that was found in the intestine tract and had a solid appearance in the hindgut. The ingestion of La is probably possible because of its precipitation either in the medium or in the animal's intestine itself. As a negative correlation can be observed between the capacity to precipitate and the lanthanide ionic radius [3], Gd tend to be more soluble than La in the test media which could explain why La was mainly ingested by the animal.

Our results highlight the importance of speciation in metals toxicity. In our tests, due to its higher solubility, Gd was found to be assimilated by daphnid and thus more toxic than La which does not accumulate in tissues.

REFERENCES

1. Tepe, N., M. Romero, and M. Bau, High-technology metals as emerging contaminants: Strong increase of anthropogenic gadolinium levels in tap water of Berlin, Germany, from 2009 to 2012. *Applied geochemistry*, 2014. 45: p. 191-197.
2. Herrmann, H., et al., Aquatic ecotoxicity of lanthanum – A review and an attempt to derive water and sediment quality criteria. *Ecotoxicology and Environmental Safety*, 2016. 124: p. 213-238.
3. Suzuki, Y., et al., Precipitation incidence of the lanthanoid(III) hydroxides. *Journal of the Less Common Metals*, 1986. 126: p. 351-356.

Probing Chromium and Manganese Speciation in Chinese RED Soils

X. Qin¹, M. Benedetti¹, D. Guinoiseau², A. Gelabert¹,
M. Desmau³, Z. Ren⁴

¹ *Institut de Physique du Globe, Paris, France*

² *Geosciences Paris-Saclay, Orsay, France*

³ *Yukon University, Whitehorse, Canada*

⁴ *South China Agricultural University, Guangzhou, China*

ABSTRACT

In China, red soils cover 30% of agricultural land, account for 80% of the country's rice production, but 35% of them are experiencing **chromium (Cr) pollution**. In these soils, **Fe and Mn oxide nodules (FMNs)** are ubiquitous and play an important role in the fate of pollutants including Cr. Toxic Cr behavior in soils is controlled by seasonal redox/pH fluctuations and thus it is also strongly correlated with the redox-sensitive Fe and Mn oxides. Therefore, identifying the **Cr speciation** and redox state in redox soils is mandatory to understand chromium cycling and the effect of environmental changes on its mobility. In this study, we performed **Cr XANES spectra analysis (BM 16 FAME-UHD, ESRF)** on two red soil profiles which are experiencing distinct redox cycles (paddy vs non-paddy soils). The speciation of Cr associated with FMNs and the surrounding soils for different horizons and hydromorphic effect has been determined. **Manganese speciation** in these samples was determined because it is the major oxidant of Cr in soils. Pre-peak can be used as a Cr redox-sensor and its analysis evidenced a **larger proportion of Cr(VI) in waterlogged horizon** of the paddy surrounding soil, along with a higher manganese valence. In addition, Chromium K-edge XANES data indicated **Cr-bearing goethite/ferrihydrite** dominated Cr speciation in FMNs as well as in surrounding soils.

Unravelling the Pathways of Cadmium in Cacao

H. Blommaert¹, A-M. Aucour², M. Wiggerhauser³, C. Moens⁴,
P. Telouk², S. Campillo¹, J. Beauchêne⁵, G. Landrot⁶, D. Testemale⁷,
S. Pin⁸, C. Lewis⁹, P. Umaharan⁹, E. Smolders⁴ and G. Sarret¹

¹ Université Grenoble Alpes, ISTERRE, Grenoble, France,

² Université de Lyon, ENS de Lyon, CNRS, UMR 5276 LGL-TPE, Villeurbanne, France,

³ Institute of Agricultural Sciences, ETH Zurich, Lindau, Switzerland,

⁴ Division of Soil and Water Management, Dept of Earth and Environmental Sci., KU Leuven, Belgium,

⁵ CIRAD, UMR EcoFoG, AgroParisTech, CNRS, Université de Guyane, Kourou, France,

⁶ Synchrotron SOLEIL, L'Orme des Merisiers, Saint-Aubin, Gif-sur-Yvette, France,

⁷ Univ. Grenoble Alpes, CNRS, Grenoble INP, Institut Néel, ligne FAME, Grenoble, France,

⁸ Université Paris-Saclay, CEA, CNRS, NIMBE, Gif-sur-Yvette, France,

⁹ Cocoa Research Centre, University of the West Indies, St. Augustine, Trinidad and Tobago

ABSTRACT

The accumulation of the potentially toxic metal cadmium (Cd) in cacao beans has recently become a subject of intense research after the European Union and the Codex Alimentarius lowered its legal limits in chocolate. The research on strategies to reduce cadmium (Cd) accumulation in cacao beans is currently limited by a lack of understanding of the Cd transfer pathways within the cacao tree¹. Moreover, studying plant samples at environmental concentrations is challenging because of the low Cd content (a few mg kg⁻¹ dw). Here, we studied the transfer of Cd from soil to the nib (seed) in a high Cd accumulating cacao cultivar by analyzing total elemental concentrations, Cd stable isotope fractionation, Cd speciation and localization. The plant Cd concentrations were 10-28 higher than the topsoil Cd concentrations. The largest fraction (57%) of total plant Cd was present in the branches where it was primarily bound to carboxyl-ligands (60-100%) and mainly localized in the phloem rays and phelloderm of the bark. Cadmium in the nibs was mainly bound to oxygen ligands (60-90%), with phytate as the most plausible ligand. A scheme of Cd pathway from roots to nib was proposed, and compared with other species. This study extended the limited knowledge on Cd accumulation in perennial, woody crops and revealed that the Cd pathway is markedly different than in annual crops, which has implications for mitigation strategies².

REFERENCES

1. Vanderschueren, R., Argüello, D., Blommaert, H., Montalvo, D., Barraza, F., Maurice, L., et al. (2021) *Science of the Total Environment*, **781**, p. 146779.
2. Blommaert H, Aucour A-M, Wiggerhauser M, Moens C, Telouk P, Campillo S, Beauchêne J, Landrot G, Testemale D, Pin S, Lewis C, Umaharan P, Smolders E and Sarret G (2022) *Front. Plant Sci.* **13**,1055912.

Synchrotron-based X-ray Imaging of Pigments and Secondary Products in Cimabue's Ceiling Paintings of the Upper Basilica of Assisi

E. Avranovich Clerici^(1,*), S. de Meyer⁽¹⁾, F. Vanmeert^(1,2),
S. Legrand⁽¹⁾, L. Monico^(3,1), G. van der Snickt⁽⁴⁾, C. Miliani⁽⁵⁾
and K. Janssens^(1,6)

(1) *AXIS Research group, NANOlaboratory Center of Excellence,
University of Antwerp, Belgium*

(2) *Laboratory Department, Royal Institute for Cultural Heritage (KIK-IRPA),
Brussels, Belgium*

(3) *CNR-SCITEC, Perugia, Italy*

(4) *ARCHES Research group, Antwerp Cultural Heritage Sciences,
University of Antwerp, Belgium*

(5) *CNR-ISPC, Napoli, Italy*

(6) *Rijksmuseum Amsterdam, The Netherlands*

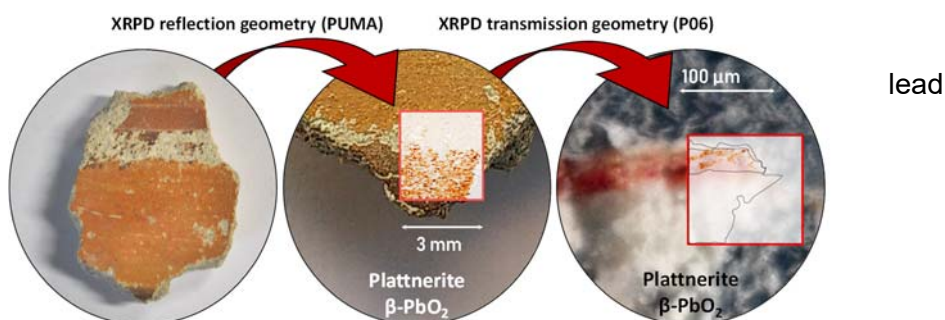
(*) ermann.avranovichclerici@uantwerpen.be

ABSTRACT

The last 20-25 years have seen an exponential growth in applications of synchrotron-based analytical techniques exploited to investigate cultural heritage-materials in an attempt to verify their originality, understand the production processes and preserve them from degradation due to the aging of these rare and precious objects. Synchrotrons have been applied to perform non-invasive investigations on a great variety of very different materials, from plastic and wooden objects to bronzes. Furthermore, thanks to the tunability of the produced beam, it is possible to use low-energy wavelengths, such as infrared to very intense ones such as hard X-rays or even particles in dedicated beamlines, to perform different types of analysis. The beams produced in synchrotrons are characterized by an extreme brilliance that allows to obtain optimal signal-to-noise ratios, enabling a very fast point acquisition and thus offering the possibility to perform imaging and tomography with a great lateral resolution. Our research group has gained a great experience in employing X-ray-based techniques using lab-based instruments and/or synchrotron facilities to image all types of heritage-related materials, especially paintings. When analysing painted masterpieces, it is not always possible to move the sample from the museum in which it is stored or, in the case of mural paintings, from the wall on which they are depicted to a synchrotron facility. In these cases, a possibility, not always well seen by curators, is to perform invasive sampling and only analyse the paint stratigraphy from cross sections. However, in rare cases such as the one that will be discussed below, it has been possible to considerably exploit synchrotron radiation.

Various types of paints, present on fragments derived from the vaults of the Upper Basilica of Saint Francis of Assisi, Italy, are studied, focusing on the pronounced colour change of the originally white,

blue/green and brown/yellow/orange areas. Here, respectively white, verdigris and/or azurite and red/yellow cinnabar and/or ochre pigments were originally used.



A series of six fragments of painted plaster, measuring several square centimetres in size, were recovered after the

Fig. 1: Example of the macro (PUMA) and micro (P06)-imaging techniques applied over the painted fragment and their cross-sections highlighting the presence of plattnerite $\beta\text{-PbO}_2$

earthquakes of September 1997 which caused a number of ceiling paintings of the Upper Basilica in Assisi, dating back to the 12th and 13th century, to shatter on the ground. The masterpieces are attributed to Cimabue and Giotto, prominent artists of their time^[1]. To characterize the original pigments and the secondary products formed during the degradation processes leading to colour changes, a combination of macroscopic and microscopic X-ray fluorescence and X-ray powder diffraction mapping was employed. Measurements were performed either directly on the fragments without any sampling at the PUMA beamline of synchrotron SOLEIL, in Saclay, France or on paint cross-sections at P06 X-ray micro/nanoprobe of the PETRA-III synchrotron in Hamburg, Germany. (Fig. 1). The combined results indicate that in many cases, the blackening of the areas painted with lead white is due to the formation of plattnerite and/or scrutinyite (two polymorphs of PbO_2), both possible oxidation products of (hydro)cerussite. In addition, the presence of other secondary products such as copper tri-hydroxychloride from pigments containing copper and calcium oxalates from the calcium containing substrate were observed. The extensive presence of chlorinated metal salts indicates to the central role of chlorine-compounds played during the degradation processes of the fresco fragments analysed^[2].

REFERENCES

^[1] Bellosi, L. Roma anno 1300: atti della IV *Stamina di studi di storia dell'arte medievale dell'Università di Roma La Sapienza* **1980**, 127-139.

^[2] Vagnini M. et al., Investigation on the process of lead white blackening by Raman spectroscopy, XRD and other methods: Study of Cimabue's paintings in Assisi, *Vibrational Spectroscopy*, **2018**, 98, 41-49.

Synchrotron μ -XRF Imaging and μ -XANES Spectroscopy at the Cultural Heritage Dedicated PUMA Beamline at SOLEIL

A. Gianoncelli⁽¹⁾, S. Raneri⁽²⁾, S. Schoeder⁽³⁾

(1) Elettra Sincrotrone Trieste, Strada Statale 14, km 163.5
in Area Science Park I-34149 Basovizza-Trieste, Italy

(2) University of Pisa, Department of Earth Sciences, Via Santa Maria, 53, 56126, Pisa, Italy

(3) Synchrotron SOLEIL, PUMA beamline, Saint-Aubin BP48, F-91192 Gif-sur-Yvette cedex, France

ABSTRACT

Archaeometry is a scientific discipline aiming at characterizing, investigating, preserving and/or dating archeological materials by applying scientific analytical techniques. Such analyses allow to retrieve historical and artistic information about the past and can be performed with standard instrumentation, devoted to a specific technique, or with dedicated instrumentation designed to better satisfy the requirements of archeological/artistic artefacts.

This is the case of PUMA, standing for French for "Photons Utilisés pour les Matériaux Anciens", a hard X-ray imaging beamline at SOLEIL synchrotron, optimized for the scientific communities of the heritage sciences. It is equipped with a 2D imaging end-station which offers a spatial resolution of a few microns with elemental (XRF), chemical (XANES) and structural (XANES and XRD) contrast.

Here we present some of the studies performed at PUMA since its opening to the expert user community in 2019 on different kind of cultural heritage materials. In particular, analyses performed on three set of samples, namely decorated ceramics [1-2], painted architectural terracottas [3] and natural stones treated with conservation products [4] are considered.

With these results we aim at highlighting the potential offered by this beamline in characterizing different kind of archaeological and historical materials, discussing possible research outcomes and new challenges in cultural heritage studies.

REFERENCES

1. A. Gianoncelli et al., *Microchemical Journal* **154**, 104629 (2020)
2. A. Gianoncelli et al., *Applied Sciences* **11** - 17, 8052 (2021).
3. G.V.M. Spagnolo, *Quaderni dell'istituto di archeologia della Facoltà di Lettere e Filosofia dell'Università di Messina* **6**, 55, (1991).
4. S. Raneri et al., *Materials Characterization* **56**, 109853 (2019).

Chemical Imaging at PUMA, SOLEIL, of Samples of Polychrome Cave Art from Font-de-Gaume Cave to Validate In-situ Results

J. Tapia¹, A. Trousseau¹, L. Tranchant², S. Schoeder²,
K. Muller², I. Reiche¹

¹*Institut de recherche de Chimie Paris, UMR 8247 CNRS Chimie Paristech,
11, Rue Pierre et Marie Curie, 75005 Paris, France*

²*IPANEMA, L'Orme des Merisiers, 91190 Saint-Aubin, France*

ABSTRACT

The polychrome decoration of the Font-de-Gaume Paleolithic cave, based on iron and manganese oxides, was characterized non-invasively and in situ by portable X-ray fluorescence (Figure 1). Micro-fluorescence and X-ray absorption imaging at the Mn and Fe K-edges at the synchrotron were also performed on calcite samples with some pigment that had been taken from the wall during a restoration campaign in the 1960s.



Here are compared the results obtained during different in situ campaigns in the cave and the analyses on the samples at the PUMA line, SOLEIL in order to be able to evaluate the validity of these analyses and to discuss their contributions and limits. The aims of study are, on the one hand, trying to improve the Palaeolithic pigments' characterization with respect to the in situ analyses in a cave that could be undertaken with a portable instrument and, on the other hand, finding differentiation criteria between the composition of the walls and the pigments that could help us to improve the performances of in situ analyses.

REFERENCES

1. Trousseau, A. et al 2021, *J. Anal. At. Spectrom.*, 36, 2449-2459.
2. Gay, M. et al 2015, *J. Anal. At. Spectrom.*, 767-776.
3. Chalmin, E. and Reiche, I. 2013. Synchrotron X-ray microanalysis and imaging of synthetic biological calcium carbonate in comparison to archaeological samples coming from the Large cave of Arcy-sur-Cure (28000-24500 BP, Yonne, France), *Microscopy and Microanalysis* 19, 1-1.
4. Reiche, I., Chalmin, E. 2014. Synchrotron methods: Color in paints and minerals, chapter 14.15 in: *Treatise on Geochemistry*, vol. 14 « Archaeology and Anthropology », Elsevier, 2nd Ed., ed. Thure Cerling, 210-239

Synchrotron X-ray Spectro-imaging Clarifies the Anatomy and Taphonomy of Amphibians from the Montceau-les-Mines Lagerstätte

P. Gueriau¹, A. Logghe², L. Tranchant^{3,1}, S. Schöder³,
S. Sanchez⁴ et J-S. Steyer²

¹Muséum national d'Histoire naturelle, Institut photonique d'analyse non-destructive européen des matériaux anciens (IPANEMA), Université Paris-Saclay/CNRS/ministère de la Culture/UVSQ/MNHN, 91190 Saint-Aubin, France

²Muséum national d'Histoire naturelle, Centre de Recherche en Paléontologie – Paris (CR2P), CNRS/MNHN/Sorbonne Université, 75231 Paris, France

³Synchrotron SOLEIL, 91190 Saint-Aubin, France

⁴Uppsala University, Subdepartment of Evolution and Development, Department of Organismal Biology, Evolutionary Biology Centre, Uppsala, Sweden

ABSTRACT

Just like the hammer, the magnifying glass and more recently X-ray tomography, X-ray fluorescence (XRF) elemental mapping has become an important tool for paleontologists. XRF mapping can be performed under the SEM (so-called “EDX” or “EDS” mapping), using benchtop instruments or at synchrotron facilities. It provides both morphological information in revealing hidden anatomies, and unexpectedly detailed paleobiological, paleoenvironmental, palaeoecological and taphonomic information through the characterization of the organic and inorganic compositions of the fossils [1–9]. In this contribution we applied synchrotron-based XRF mapping to two branchiosaurid amphibians from the Upper Carboniferous Montceau-les-Mines Lagerstätte (see [10] for a general review of the biota and its taphonomy; and [11] for a review of the amphibians). The distribution of arsenic unveils large remains of external cutaneous tissues, offering new insights into the ecology of these organisms. The distribution of yttrium, which substitutes for calcium in bone apatite [6], reveals previously indiscernible skeletal features, particularly of the skull, allowing for more detailed anatomical descriptions. Surprisingly, it also uncovers the presence of a halo enriched in yttrium around the carcasses, restricted to the main body outline but not encompassing the head and the tip of the limbs and tail. We further investigated the origin of this halo using X-ray absorption spectroscopy (XAS) and mapping (see-XAS [12]), and propose an updated taphonomic scenario for the formation of concretions at the Montceau-les-Mines Lagerstätte, with implications for other concretion-bearing deposits.

REFERENCES

1. U. Bergmann, P. L. Manning and R. A. Wogelius, *Annu. Rev. Anal. Chem.* **5**, 361-389 (2012).
2. A. Brayard, P. Gueriau, M. Thoury, G. Escarguel and the Paris Biota team, *Geobios* **54**, 71-79 (2019).
3. D. Davesne, P. Gueriau, D. B. Dutheil and L. Bertrand, *Sci. Rep.* **8**, 8509 (2018).
4. P. Gueriau et al., *PLoS One* **9**, e86946 (2014).
5. P. Gueriau, S. Bernard and L. Bertrand, *Elements* **12**, 45-50 (2016).
6. P. Gueriau, C. Jauvion and C. Mocuta, *Palaeontology* **61**, 981-990 (2018).
7. P. Gueriau et al., *Geology* **48**, 1164-1168 (2020).
8. P. Gueriau et al., *R. Soc. Open Sci.* **7**, 201037 (2020).
9. C. Jauvion et al., *Palaeontology* **63**, 395-413 (2020).
10. V. Perrier and C. Charbonnier, *C. R. Palevol* **13**, 353-367 (2014).
11. R. Werneburg, *Semana* **34**, 11-51 (2019).
12. S. X. Cohen, S. M. Webb, P. Gueriau, P., E. Curis and L. Bertrand, *J. Synchrotron Radiat.* **27**, 1049-1058 (2020).

Structural Studies of Antibody Antigen Complexes

F. Rey

Institut Pasteur, Paris, France

ABSTRACT

In this presentation, I will summarize our structural biology studies combining X-ray crystallography and cryo-electron microscopy to understand the epitopes targeted by neutralizing antibodies directed against pathogenic viruses. I will show examples of results with dengue and Zika virus, with hantaviruses and with SARS-CoV-2. The results provide insight into the mechanism of neutralization in each case and suggest ways to prepare next-generation immunogens for epitope-focused vaccine design.

Why Do We See Amyloid- β Plaques in Phase-contrast Imaging?

M. Chourrout¹, C. Sandt², T. Weitkamp², D. Meyronet³, T. Baron⁴,
J. Klohs⁵, N. Rama⁶, H. Boutin⁷, M. Wiart⁸, S. Bohic⁹,
E. Brun⁹ and F. Chauveau¹

¹ Lyon Neuroscience Research Center (CRNL), Neurocampus, CH Vinatier, 69500 Bron, France

² SOLEIL synchrotron, L'Orme des Merisiers, D128, 91190 Saint-Aubin, France

³ Hospices Civils de Lyon, 3 Quai des Célestins, 69002 Lyon, France

⁴ ANSES – Lyon laboratory, 31 avenue Tony Garnier, 69364 Lyon Cedex 7, France

⁵ ETH Zurich, OCT, Binzmuehlestrasse 130, 8092 Zurich, Switzerland

⁶ Cancer Research Center of Lyon (CRCL), 28 Rue Laennec, 69008 Lyon, France

⁷ The University of Manchester, Oxford Road, Manchester, M13 9PL, United Kingdom

⁸ CarMeN Laboratory, CENS ELI, 165 Chemin du Grand Revoyet, 69310 Pierre Bénite, France

⁹ STROBE, 71 avenue des martyrs, 38000 Grenoble, France

ABSTRACT

Synchrotron X-ray phase-contrast tomography (XPCT) is well-suited for the virtual histology of amyloid seeding and spreading in Alzheimer's Disease (AD): one can explore the whole brain in 3D with a native rendering of anatomical structures and the technique easily detects amyloid- β (A β) plaques in label-free samples [1–4]. However, different transgenic rodent strains give rise to different XPCT contrasts of A β plaques (hyper- or hypointense), which are still unexplained. Here we explored 2 hypotheses: it could be due to variations of amyloid fibrillation and/or of metal concentrations.

XPCT plus Fourier-Transform Infrared (FTIR) and X-Ray Fluorescence (XRF) spectroscopies were conducted at SOLEIL synchrotron on human samples (genetic AD vs. sporadic AD patients) and transgenic rodent models (APPPS1, ArcA β , J20, TgF344; cf. alzforum.org/research-models). Each sample was cut into halves which underwent specific preparations. For FTIR and XRF, cryosections were deposited on SiRN membranes and plaques were stained with p-FTAA [9]; for XPCT, the whole tissue was fixed in FA. Subsequent analyses were performed to extract the composition of A β plaques:

- Segmentation and morphological description of A β plaques from XPCT 3D images;
- Quantification of amyloid fibrillation via analysis of β -sheet contribution in the Amide I band of FTIR spectra (β -induced over α -induced absorptions);
- Quantification of metals (Fe, Cu, Zn) via peak-fitting of their signatures in XRF spectra.

A β plaques from the genetic AD patient were successfully detected in XPCT, while those from the sporadic AD patient were not revealed. This could be explained by the increased fibril and metal levels we measured in the genetic AD case compared to the sporadic AD case (Fe: +109%, Zn: +97%, Cu: +88%; β/α : +55%).

To investigate further, we also studied transgenic rodents. Plaques from J20 mice and TgF344 rats appeared bright; plaques from APPPS1 and ArcA β mice had a dark rim with a slightly brighter core. Amyloid fibrillation was relatively similar between the 3 strains (APPPS1: 0.65 ± 0.12 (mean \pm SD); ArcA β : 0.62 ± 0.09 ; J20: 0.68 ± 0.13 , TgF344: 0.73 ± 0.08); while the higher fibrillation level was specific to A β inclusions, this measurement could not reliably explain the differences between the rodent models. On the other hand, bright-plaque strains had higher levels of metals: J20 had more zinc (5.11 ± 3.76 ppm) and iron (4.32 ± 3.57 ppm)

bound in A β than APPPS1 (Zn: 1.63 \pm 0.75 ppm, Fe: 1.88 \pm 1.02 ppm) and ArcA β (Zn: 3.05 \pm 2.32 ppm, Fe: 3.41 \pm 2.15 ppm); TgF344 had more copper (3.94 \pm 3.67 ppm) than all other strains (APPPS1: 0.47 \pm 0.19 ppm, ArcA β : 0.84 \pm 0.55 ppm, J20: 1.00 \pm 0.77 ppm). This could explain why A β plaques from J20 and TgF344 were hyperintense.

Contrast formation in XPCT images can be explained by higher concentrations of metals in the A β plaques from rodents and from the genetic AD patient; the sporadic AD patient had rather diffuse plaques which could not be detected in XPCT images [6]. Additional factors, other than the overall β -sheet content, are likely to contribute to the XPCT contrast and remain to be identified.

REFERENCES

1. Massimi, L., Pieroni, N., et al. 2020, 'Assessment of plaque morphology in Alzheimer's mouse cerebellum using three-dimensional X-ray phase-based virtual histology', *Scientific Reports*, 10 (1), 11233.
2. Töpperwien, M., van der Meer, F., et al. 2020, 'Correlative x-ray phase-contrast tomography and histology of human brain tissue affected by Alzheimer's disease', *NeuroImage*, 210 116523.
3. Noda-Saita, K., Yoneyama, A., et al. 2006, 'Quantitative analysis of amyloid plaques in a mouse model of Alzheimer's disease by phase-contrast X-ray computed tomography', *Neuroscience*, 138 (4), 1205–1213.
4. Chourrout, M., Roux, M., et al. 2021, 'Brain virtual histology with X-ray phase-contrast tomography, Part II: 3D morphologies of amyloid- β plaques in Alzheimer's disease models', *Biomedical Optics Express*.
5. Åslund, A., Sigurdson, C.J., et al. 2009, 'Novel Pentameric Thiophene Derivatives for in Vitro and in Vivo Optical Imaging of a Plethora of Protein Aggregates in Cerebral Amyloidoses', *ACS Chemical Biology*, 4 (8), 673–684.
6. Chourrout M., Sandt C., et al. 2022, 'Virtual histology of Alzheimer's Disease: why are amyloid- β plaques visible with X-ray phase-contrast imaging?', *BioRxiv*, 2022.09.27.509706, <https://doi.org/10.1101/2022.09.27.509706>

Synchrotron Based X-ray Microtomography Reveals Cellular Morphological Features of Developing Wheat Grain

D. Legland^{1,2}, C. Alvarado¹, E. Badel³, F. Guillon¹, A. King⁴, T.D.Q. Le^{1,2}, C. Rivard^{4,5}, L. Paré^{1,2}, A-L. Chateigner-Boutin¹, C. Girousse⁶

¹ INRAE, UR BIA, 44316 Nantes, France

² INRAE, PROBE Research Infrastructure, BIBS Facility, 44316 Nantes, France

³ Université Clermont Auvergne, INRAE, PIAF, 63000 Clermont-Ferrand, France

⁴ Synchrotron SOLEIL, L'Orme des Merisiers, Saint-Aubin, 91192 Gif-sur-Yvette, France

⁵ INRAE, TRANSFORM, 44316 Nantes, France

⁶ INRAE, Université Clermont-Auvergne, UMR GDEC, 63000 Clermont-Ferrand, France

ABSTRACT

Wheat is one of the most important crops in the world, mainly used for human consumption and animal feed. To overcome the increasing demand in production, it becomes necessary to better understand the mechanisms involved in the growth of the wheat grain.

X-ray micro-tomography has proven to be useful for the anatomical study of plant organs^{1,2,3}. We investigated the potential of phase-contrast micro-tomography provided by the Psiché beamline to study the changes of anatomy of the wheat grain during its development⁴. A first setup provided 3D images of entire grains at various development stages. Resolution and contrast were greatly improved compared to laboratory tomography, allowing to identify a large number of tissues, and to visualize individual cells. The development of specific image processing workflows allowed the semi-automated identification of different regions within the grain and the quantification of changes of tissue morphology from large 3D images. A second setup with higher resolution resulted in finer details, making it possible to identify additional tissues and cells. In particular, it was possible to visualize the 3D architecture of thin cellular layers located within dense tissues. Three-dimensional rendering of the grain also revealed a spatio-temporal heterogeneity and diversity in cell shape and orientations, in particular outer layers.

X-ray phase-contrast tomography thus appears as a promising imaging method for the study of 3D-anatomy of growing plant organs and tissues, and for deciphering the mechanisms involved in the final shape and size of the wheat grain.

REFERENCES

1. Stuppy, W. H.; Maisano, J. A.; Colbert, M. W.; Rudall, P. J. & Rowe, T. B. *Trends in Plant Science*, **8**, 2-6 (2003).
2. Cloetens, P.; Mache, R.; Schlenker, M. & Lerbs-Mache, S. *Proceedings of the National Academy of Sciences*, **103**, 14626-14630 (2006).
3. Le, T. D. Q.; Alvarado, C.; Girousse, C.; Legland, D. & Chateigner-Boutin, A.-L. *Plant Methods*, **15**, 84 (2019).
4. Legland, D., Alvarado, C., Badel, E., Guillon, F., King, A., Le, T.D.Q., Rivard, C., Paré, L., Chateigner-Boutin, A.L., Girousse, C. *Applied Sciences* **12**(7), 3454 (2022).

Multimetal Methyltransferase Making Methanogenesis

C.D. Fyfe

Université Paris-Saclay, INRAE, AgroParisTech, Micalis Institute, ChemSyBio

ABSTRACT

B12-dependent radical SAM enzymes are one of the largest groups of radical SAM enzymes with more than 200,000 members¹. This family of metalloenzymes are unique in their ability to form carbon-carbon bonds between unactivated sp³-hybridized carbons. Using biochemical and biophysical techniques including X-ray crystallography and electron paramagnetic resonance we have investigated methanogenesis marker protein 10 (Mmp10). Mmp10 has been shown to perform a post-translational methylation of an arginine within the active site of methyl-coenzyme M reductase². This is one of many post-translational modifications that are profoundly important for the methane production by microbes using methyl-coenzyme-M-reductase³. Our crystallographic snapshots of Mmp10 reveal unique features including four distinct metal centres and a tyrosine that can coordinate the radical SAM clusters fourth iron allowing it to switch between radical and nucleophilic chemistry(Figure 1.). The various snapshots we obtain have shown not only how this enzyme binds it protein substrate but also how it can utilise SAM in multiple ways to methylate its substrate⁴.

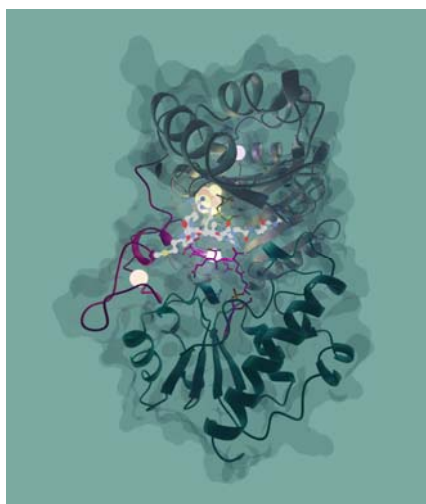


Figure 1. Mmp10 with its four metal centres and peptide substrate bound.

REFERENCES

- Holliday GL, Akiva E, Meng EC, Brown SD, Calhoun S, Pieper U, Sali A, Booker SJ, Babbitt PC. *Methods Enzymol.* 2018;606:1-71. doi: 10.1016/bs.mie.2018.06.004. Epub 2018 Jul 24. PMID: 30097089; PMCID: PMC6445391.
- Radle MI, Miller DV, Laremore TN, Booker SJ. *J Biol Chem.* 2019 Aug 2;294(31):11712-11725. doi: 10.1074/jbc.RA119.007609. Epub 2019 May 20. PMID: 31113866; PMCID: PMC6682749.
- Gunsalus R. P., and Wolfe R. S. (1978) Chromophoric factors F342 and F430 of Methanobacterium thermoautotrophicum. *FEMS Microbiol. Lett.* 3, 191–193 10.1111/j.1574-6968.1978.tb01916.x
- Fyfe CD, Bernardo-García N, Fradale L, Grimaldi S, Guillot A, Brewee C, Chavas LMG, Legrand P, Benjdia A*, Berteau O.* - 2022 - Crystallographic snapshots of a B12-dependent radical SAM methyltransferase. *Nature (7896)*:336-342.

PARALLEL SESSION

New Materials

(Structure / Electronic Properties / Surfaces & Interfaces)

*SOLEIL - Main Building
Libra, Phénix, PyXIS & Colomba Rooms*

Thursday, January 19th

Chairpersons:

E. Frantzeskakis, A. Bordage, D. Pierucci, F. Cheynis

- IT-07 From multiferroicity to superconductivity : 1D Fe spin ladder under pressure
V. Balédent
- OC-19 Operando XAS investigation of bimetallic iron–molybdenum sulfide electrocatalysts for the hydrogen evolution reaction in proton exchange membrane electrolyzers
A. Khan
- OC-20 UV and X-ray stability of CsPbBr₃ perovskite nanocrystals
A. Ali
- OC-21 The effect of side chain structure on self-organization properties and the electronic structure of low band gap polymers
D. Batchelor
- IT-08 Multi-beam lines investigation of HgTe nanocrystals electronic structure
E. Lhuillier
- OC-22 In situ XPS Synchrotron study of solid-liquid interphase in lithium-ion batteries
F.G. Capone
- OC-23 Resonant Auger spectroscopy on adsorbed xenon on gold, silver and copper substrates
F.O.L. Johansson
- OC-24 Self-assembled monolayers of functionalised spin crossover complexes
P. Rosa

PARALLEL SESSION

New Materials

(Structure / Electronic Properties / Surfaces & Interfaces)

*SOLEIL - Main Building
Libra, Phénix, PyXIS & Colomba Rooms*

Friday, January 20th

Chairpersons:

E. Frantzeskakis, A. Bordage, D. Pierucci, F. Cheynis

- IT-09 Fundamental mechanisms of stress-build-up during thin film formation:
Multimethod real-time Synchrotron experiments
B. Krause
- OC-25 Probing the chemical and electronic structure of BaTiO₃ ultrathin films using
X-ray spectroscopy
S. Gonzalez
- OC-26 Carbon-based defects in pristine α boron
Y. Cho
- OC-27 Band structure and Rashba effect of ferroelectric α -GeTe as function of the
thickness
A. Llopez

From Multiferroicity to Superconductivity: 1D Fe Spin Ladder under Pressure

V. Balédent, W. Zheng, A. Roll, P. Foury

Université Paris-Saclay, CNRS, Laboratoire de Physique des Solides, 91405, Orsay cedex, France

ABSTRACT

Mn-based compounds have long been the main source of magnetoelectric systems with improper ferroelectricity. Indeed, their multiple stable valences, as well as their high magnetic moment for 3d ions allow to produce Type II multiferroicity, where ferroelectricity is induced by magnetic ordering. The families RMnO_3 and RMn_2O_5 (R being a rare earth) are the archetypes of these materials, presenting a large magnetoelectric coupling. However, these properties are limited to low temperature, generally below 50 K [1]. The research of such properties has thus turned to iron-based compounds. This interest is motivated by the fact that iron presents the same advantages as Mn (large magnetic moment and multiple valences), with generally higher magnetic order temperatures due to stronger magnetic exchange interactions, above 100 K [2]. In this context we studied the quasi-1D Fe spin ladder BaFe_2Se_3 . We will demonstrate here the necessity to combine multiple synchrotron based techniques, as well as neutron scattering and laboratory experiments to reveal the complexity and richness of the pressure-temperature phase diagram of BaFe_2Se_3 . At ambient pressure, the system is polar at room temperature and the structure evolves under the magnetic transition at 250K to become multiferroic [3,4]. The associated magnetic structure shows a strong frustration originating from competing magnetic interactions and anisotropy [5,6]. Above 4 GPa a new magnetic phase is revealed, concomitant with a structural transition [7], with no change in the local electronic structure and minute change of the local magnetic moment. The metallicity shows a two steps increase, the first one at 4 GPa, and another one at higher pressure, saturating before the appearance of superconductivity. Both results shed a new light on the possible pairing mechanism responsible for the superconducting phase.

REFERENCES

- [1] S. Chattopadhyay, V. Balédent et al. *Physical Review B* 93, 104406 (2016)
- [2] S. M. Disseler et al. *Phys. Rev. Lett.* 114, 217602 (2015)
- [3] W. Zheng, V. Balédent et al. *Rapid Com. Physical Review B* 101, 020101(R) (2020)
- [4] M. J. Weseloh, V. Balédent et al. *Journal of Physics : Condensed Matter* 34, 255402 (2022)
- [5] W. G. Zheng, V. Balédent et al. *Nature Communication Physics* (2022)
- [6] A. Roll, V. Balédent et al. in preparation (2022)
- [7] A. Roll, V. Balédent et al. in preparation (2022)

Operando XAS Investigation of Bimetallic Iron–molybdenum Sulfide Electrocatalysts for the Hydrogen Evolution Reaction in Proton Exchange Membrane Electrolyzers

A. Khan¹, A. Morozan², V. Artero², A. Zitolo¹

¹Synchrotron SOLEIL, L'orme des Merisiers, BP 48 Saint Aubin, 91192 Gif-sur-Yvette, France

²Laboratoire de Chimie et Biologie des Métaux, Univ. Grenoble Alpes, CNRS, CEA/IRIG, 38054, Grenoble, France

anastassiya.khan@synchrotron-soleil.fr

ABSTRACT

Nowadays green hydrogen production has been seen as a key element for the future development and large-scale implementation of fuel cell technology. Proton exchange membrane electrolyzers (PEMEL) represent the most advanced electrolysis technology for producing pure hydrogen from water. The preparation of efficient, cost-effective, and stable noble-metal-free electrocatalysts for the hydrogen evolution reaction (HER) at the cathode of PEMEL remains one of the main issues that need to be solved to allow the widespread use of hydrogen as an energy carrier. The comprehensive characterization of the structure-electrocatalytic activity relationships can significantly contribute to the understanding of the origin of the enhanced catalytic activity and provide some important insights for further improvements.

Molybdenum sulfide (MoS_x) is a well-studied material showing promising HER catalytic activity, especially in its amorphous state and when doped with other transition metals¹. The successful implementation of a bimetallic iron-molybdenum sulfide electrocatalyst for HER into a PEM electrolyzer has been recently reported². However, the structure of their active sites requires a more elaborate investigation. In this study, we employed *operando* X-ray absorption spectroscopy to identify potential-induced structural and electronic changes in FeMoS_{mw} bimetallic iron–molybdenum sulfides and MoS_{mw} obtained by a microwave irradiation synthetic approach². Extended X-ray absorption fine structure (EXAFS) spectra at Mo and Fe K-edge under *operando* conditions provided us with accurate structural characterization of the catalytic active sites: while an amorphous MoS_3 phase is detected and retained in both MoS_{mw} and FeMoS_{mw} at low potential, a FeS phase is observed at Fe K-edge, likely explaining the better performance of the bimetallic iron-molybdenum sulfides electrocatalysts compared to molybdenum sulfides.

REFERENCES

1. Ren, X.; Wang, W.; Ge, R.; Hao, S.; Qu, F.; Du, G.; Asiri, A. M.; Wei, Q.; Chen, L.; Sun, X. An amorphous FeMoS_4 nanorod array toward efficient hydrogen evolution electrocatalysis under neutral conditions. *Chem. Commun.* 2017, 53, 9000–9003.
2. Morozan, A.; Johnson, H.; Roiron, C.; Genay, G.; Aldakov, D.; Ghedjatti, A.; Nguyen, C.; Tran P.; Kinge, S.; Artero, V. (2020). Nonprecious Bimetallic Iron–Molybdenum Sulfide Electrocatalysts for the Hydrogen Evolution Reaction in Proton Exchange Membrane Electrolyzers. *ACS Catalysis*. 10. 10.1021/acscatal.0c03692.

UV and X-ray Stability of CsPbBr₃ Perovskite Nanocrystals

A. Ali^a, F.O.L. Johansson^{a,b}, M. Ahmad^c, H. Cruguel^a,
E. Giangrisostomi^d, R. Ovsyannikov^d, L. Dudy^e, M.G.Silly^e,
M. Madsen^c, E. Lhuillier^a, N. Witkowski^{a*}

^a Sorbonne Université, CNRS, Institut des NanoSciences de Paris, INSP, F-75005, Paris, France.

^b Division of Applied Physical Chemistry, Department of Chemistry, KTH – Royal Institute of Technology, SE-100 44 Stockholm, Sweden.

^c SDU NanoSYD, Mads Clausen Institute, University of Southern Denmark, Sønderborg DK-6400, Denmark.

^d Institute for Methods and Instrumentation in Synchrotron Radiation Research, PS-ISRR, Helmholtz-Zentrum Berlin für Materialien und Energie GmbH, Albert-Einstein-Strasse 15, 12489 Berlin, Germany.

^e Synchrotron SOLEIL, 91192 Gif-sur-Yvette, France.

ABSTRACT

Understanding of electronic band structure and charge carrier dynamics of halide perovskites and their interface is critical for the advancement of perovskite photovoltaics[1,2]. Inorganic Cesium lead bromide (CsPbBr₃) perovskite nanocrystals (NCs) with a bandgap of 2.3 eV are regarded as one of the potential candidates as an active layer in solar cells devices, thanks to significant progress made recently in terms of improving its intrinsic properties and stability under environmental conditions. However, stability under UV and X-ray exposure remains an open question[3-6]. The stability of spin-coated CsPbBr₃ NCs deposited on gold (Au) substrates is investigated here under the impact of the UV laser light and X-rays. Under the UV laser pulse, the NCs exhibit distinctly different behavior depending upon the energy of the laser pulse, its fluence and time NCs exposed to it. When the NCs are exposed to UV laser pulses with the photon energy of 3.6 eV (greater than the bandgap), the NCs are modified irreversibly. Both metallic lead (Pb⁰) and ionic lead (Pb⁺²) with a new component of Pb^{4f} are detected in the Pb^{4f} core-level spectra. Similarly, when NCs exposed exclusively to X-ray with high flux, same components of Pb^{4f} were found in Pb^{4f} spectrum. The modification is more or less similar in either case; however, under UV laser exposure, a large chemical shift of 0.69 eV towards higher binding energy observed after the exposure, which is not the case with X-ray exposure alone. The chemical shift could be attributed to the accumulation of charge carriers at the interface under UV laser and getting trapped by the (Pb⁰) donor type surface states[6]. Therefore, depending on the type of radiation exposure either UV laser or X-rays, the CsPbBr₃ NCs show different behavior and thus the energy level alignments. We show that the chemical properties of NCs are sensitive to both UV laser and X-rays irradiation, and investigation of these changes under the type of radiation exposure might help us understand the underlying phenomenon that governs these changes.

REFERENCES

- [1] Zu, Fengshuo, et al. ACS applied materials & interfaces 9.47 (2017): 41546-41552.
- [2] Amelot, Dylan, et al. The Journal of Physical Chemistry C 124.6 (2020): 3873-3880.
- [3] Zhang, Yi, et al. Advanced Energy Materials 9.22 (2019): 1900243.
- [4] Akkerman, Quinten A., et al. Nature Energy 2.2 (2016): 1-7.
- [5] Zu, Fengshuo, et al. Solar RRL (2022): 2101065.
- [6] Zu, Feng-Shuo, et al. Advanced Optical Materials 5.9 (2017): 1700139.

The Effect of Side Chain Structure on Self-organization Properties and the Electronic Structure of Low Band Gap Polymers

S. Bölke^a, D. Batchelor^b, A. Früh^a, B. Lassalle-Kaiser^d, T. Keller^c,
F. Trilling^c, M. Forster^c, U. Scherf^c, T. Chassé^a, H. Peisert^a

^a *Institut für Physikalische und Theoretische Chemie, Eberhard Karls Universität Tübingen, Auf der Morgenstelle 18, 72076 Tübingen, Germany*

^b *Karlsruher Institut für Technologie, Institute for Photon Science and Synchrotron Radiation (IPS), Hermann-von-Helmholtz-Platz 1, D-76344 Eggenstein-Leopoldshafen, Germany*

^c *Makromolekulare Chemie (buwMakro) und Wuppertal Center for Smart Materials and Systems (CM@S), Bergische Universität Wuppertal, Gausstrasse 20, 42119 Wuppertal, Germany*

^d *Synchrotron SOLEIL, L'Orme des Merisiers, Départementale 128, 91190 Saint-Aubin*

ABSTRACT

The properties of low band gap (LBG) polymers thin films and their interfaces are strongly dependent on the growth and morphology and also the ability for self-organisation in the film. This has important ramifications for solar cell device development. We have studied the effect of the position of alkoxy and alkyl side chains in four conjugated, alternating oligothiophene-benzothiadiazole copolymers using X-ray absorption spectroscopy (XAS Sulphur K-Edge, Fluorescence-FY and Total electron yield-TEY), photoelectron spectroscopy (UPS, XPS), and polarization modulation-infrared reflection-adsorption spectroscopy (PMIRRAS). Growth of the films is also studied on different substrates and varying the annealing temperature. The Interface Charge Transfer (ICT) model is applied to explain the interface properties on the substrates with their different work functions. We find that the position of the side chains strongly affects the self-organisation properties of the polymers and hence the orientation in the films and to a lesser extent the electronic structure. Annealing leads to improved orientation and ordering of the films. The surface and bulk structure is also discussed using the different surface sensitivity of the methods.

Multi-beam Lines Investigation of HgTe Nanocrystals Electronic Structure

E. Lhuillier^a, Y. Prado^a, M. Silly^b, F. Capitani^b,
J. Avila^b, B. Baptiste^c, S. Klotz^c, D. Pierucci^a,

^a Sorbonne Université, CNRS, Institut des NanoSciences de Paris,
INSP, F-75005 Paris, France.

^b Synchrotron-SOLEIL, Saint-Aubin, BP48, F91192 Gif sur Yvette Cedex, France.

^c Sorbonne Université, CNRS, Institut de Minéralogie, de Physique des Matériaux et de Cosmochimie, IMPMC, F-75005 Paris, France.

* email : el@insp.upmc.fr

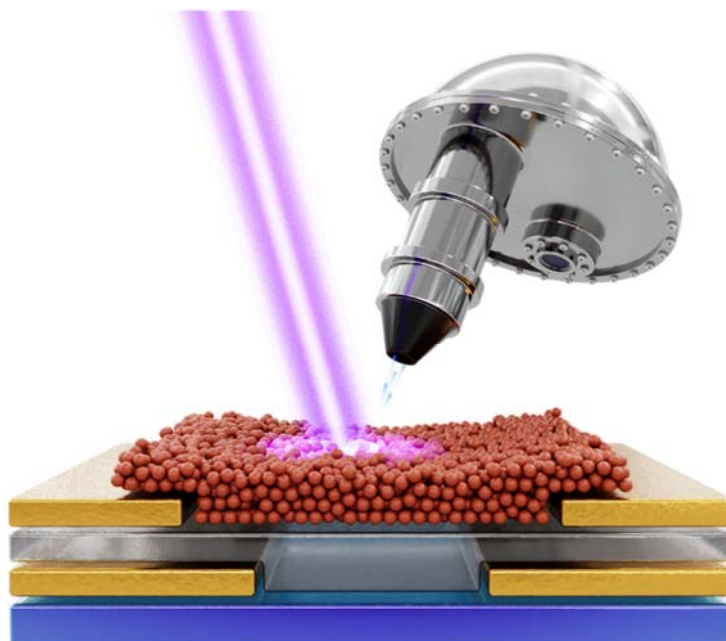
ABSTRACT

Nanocrystals are semiconductor nanoparticles. Through quantum confinement their optical spectra can easily be tuned from UV to the THz. To address the infrared spectral range, materials with bulk narrow band gap are suitable. In this framework, bulk semimetal such as HgTe are of utmost interest. Over the past decade, large progresses have been obtained regarding the device integration of such material. This includes field-effect transistor, photodiode, light emitting diode and camera [1].

However, the limited knowledge of their electronic structure certainly slows the rational optimization of these devices. Bulk HgTe already presents a peculiar band structure being an inverted semimetal. On top of that, comes the quantum confinement and a strong dependence of the doping with the surface chemistry. This is why for the last few years we initiate a systematic investigation of the material electronic structure in which infrared and photoemission beamline of soleil have been central instruments.

On Smis beamline, we have initiated a systematic investigation of HgTe quantum electronic phase diagram as a function of the temperature, pressure and quantum confinement [2-3]. We demonstrate that HgTe experiences two phases structural (and associated electronic) changes from zinc-blende to cinnabar and to rocksalt in the 0 to 10 GPa range. The phase changes are observed at higher threshold pressure compared to the bulk meaning that the nano aspect further stabilizes the low pressure phase. This result highlights that core-shell growth may be grown without the risk of inducing phase change.

We then use photoemission (on Tempo) to unveil the material band alignment and doping of this material as a function of quantum confinement and surface chemistry. Beyond the investigation of the active material, time resolved photoemission emission can be used to unveil the coupling between layer in device such as LED [4-6]. Finally, I will say a few words about our most recent results relative to the *in situ* mapping of the energy landscape that has been obtained using the nanobeam of Antares.



REFERENCES

- [1] *Mercury chalcogenide quantum dots: Material perspective for device integration*, C Gréboval et al, *Chemical Reviews* 121, 3627 (2021)
- [2] *Vanishing Confinement Regime in Terahertz HgTe Nanocrystals Studied under Extreme Conditions of Temperature and Pressure*, S Pierini et al, *J. Phys. Chem. Lett.* 13, 6919 (2022)
- [3] *The strong confinement regime in HgTe two-dimensional nanoplatelets*, N Moghaddam et al, *J. Phys. Chem. C* 124, 23460 (2020)
- [4] *Electroluminescence from Nanocrystals above 2 μm* , J Qu et al, *Nature Photonics* 16, 38 (2022)
- [5] *Extended Short-Wave Photodiode Based on CdSe/HgTe/Ag₂Te Stack with High Internal Efficiency*, P Rastogi et al, *J. Phys. Chem. C* 126, 13720 (2022)
- [6] *Time-resolved photoemission to unveil electronic coupling between absorbing and transport layers in a quantum dot-based solar cell*, C Gréboval et al, *J. Phys. Chem. C* 124, 23400 (2020)

In situ XPS Synchrotron Study of Solid-liquid Interphase in Lithium-ion Batteries

F.G. Capone^{1,2}, J-P. Rueff², A. Grimaud³

1. PHENIX, Sorbonne Université, CNRS UMR 8234, 75252, Paris, France
2. SOLEIL Synchrotron, F91192 Gif sur Yvette Cedex, Saint-Aubin BP48, France
3. Réseau sur le Stockage Electrochimique de l'Energie (RS2E), CNRS FR 3459, 33 rue Saint Leu, Amiens Cedex 80039, France

ABSTRACT

Lithium-ion batteries (LIBs) represent one of the pillars of the energy transition demanded by the climate changes [1]. While the choice of the materials used as positive and negative electrodes determines the power energy, the voltage window is defined by the thermodynamic stability of the employed organic electrolytes. When pushing the batteries outside the stability window of the electrolyte, the electrolyte can be decomposed, and a few Å-thin and chemically inhomogeneous layer called solid-electrolyte interphase is formed on the positive (CEI) and negative (SEI) electrodes. While the SEI is responsible of the initial irreversible capacity lost during the firsts cycles, its electronic insulating character prevents from the short-circuit of the battery and further degradation of the electrolyte upon cycling. It is therefore clear why the understanding of the formation and stability of the SEI is of pivotal importance for improving safety [2], lifespan and power density [3] of the next battery generation. Thanks to its high chemical sensitivity, XPS is the suitable tool to study the heterogeneous and mosaic-like SEI, providing accurate information about its chemical composition. On the other hand, XPS requires UHV environment, and it is extremely surface sensitive, thus ex situ electrodes are heavily manipulated before the XPS analysis to remove the salt excess, inducing significant changes in the SEI [4]. My PhD research project consists in the development of two approaches enabling in situ XPS analysis of the SEI [5], in the framework of the European Battery Interfaces Genome – Materials Accelerations Platform (BIG-MAP). First, the solid-liquid interphase is probed through the liquid phase [IA(CI)] of the electrolyte using a “dip & pull” setup combined with Near Ambient Pressure Photo-electron Spectroscopy (NAP-PES) setup. We have applied this approach recently at HIPPIE beamline of Sweden Synchrotron Max-IV, where we have investigated the interphase formed on a glassy carbon electrode cycled against metallic lithium as a function of applied voltage. Moreover, we have proposed to study the formation and stability of the interphase through the solid phase with Hard X-Rays PES (HAXPES). Therefore, a tailored liquid cell have been designed and developed to fit the UHV analysis chamber at GALAXIES beamline (SOLEIL) and to reproduce realistic electrochemical properties. While the cell development is still in progress, the first tests showed the feasibility of the experiment and guided us to the last steps needed to obtain reproducible and trustable results. These two approaches represent a first step towards obtaining crucial information regarding the SEI growth and stability and then to move forward in the characterization and optimization of lithium-ion batteries.

REFERENCES

1. Gröger, O., et al., (2015). Journal of The Electrochemical Society, 162(14), A2605.
2. Gauthier, M., et al., (2015). The journal of physical chemistry letters, 6(22), 4653-4672.
3. Peled, E., et al. (1995). MRS Online Proceedings Library Archive, 393.
4. Edström, K., et al. (2006). Journal of Power Sources, 153(2), 380-384.
5. Atkins, D., et al (2021) Advanced Energy Materials, 2102687.

Resonant Auger Spectroscopy on Adsorbed Xenon on Gold, Silver and Copper Substrates

F.O.L. Johansson^{1,2,3}, E. Berggren¹, L.M. Cornetta¹, D. Céolin⁴,
M. Fondell⁵, H. Ågren¹ and A. Lindblad¹

¹*Division of X-ray Photon Science, Department of Physics and Astronomy,
Uppsala University, Box 516, SE-751 20 Uppsala, Sweden*

²*Division of Applied Physical Chemistry, Department of Chemistry,
KTH Royal Institute of Technology, SE-100 44 Stockholm, Sweden*

³*Sorbonne Université, CNRS, Institut des NanoSciences de Paris, INSP, F-75005, Paris, France*

⁴*Synchrotron SOLEIL, l'Orme des Merisiers, Saint-Aubin,
Boîte Postale 48, 91192 Gif-sur-Yvette Cedex, France*

⁵*Institute Methods and Instrumentation for Synchrotron Radiation Research PS-ISRR,
Helmholtz-Zentrum Berlin für Materialien und Energie,
Albert-Einstein-Straße 15, 12489, Berlin, Germany*

ABSTRACT

An investigation of the radiationless decay of core excited Xe atoms (Xe $2p_{3/2} \rightarrow nd$ ($n \geq 5$) absorption) in the region of Xe $L_3M_{4,5}M_{4,5}$ Auger electron kinetic energies, has been performed at the GALAXIES beamline for Xe adsorbed on Cu, Ag and Au metals. By doing so we differentiate between contributions from coherent and incoherent decay channels of the core excited state that build up the X-ray absorption cross section [1].

The intensity distribution of the decay channels is different compared with Xe in the gas-phase [2,3] with no post-collision interaction shifts in the incoherent decay channel for the condensed system is observed within the energy range recorded. Charge transfer of the core excited electron occurs within tens of attoseconds in all studied systems for excitation energies approaching the ionization threshold of the condensed system, whereas charge transfer times are substrate dependent for lower excitation energies with distinct difference for Au compared with Ag and Cu, which show similar dynamics.

The determination of partial yields in the decay channels allows for observation of a decay channel present in the Xe/Cu and Xe/Ag systems but not in the case of Xe/Au. This extra decay channel is seen on the high kinetic energy side of the incoherent Auger line. Theoretical calculations allow us to interpret this channel as emanating from varying amount of ground state hybridization between Xe and the substrates. This impacts the energy of the Auger final states enabling an identification of these states as system specific features in the experimental data.

REFERENCES

1. N. Mårtensson, M. Weinelt, O. Karis, M. Magnuson, N. Wassdahl, A. Nilsson, J. Stöhr, and M. Samant, Applied Physics A: Materials Science & Processing 65 (1997)
2. R. K. Kushawaha, K. Jänkälä, T. Marchenko, G. Goldsztejn, R. Guillemin, L. Journal, D. Céolin, J. P. Rueff, A. F. Lago, R. Püttner, M. N. Piancastelli, and M. Simon, Physical Review A, 92, 013427 (2015)
3. G. B. Armen, S. H. Southworth, J. C. Levin, U. Arp, T. LeBrun, and M. A. MacDonald Physical Review A, 56, 2, (1997)

Self-assembled Monolayers of Functionalised Spin Crossover Complexes

P. Rosa¹, R. Rodrigues de Miranda¹, M. Penicaud¹, E. Bryan²,
N. Giacconi³, M. Gonidec¹, S. Heutz, M. Mannini³, L. Poggini⁴, E. Otero⁵

¹ Univ. Bordeaux, CNRS, Bordeaux-INP, ICMCB, UMR 5026, 87 avenue du Dr. A. Schweitzer
F-33600 Pessac, France

² Department of Materials, London Centre for Nanotechnology, Imperial College London,
South Kensington Campus, UK-SW7 2AZ London, United Kingdom

³ LaMM, Università degli Studi di Firenze, Dipartimento di Chimica 'Ugo Schiff',
Via della Lastruccia 13, I-50019 Sesto Fiorentino (FI), Italy

⁴ ICCOM, Via Madonna del Piano 10, I-50019 Sesto Fiorentino (FI), Italy

⁵ DEIMOS beamline, SOLEIL synchrotron light source, L'Orme des Merisiers,
F-91190 Saint-Aubin, France

ABSTRACT

Spin crossover complexes (SCOs) are transition metal complexes that exhibit reversible state switching at ambient conditions, making them promising candidates for molecular electronics and spintronics, for example in memory devices.¹ In iron (II) complexes, switching occurs between a diamagnetic low spin state (S=0) and a paramagnetic high spin state (S=2), and is photo- or thermally-induced. The switching is accompanied by a change in the electronic and magnetic properties, such that molecular junctions of these SCOs exhibit a change in conductance depending on the spin state.

A major advantage of SCO thin-film devices over conventional 2D materials is that the organic ligands can be tailored to add any number of desired properties, such as photoactivity² or the ability to self-assemble on a surface.³ However, the structural and electronic complexity of these molecules mean it can be hard to predict the exact conditions where switching will occur. One of our goals is to control the spin state switching of iron (II) SCCs on surfaces. We aim to perform this tuning in two ways: by functionalising the organic ligands,⁴ or by changing the 'spinterface' between the molecules and substrate. The latter can be done by varying the substrate material, for instance by using a ferroelectric substrate that can be electrically polarised.⁵

We started synthesizing a library of functionalised iron (II) SCOs and characterizing it, in bulk by standard physical-chemical techniques, and as (sub)monolayer films by microscopy, PM-IRRAS and X-ray absorption, in order to increase our understanding of the SCO phenomenon at the nanoscale and the subtleties of the spinterface, with the end goal of bringing SCOs closer to technological applications in molecule-based electronics and spintronics.

REFERENCES

¹ J.-F. Létard, P. Guionneau, L. Goux-Capes, *Top. Curr. Chem.* **235**, 221 (2004).

² L. Poggini, M. Milek, G. Londi, A. Naim, G. Poneti, L. Squillantini, A. Magnani, F. Totti, P. Rosa, M. M. Khusniyarov, M. Mannini *Mater. Horiz.* **5**, 506 (2018).

³ K. S. Kumar, M. Studniarek, B. Heinrich, J. Arabski, G. Schmerber, M. Bowen, S. Boukari, E. Beaurepaire, J. Dreiser, M. Ruben *Adv. Mater.* **30**, 1705416 (2018).

⁴ S. Ossinger, L. Kippen, H. Naggert, M. Bernien, A. J. Britton, F. Nickel, L. M. Arruda, I. Kumberg, T. A. Engesser, E. Golias, C. Näther, F. Tuczek, W. Kuch *J. Phys. Condens. Matter* **32**, 11400 (2019).

⁵ X. Zhang, T. Palamarciuc, J.-F. Létard, P. Rosa, E. V. Lozada, F. Torres, L. G. Rosa, B. Doudin, P. A. Dowben *Chem. Commun.* **50**, 2255 (2014).

Fundamental Mechanisms of Stress-build-up during Thin Film Formation: Multimethod Real-time Synchrotron Experiments

B. Krause

*Institut für Photonenforschung und Synchrotronstrahlung (IPS), Karlsruher Institut für Technologie,
Eggenstein-Leopoldshafen 76344, Germany*

ABSTRACT

Since the early days of thin film growth, the stress build-up during deposition has been one of the most important driving forces for fundamental research and industrial development. Residual stresses affect the lifetime of coatings, sensors, or electronic devices – via obvious degradation (crack formation, delamination) or subtle changes of the performance parameters (e.g. shift of photoemission lines, resistance changes...). At the same time, stresses are powerful tools allowing for control of nanostructure formation, optoelectronic properties, and even offering a simple way to monitor growth processes.

In contrast to epitaxial systems, where the stress evolution is often dominated by interface-related stresses, polycrystalline systems reveal a complex stress evolution, resulting from superposed, reversible and irreversible stress contributions related to the interface formation and microstructure evolution during deposition. The scientific community has accepted this challenge, and developed elaborate models reproducing the experimentally observed stress evolution. The validity of these models, however, is difficult to confirm experimentally.

We will show that the combination of optical stress measurements and surface-sensitive real-time synchrotron methods can overcome this problem. We have established a portfolio of simultaneous grazing incidence x-ray methods (diffraction, small-angle scattering, reflectivity) to correlate the instantaneous stress changes, recorded by optical curvature measurements, with specific aspects of microstructure formation occurring during sputter deposition of thin films. This includes, e.g., the evolution of morphology, crystal structure, phase formation, grain size, and texture. We will demonstrate the strength of this approach, presenting recent results obtained at the SixS beamline of the synchrotron SOLEIL. Based on the study of several metal/semiconductor and metal/oxide systems, we will give insight into the current understanding of the stress evolution during sputter deposition of nanoscale layers.

Probing the Chemical and Electronic Structure of BaTiO₃ Ultrathin Films using X-ray Spectroscopy

S. Gonzalez^{a*}, M. Bugnet^c, P. Schöffmann^d, E. Otero^d,
P. Rojo-Romeo^b, B. Vilquin^b, B. Gautier^a, G. Herrera^e,
O. Boisron^e, P. Ohresser^d, V. Dupuis^e, I.C. Infante^a

a. Univ. Lyon, INSA Lyon, CNRS, ECL, UCBL, CPE Lyon, Institut des Nanotechnologies de Lyon, UMR5270, 69621 Villeurbanne, France

b. Univ. Lyon, ECL, CNRS, CPE Lyon, Institut des Nanotechnologies de Lyon, UMR5270, France

c. Univ. Lyon, CNRS, INSA Lyon, UCBL, MATEIS, UMR 5510, 69621 Villeurbanne, France

d. Synchrotron SOLEIL, CNRS-CEA, L'Orme des Merisiers, Saint-Aubin, 91192, France

e. Univ. Lyon, Université Claude Bernard Lyon 1, Institut Lumière Matière, CNRS UMR 5306, France

ABSTRACT

Nano ferroelectricity has promising technological applications as energy-saving, low-sized electronic devices. Tunnel junctions and transistors using ferroelectric gates are examples of potential applications [1]. BaTiO₃ (BTO) is a lead-free ferroelectric showing fascinating properties when connected to an electrode, in particular a “positive dead-layer” [2] or interface ionic relaxation [3], making BTO a promising candidate for integration in multifunctional structures with ultimate nanoscale dimensions. For this purpose, the physical and chemical properties of interfaces and ultrathin layers based on BTO have to be understood and means to control their properties must be sought out. In this work, we propose to study ultrathin BTO films grown by industrially scalable magnetron sputtering on conductive Nb-doped SrTiO₃ substrates and on structurally compatible conductive layers of SrRuO₃, to explore the electronic structure and chemical reconstruction within the films and at the different interfaces.

The average structure and strain of BTO films from 1 to 16 nm were investigated using X-ray diffraction. A thorough spectroscopic analysis of the films was carried out to study the relationship between strain and materials and processing parameters. Combining synchrotron X-ray absorption spectroscopy in capacitors and laboratory X-ray photoelectron spectroscopy, we probed the electronic structure under the influence of different UHV annealing conditions, studied the promotion of electronic and ionic defects, e.g. oxygen vacancies. Structural and polarization states of differently strained BTO films were analyzed through X-ray natural linear dichroism at the Ti-L_{2,3} edges. Multiplet calculations were made, supporting the experimental evidence of the contribution of the strain to the polarization of the films. Finally scanning transmission electron microscopy and electron energy loss electron spectroscopy provided the atomic scale fingerprint of the electronic structure through the films and at the interfaces.

These results are crucial to understand and master the underlying physical mechanisms leading to the ferroelectric properties of operating BTO-based devices.

This work is supported by collaborative VOLCONANO ANR-19-CE09-0023 project.

REFERENCES

1. S Scott, J.F. Science 315, 954 -959 (2007)
2. A Stengel, M., Vanderbilt, D. & Spaldin, N.A. Nature Materials 8, 392-397 (2009)
3. Gerra G., Tagantsev A. K., and Setter N., Physical Review Letters 98, 207601 (2007)

Carbon-based Defects in Pristine α Boron

Y. Cho¹, A. Chakraborti^{1,2,3}, J. Sjakste¹, Y. Le Godec², N. Vast¹

¹ *Laboratoire des Solides Irradiés, Ecole Polytechnique, CEA/DRF/IRAMIS, CNRS, Institut Polytechnique de Paris, Palaiseau, France*

² *Institut de Minéralogie, de Physique des Matériaux et de Cosmochimie (IMPMC), Sorbonne Université, CNRS, Muséum National d'Histoire Naturelle, IRD, Paris, France*

³ *Currently at Bayerisches Geoinstitut, Universität Bayreuth, Bayreuth D95440, Germany*

ABSTRACT

During the high pressure and high temperature (HPHT) synthesis of boron carbide using β -rhombohedral boron and amorphous carbon, red α -boron was formed at some P, T values [1, 2]. In other experiments, α boron turns out to show a variety of colors, and depending on the size of the crystals and experimental conditions, the resulting color was reported to be red [2-7], black [3,5,7], or even yellowish [6]. Our experimental works suggest that the presence of carbon atoms plays a key role in the formation of red α -boron. In our theoretical work, carbon atoms were tentatively inserted into elemental α boron to investigate a possible thermodynamic process that forms the red α -boron. The physical properties of defective supercells have been computed within the density functional theory (DFT) [2]. The formation energy reveals some low-energy defects that do not show drastic changes in properties such as lattice parameters and band gap. The consequences on the optical properties will be discussed from the theoretical viewpoint.

REFERENCES

- [1] A. Chakraborti, N. Guignot, N. Vast, Y. Le Godec, J. Phys. Chem. Solids. 159, 110253 (2021).
- [2] A. Chakraborti, Y. Cho, J. Sjakste, B. Baptiste, L. Henry, N. Guignot, Y. Le Godec, N. Vast, Forcing the stability of alpha boron at high pressure and high temperature with carbon, to be submitted (2022).
- [3] F. H. Horn, J. Appl. Phys. 30, 1611 (1959).
- [4] L. V. McCarty, J. S. Kasper, F. H. Horn, B. F. Decker, A. E. Newkirk, J. Am. Chem. Soc. 80, 2592 (1958).
- [5] B. F. Decker and J. S. Kasper, Acta Cryst. 12, 503 (1959).
- [6] G. Parakhonskiy, N. Dubrovinskaia, L. Dubrovinsky, S. Mondal, S. van Smaalen, Journal of Crystal Growth 321, 162-166 (2011).
- [7] K. C. Buschbeck. Gmelin Handbook of Inorganic Chemistry (Springer-Verlag, Berlin), 13, Suppl. 2 (1982).

Band Structure and Rashba Effect of Ferroelectric α -GeTe as Function of the Thickness

A. Llopez¹, B. Croes¹, F. Leroy¹, S. Curiotto¹, P. Müller¹,
Y. Fagot-Revurat², B. Kierren², B. Tegomo-Chiogo²,
C. Tagne-Kaegom², F. Cheynis¹

¹ CINaM, Aix Marseille Université & CNRS, Marseille, France

² IJL, Université de Lorraine & CNRS, Nancy, France

ABSTRACT

Ferroelectric Rashba semiconductors (FERSC) displaying large spin-orbit coupling and switchable electric polarization stand out as versatile platforms for the realization of low-power all-electrically controlled spintronics devices. Remarkably, it has been predicted in 2013 [1] and experimentally confirmed in 2018 [2,3] that the spin texture in GeTe induced by the Rashba effect can be controlled by the reversal under an electric field of its ferroelectric polarization. To be integrated into microelectronic devices both ferroelectric polarization and Rashba effect with a large Rashba parameter αR are required and need to be controlled when the material is reduced to only several nanometers in thickness.

We have measured the bands structure of GeTe samples of different thicknesses are measured by ARPES (figure.1) and Rashba parameter αR are measured by taking count of the maxima of Rashba bands. A clear change in of GeTe bands structure is observed below 5nm thickness and contrary to the previous study [4] we measured and increase in the Rashba parameter below 5nm thickness (figure.2)

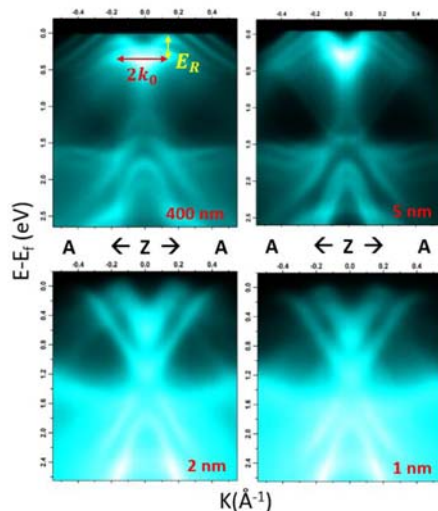


Figure 2 : Bands structure of 400 , 5 , 2 and 1nm thickness GeTe samples measured by ARPES.

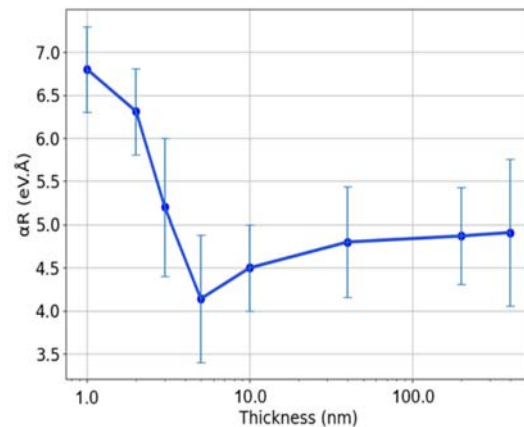


Figure 1 : Rashba parameter αR of GeTe as a function of the thickness.

REFERENCES

- [1] D. Di Sante et al., Adv. Mater. 25 (2013) 509–513
- [2] C. Rinaldi et al., Nano Lett. 18 (2018) 2751–2758
- [3] J. Krempaský et al., Phys. Rev. X 8 (2018) 021067
- [4] X. Yang et al., Nano Lett. (2021), 21, 77–83

POSTERS SESSION

List of Student Posters

- PO-DR-01** Study of the electronic structure of iron metal complexes in aqueous solution by X-ray photoemission spectroscopy
N.H. Azzouza
- PO-DR-02** Application of photoelectron spectroscopy to study electronic ligand effects on iron cyclopentadienone complexes
L. Bourehil
- PO-DR-03** First investigation of non-radiative relaxation process of solvated urea (CH₄N₂O) using photoelectron spectroscopy
M. Fournier
- PO-DR-04** Differential evolution driven algorithm transform demodulated signal from modulation excitation experiments back to time domain
L. Jiang
- PO-DR-05** Understanding the dissociation of doubly-ionized water in liquid water
A. Rajpal
- PO-DR-06** Ultradispersed MoS_x catalysts: Evolution of active species and effect of the support
D. Ryaboshapka
- PO-DR-07** NAP-XPS on alkali halide aqueous solution surfaces interfaces: Radiolysis issues
H. Tissot
- PO-DR-08** In vivo speciation and molecular mechanisms of the uptake of uranium by *ascophyllum nodosum*
M. Zerbini
- PO-LS-09** Use of metals in microplastics to track microplastics during digestion
N. Belkessa
- PO-LS-10** Brain virtual histology with X-ray phase-contrast tomography
M. Chourrout
- PO-LS-11** Investigation of magnetite/cobalt interactions at nanoscale
L. Fablet
- PO-LS-12** X-ray microtomography of non-small cell lung cancer tumours (NSCLC) treated with cold atmospheric plasma
K. Géraud
- PO-LS-13** Unmasking the otolith using Synchrotron-based scanning X-ray fluorescence
V. Haÿ
- PO-LS-14** Impact of the polymer degradation on the metallic additives distribution in microplastics
I. Khatib
- PO-LS-15** Mouse arterial wall analysis from Synchrotron micro-CT imaging
X. Liang

- PO-NM-16** Surface chemistry engineering of mercury telluride nanocrystals for infrared LEDs
E. Bossavit
- PO-NM-17** The impact of substitutions in goethite on rare earth element adsorption
A. Buist
- PO-NM-18** Exploring the application of inelastic X-ray scattering for novel spectral imaging and spectroscopy of contemporary art materials
L. Dalecky
- PO-NM-19** Investigation of the crystal electric field in rare-earth titanate pyrochlores by resonant inelastic x-ray scattering
O. Duros
- PO-NM-20** ARPES investigations of the topological states in TaTe₄ and NbTe₄
P. Gonçalves
- PO-NM-21** Investigation of the structure evolution of thermal treated imogolite nanotubes
Y. Pan
- PO-NM-22** Influence of the crystal structure and nature of the ligands on the valence of uranium in binary chalcogenides: a HERFD-XANES and RIXS study
T. Stephant

Study of the Electronic Structure of Iron Metal Complexes in Aqueous Solution by X-ray Photoemission Spectroscopy

N.H. Azzouza^{1,2}, D. Céolin², L. Journal¹

¹ Sorbonne Université, CNRS, UMR 7614, Laboratoire de Chimie Physique-Matière et Rayonnement, 4 Place Jussieu, F-75005 Paris, France

² Synchrotron SOLEIL, L'Orme des Merisiers, Saint-Aubin, F-91192 Gif-sur-Yvette Cedex, France

ABSTRACT

Metal complexes are essential for many biological systems. This is for instance the case for iron complexes which act as redox centers in metalloproteins such as hemoglobin. Their properties depend on their chemical environment, i.e., the interaction of the center with the ligands, and of the complex with the solvent. A detailed description of their electronic structure allows a better understanding of the processes in which they are involved [1]. Numerous studies [2-4] have focused on the electronic structure of iron complexes. Nevertheless, to our knowledge, there are very few experimental x-ray photoemission spectroscopy (XPS) results for these systems diluted in aqueous solution. XPS spectroscopy is a very powerful tool to probe the interaction of a metal center with its ligands and the solvent.

We present the XPS spectra of potassium hexacyanoferrate (II) $K_4[Fe(CN)_6]$ and potassium hexacyanoferrate (III) $K_3[Fe(CN)_6]$ complexes in aqueous solution. These two complexes have the same octahedral geometry and differ only in their charge state $2+/3+$ respectively. The measurements were performed at the GALAXIES beamline of SOLEIL [5] using a liquid micro-jet adapted to the high energy photoemission spectrometer (HAXPES) [6]. The spectra were measured at the iron K, L and M thresholds and at the carbon and nitrogen K threshold. All of them show notable differences and a dependence of the electronic structure of these complexes on their charge state. For example, we observed a strong intensity variation of the satellite structures in the N1s and to a less extend C1s photoelectron spectra. Moreover, the Fe^{3+} 2p spectrum exhibit a low kinetic energy shoulder, whereas it is absent in the Fe^{2+} 2p one. More results will be shown in the poster.

REFERENCES

1. R. Golnak et al., Scientific Reports, 2016, 6, 24659.
2. R.K. Hocking, E.C. Wasinger, F.M.F. de Groot, K.O. Hodgson, B. Hedman, E.I. Solomon, J. Am. Chem. Soc. 2006, 128, 32, 10442–10451.
3. T. Yamashita, P. Hayes, Applied Surface Science, 2008, Vol 254, Issue 8, 2441-2449.
4. A. Cano, J. Rodríguez-Hernández, L. Reguera, E. Rodríguez-Castellón, E. Reguera, Eur. J. Inorg. Chem., 2019, 1724.
5. J.P. Rueff, J.M. Ablett, D. Ceolin, D. Prieur, T. Moreno, V. Balédent, B. Lassalle-Kaiser, J.E. Rault, M. Simon, A. Shukla, Journal of Synchrotron Radiation., 2015, 22(1), 175-179.
6. D.Céolin, J.M. Ablett, D.Prieur, T.Moreno, J.P Rueff, T. Marchenko, L.Journal, R. Guillemin, B. Pilette, T. Marin, M. Simon, Journal of Electron Spectroscopy and Related Phenomena., 2013, 190 part B: 188–192.

Application of Photoelectron Spectroscopy to Study Electronic Ligand Effects on Iron Cyclopentadienone Complexes

L. Bourehil^{1,2}, D. Lesage¹, L. Bettoni³, N. Joly³, J-L. Renaud³,
Y. Gimbert^{1,4}, G. Garcia², H. Dossmann¹

1 Sorbonne Université, CNRS, Institut Parisien de Chimie Moléculaire, IPCM, F-75005 Paris, France

2 Synchrotron SOLEIL, L'Orme des Merisiers, St Aubin, BP 48, 91192 Gif-sur-Yvette Cedex, France

3 Université Normandie, LCMT, ENSICAEN, UNICAEN, CNRS, F-14050 Caen, France

4 Université Grenoble Alpes, CNRS, DCM, F-38000 Grenoble, France.

ABSTRACT

Organometallic chemistry is a key process in homogenous catalysis and gives access to a wide range of products and reactions. Through their steric and electronic effects, ligands are able to orientate the reactivity of the complexes and can thus influence the selectivity in the chemical transformations. Usually, the metal-ligand bond is depicted by the Dewar-Chatt-Duncanson model^{1,2} involving two opposite interactions, a σ -donor and a π -acceptor effect. Over the years, many experimental methods have been developed to measure these electronic effects, the most common being that of Tolman (Tolman electronic parameter), which is limited to organometallic complexes possessing probe ligands such as CO and based on the A1-symmetrical CO-stretching frequency shift.³

We have recently developed the use of new experimental gas-phase approaches to measure these effects, one based on photoelectron spectroscopy (PES) coupled to synchrotron radiation, and the other on mass spectrometry using activation by higher energy collision dissociation (HCD). Under the first method, the satisfying results obtained on model systems⁴ have encouraged us to apply this method to catalysts developed for hydrogenation reactions,⁵ and to probe the electronic interaction between the ligand and the metal centre. Results obtained for tricarbonyl iron complexes of the $(\text{Fe}(\text{CO})_3\text{L})$ type, with L being substituted cyclopentadiene ligands, are presented here. The photoelectron spectra provide access to the ionization energies and state-selected Fe-CO dissociation energies.

REFERENCES

1. E. C. Constable, John Wiley & Sons 1996, 22-45.
2. A. Zecchina, S. Califano, John Wiley & Sons 2017, 59-90.
3. C.A. Tolman, Chemical Reviews 1977, 77, 313-348.
4. H. Dossmann, et al. Journal of Physical Chemistry A 2020, 124, 8753-8765.
5. L. Bettoni, et al. Chemical Communications 2020, 56, 12909-12912.

First Investigation of Non-radiative Relaxation Process of Solvated Urea ($\text{CH}_4\text{N}_2\text{O}$) using Photoelectron Spectroscopy

M. Fournier^{1,2}, L. Huart^{2,3,4}, C. Nicolas², J-P. Renault³,
M-A. Hervé Du Penhoat⁴, F. Penent¹, I. Ismail¹, L. Journel¹,
B. Lutet-Toti¹, A. Kumar² and J. Palaudoux¹

¹LCPMR, Sorbonne-Université – UPMC, UMR CNRS 7614, Paris, France

²Synchrotron SOLEIL, Saint-Aubin, France

³NIMBE UMR CEA-CNRS 3685, Saclay, France,

⁴IMPMC, Sorbonne-Université – UPMC, UMR CNRS 7590, Paris, France

ABSTRACT

The comprehension of mechanisms involved in biological damage induced by ionizing radiation at the femto-pico second scale is still incomplete in soft X-ray regime. In addition to radicals, electrons emitted after a core-ionization can also be responsible of damages. Indeed, they can be seen as secondary particles that will deposit their energies in nanometric volumes¹. This raises the question of knowing the origin of these electrons and their kinetic energies distribution.

More generally, when an atom (or a molecule) is exposed to X-ray, a photoelectric effect occurs. Following a core-shell ionization, this atom (or molecule) can relax through different non radiative processes. In this study, we will focus on one specific relaxation process: the Auger decay. Disentangle the different Auger processes, involved after a photoionization of a biomolecule in solution, is still challenging due to the complexity of its environment. Coincidence spectroscopy between photoelectrons and Auger electrons is an interesting method to filter the events coming from the solvent from those coming from the biomolecule. For this purpose, a magnetic bottle time-of-light spectrometer has been designed by our scientific group and coupled to the PLEIADES micro-jet source. First encouraging results, as a proof of concept was obtained with sodium benzoate molecules²⁻⁴.

Therefore, we have extended our studies to urea ($\text{CH}_4\text{N}_2\text{O}$), which is one of the smallest system available with a biological interest. The three core-ionization thresholds accessible (C 1s, N 1s and O 1s) were probed. In order to assure a comprehensive study of our molecule, we also used a classical X-ray electron spectroscopy to focus on the photoelectrons and the valence electrons emitted.

REFERENCES

1. L. Huart, *J. Phys. Chem. A*, 124, 10, 1896–1902 (2020)
2. M. Fournier et al, *EPJ Web Conf.* 273, 01009 (2022)
3. L. Huart et al, *Physical Chemistry Chemical Physics*, on line first, (2023)
4. L. Huart, Thesis, (2022)

Differential Evolution Driven Algorithm Transform Demodulated Signal from Modulation Excitation Experiments Back to Time Domain

L. Jiang¹, S. Cristol¹, A. Tougeri¹, V. Briois², A. Beauvois²

¹ Univ. Lille, CNRS, Centrale Lille, ENSCL, Univ. Artois, UMR 8181 – UCCS – Unité de Catalyse et Chimie du Solide, Lille F-59000, France

² Synchrotron SOLEIL, UR1-CNRS L'Orme des Merisiers, Saint-Aubin, BP 48, Gif-sur-Yvette Cedex 91192, France

ABSTRACT

Modulation excitation spectroscopy (MES) coupled with Phase Sensitive detection (PSD) is a suitable technique to trace the dynamic behavior of active sites for heterogeneous catalyst. [1] MES technique consists sending periodic perturbation to catalytical system and recording system's response, during which only the active species' concentration profile would be affected, and spectator species signal along with noise could be canceled out later by off-line mathematical treatment PSD, which is expressed as following: $A_{exp}(E, \varphi PSD) = 2T \int_0^T G(E, t) \cdot \sin(\omega t + \varphi PSD) dt$ eq.1

Where recorded data is transformed from regular spectra (time domain) $G(E, t)$ to demodulated spectra (phase domain) $A_{exp}(E, \varphi PSD)$ and φ the external perturbation frequency. Processing demodulated signal is actually bottleneck of MES-PSD approach with changed spectra shape, making quantitative interpretation difficult. Transforming demodulated signal back to time domain is a possible way to solve this problem, thus, an algorithm driven by differential evolution [2] has been developed in this work to achieve this process and isolate pure spectra with their kinetics. The principle is to reconstruct experimental demodulated spectra $A_{exp}(E, \varphi PSD)$ by following equation adapted from eq.1: $A_{model}(E, \varphi PSD) = 2T \int_0^T \sum_i [C_i \cdot \sin(\omega t + \varphi_i) + h_i] \cdot S_i(E) \sin(\omega t + \varphi PSD) dt$ eq.2

This algorithm has been applied to a data-set of Modulation Excitation X-ray Absorption Spectroscopy (ME-XAS) experiments achieved for iron molybdate catalyst (Mo/Fe=2.2) [3] during selective oxidation of methanol to formaldehyde. The pure regular spectra of interest are isolated with success by our algorithm.

REFERENCES

- [1]: Müller P, Hermans I. Applications of modulation excitation spectroscopy in heterogeneous catalysis[J]. Industrial & Engineering Chemistry Research, 2017, 56(5): 1123
 [2]: Qin A K, Huang V L, Suganthan P N. Differential evolution algorithm with strategy adaptation for global numerical optimization[J]. IEEE transactions on Evolutionary Computation, 2008, 13(2): 398
 [3]: Soares A P V, Portela M F, Kiennemann A. Methanol selective oxidation to formaldehyde over iron-molybdate catalysts[J]. Catalysis Reviews, 2005, 47(1): 125

Understanding the Dissociation of Doubly-ionized Water in Liquid Water

A. Rajpal^{a,b,c}, L. Huart^{a,b,c}, C. Nicolas^c, C. Chevallard^a, P. Mercere^c,
M-F. Politis^d, J-M. Guigner^b, M-A. Hervé du Penhoat^b, J-P. Renault^a

^a Université Paris-Saclay, CEA, CNRS, NIMBE, Gif-sur-Yvette 91191, France

^b IMPMC, Sorbonne Université, UMR CNRS 7590, MNHN, Paris 75005, France

^c Synchrotron SOLEIL, Saint Aubin 91190, France

^d LAMBE UMR 8587, Université d'Evry val d'Essonne, CNRS, CEA, Université Paris-Saclay, Evry 91025, France

ABSTRACT

Water radiolysis is a widely studied phenomenon, resulting in the formation of reactive oxygen species (ROS) in ionization tracks. These ROS can result in lethal or sub-lethal damage. The *superoxide radical* (HO_2) is one such ROS, generated in heavy-ion tracks due to multiple ionization^{1,2}. Another pathway of its production is the reaction of electrons with molecular oxygen.³ However, since this species is biologically toxic, due to its ability to act as a reductant or as an oxidant that might cause major indirect damages, it becomes crucial to investigate it. We, therefore, study the formation of this species following water molecules' K-shell ionizations, using theoretical and experimental techniques.

Experimentally, we utilize soft X-rays (100-1800eV), as they offer an advantage of dominant core-shell ionization. But, owing to their poor penetration in liquid, there is a scarcity of experimental knowledge in this energy range. Hence, we expose the sample in a microfluidic cell to synchrotron soft X-rays.⁴ The absorption of photons in liquid water, above the O K edge, results in a doubly ionized water molecule produced after an Auger relaxation process, surrounded by singly ionized water molecules originating from the photo- and Auger electrons tracks. Thereafter, the dissociation of the ionized water molecules and intra-track reactions may result in the generation of the HO_2 species, via the reaction $\text{O} + \text{OH} \rightarrow \text{HO}_2$. Superoxide radicals reduce the probe (Water-soluble tetrazole salt, WST8) present in the sample, giving a characteristic signal in the UV, which corresponds to WST8 formazan. The addition of superoxide dismutase (SOD), scavenges the HO_2 species leading to a lowering in reduction hence confirming that HO_2 is one of the causes of this reduction. Performing these experiments in oxic and anoxic conditions, with and without SOD, can help give a better understanding of the various HO_2 formation pathways. *Theoretically*, we simulate the dynamics of a doubly ionized water molecule and a hydroxyl radical in liquid water using Time-Dependent Density Functional Theory and Car Parrinello Molecular Dynamics approaches. The results obtained give an understanding of the production of this species (HO_2), in addition to the formation of H_2O_2 .

REFERENCES

- (1) Gervais, B.; Beuve, M.; Olivera, G. H.; Galassi, M. E.; Rivarola, R. D, *Chem. Phys. Lett.* **2005**, 410 (4–6), 330–334.
- (2) Gervais, B.; Beuve, M.; Olivera, G. H.; Galassi, M. E, *Phys. Chem.* **2006**, 75 (4), 493–513.
- (3) Hayyan, M.; Hashim, M. A.; AlNashef, I. M, *Chem. Rev.* **2016**, 116 (5), 3029–3085.
- (4) Huart, L.; Nicolas, C.; Hervé du Penhoat, M.-A.; Guigner, J.-M.; Gosse, C.; Palaudoux, J.; Lefrançois, S.; Mercere, P.; Dasilva, P.; Renault, J.-P.; Chevallard, C., *J. Synchrotron Radiat.* **2021**, 28 (3), 778–789.

Ultradispersed MoS_x Catalysts: Evolution of Active Species and Effect of the Support

D. Ryaboshapka¹, L. Piccolo¹, C. Geantet¹, P. Bargiela¹,
M. Aouine¹, P. Afanasiev¹, V. Briois²

¹Univ. Claude Bernard Lyon 1, CNRS, UMR5256, IRCELYON, F-69626, Villeurbanne, France

²SOLEIL synchrotron, UR1-CNRS, L'Orme des Merisiers, BP48, 91192 Gif-sur-Yvette, France

ABSTRACT

In the field of hydrodesulfurization (HDS) catalysis, lamellar MoS₂ is the most studied system. Active sites are located at the edges/corners of MoS₂ slabs. Recently along with slabs, clusters of several atoms and single atoms (SAs) of Mo were observed by STEM in sulfide catalysts (1,2) and proven to have high HDS activity (3). However, the structure and evolution of such species during catalyst activation and under reaction conditions are still unknown.

In this work, we have prepared sulfide Mo catalysts containing mostly MoS_x clusters and SAs and studied their activity in HDS and the effect of the support on the formation of these species. Five catalysts were synthesized: MoS_x supported on activated carbon (AC), graphene, silica (KIT-6), TiO₂ and Al₂O₃ with 1 wt.% Mo. Conventional characterizations (TEM, UV-vis DRS) and STEM-ADF confirmed the absence of MoS₂ slabs. For all samples, the specific HDS activity per Mo atom was higher than that of a 10%MoS₂/Al₂O₃ reference (Fig. 1a). The structure and evolution of the Mo species during sulfidation and HDS reaction were studied by means of operando QXAS at the ROCK beamline of SOLEIL synchrotron.

As determined from MCR-ALS analysis of QXAS spectra, the evolution during sulfidation of the initial oxidic Mo oligomers proceeds via an oxysulfidic state, then MoS₃-like species, and finally MoS_x species are formed. On all the supports, the coordination number (CN) of Mo is equal to or lower than 1 (Fig. 1b), and much lower than for 10%MoS₂/Al₂O₃ (CN = 2.3). The lowest Mo CNs were obtained on TiO₂, AC and graphene. The mechanisms of ultradispersion stabilization seem different: carbons provide a large enough surface area to distribute the Mo precursor, while TiO₂ binds it strongly, allowing to obtain highly dispersed MoS_x clusters and SAs.

In conclusion, for the first time, we demonstrated that MoS_x clusters supported on carbons and oxides are active in HDS in the absence of MoS₂ slabs. The support greatly influences the nature of the species: silica and alumina favor the formation of larger and less active clusters, while more active sulfidic oligomers are obtained on carbons and titania

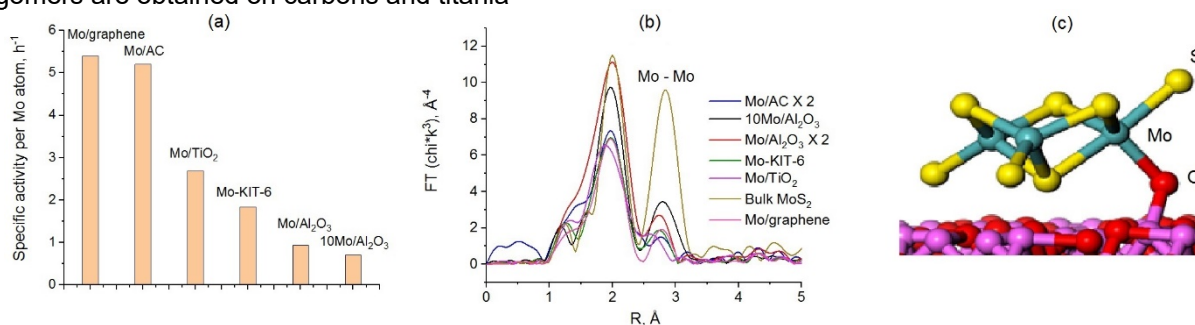


Figure 1: (a) Specific HDS activities per atom of Mo for the sulfided samples, (b) EXAFS spectra of the sulfidic Mo species in ultradispersed samples and reference, (c) possible model of MoS_x cluster on the surface of Al₂O₃.

REFERENCES

- 1 L. Zavala-Sanchez et al., *Catal. Today* **377**, 127-134 (2021).
- 2 M. Girleanu et al., *Microporous Mesoporous Mater.* **217** 190-195 (2015).
- 3 D. Ryaboshapka et al., *App. Catal. B Environ.* **302** 120831 (2022).

NAP-XPS on Alkali Halide Aqueous Solution Surfaces Interfaces: Radiolysis Issues

H. Tissot¹, R. Coustel², C. Carteret², A. Boucly,³ J.-J. Gallet³,
F. Bournel³, F. Rochet³

1. UCCS, Unité de Catalyse et Chimie du Solide, UMR 8181, F-59000 Lille, France

2. Laboratoire de Chimie Physique et Microbiologie pour les Matériaux et l'Environnement
54600 Villers-lès-Nancy, France

3. Laboratoire de Chimie Physique matière et Rayonnement, UMR 7614, France

ABSTRACT

We used Near Ambient Pressure X-ray Photoemission Spectroscopy (NAP-XPS) to follow in situ and in real time the chemistry of concentrated sodium halide solutions, NaCl, NaBr and NaI under irradiation. A “drying” MgCl₂ brine was also examined which gave the possibility of examining the effect of concentration. Without questioning the enormous interest of using NAP-XPS on gas/solid and gas/liquid interfaces at thermodynamic equilibrium, it is admitted that during NAP-XPS experiments the X-ray beam may induce beam damage. Effects seem more significant when the beam is used to probe liquid water samples condensed on cooled substrates or hydrated solids in equilibrium with H₂O gas.

The focus here is on the chemistry of halides than can pass through higher degrees of oxidation by reacting with water radiolysis products, or by being oxidized by direct photoemission (especially at high concentration). Studies have shown that the action of ionizing radiation on aqueous solutions of chlorides induces consecutive oxidation steps resulting finally in stable compounds. These species are observed on the XPS spectra. Core-level halide components, chemically shifted to higher binding energy from the plain X⁻ halide peak, are observed. In contrast, liquid jet X-ray photoemission spectroscopy studies of alkali halide solutions exhibit a single chemical environment for the halide specie.

REFERENCES

1. Tissot, H.; Olivieri, G.; Gallet, J.-J.; Bournel, F.; Silly, M. G.; Sirotti, F.; Rochet, F. Cation Depth-Distribution at Alkali Halide Aqueous Solution Surfaces. *J. Phys. Chem. C* **2015**, *119* (17), 9253–9259.
2. Tissot, H.; Gallet, J.-J.; Bournel, F.; Olivieri, G.; Silly, M. G.; Sirotti, F.; Boucly, A.; Rochet, F. The Electronic Structure of Saturated NaCl and NaI Solutions in Contact with a Gold Substrate. *Top. Catal.* **2016**, *59* (5–7), 605–620

In Vivo* Speciation and Molecular Mechanisms of the Uptake of Uranium by *Ascophyllum Nodosum

M. Zerbini¹, P.L. Solari², C. Leblanc³, C. Den Auwer¹ and M.R. Beccia¹

¹ Institut de Chimie de Nice/ Université Côte d'Azur/ France

² MARS Beamline/ Synchrotron SOLEIL/ France

³ Station Biologique de Roscoff/ Sorbonne Université/ CNRS/ France

ABSTRACT

Uranium is naturally present at trace level, but the recent growing use of nuclear energy and the accidental release of nuclear wastes have brought an increasing of the amount in the environment (1). As seawater is the major recipient of human pollutants, its ecosystem is considered at risk and in recent years important research has been done to understand the impact of the radionuclide in the marine environment (2).

Ascophyllum nodosum is a macroalga belonging to the *Fucacea* family, living along the coast of the Atlantic Ocean in Nord Europe and Nord America. It is widely studied and often used as bio-indicator for metal ion pollution because of its high tolerance to chemical toxicity and high CF (Concentration Factor) (3). Uranium is known not to have any role in organism life, but it can be accumulated in tissue and become a threatening heavy metal due to its chemical toxicity (its radiotoxicity is considered negligible). However, its chemical behavior (solubility, migration and bioavailability) strongly depends on its speciation related to the environmental characteristic such as pH, ionic strength and content of organic matter. For this reason, a single determination of the accumulation rate is not sufficient to identify the risk of the contamination, but a speciation study is required.

We present here a multi-scale investigation, aiming at understanding the impact of uranium accumulation in algae tissues at molecular level and describing the uptake mechanism.

A contamination of specimens of *A. nodosum* in closed aquaria has been pursued with uranium, whose main species in seawater is $\text{CaUO}_2(\text{CO}_3)_3$ (4).

Uranium uptake in different algal compartments has been quantified by ICP-MS. Uranium localization at tissue and cellular level was obtained by combining microscopy imaging (SEM and TEM) and XAS spectroscopy.

Ours results show a higher uranium accumulation in the receptacles, the reproductive part of the algae, and a lower amount in the other comparts of the algae. The analysis of the *in vivo* uranium speciation suggests that in the main tissue of *A. nodosum* (thallus and lateral branches) the alginate polymer is involved in the radionuclide uptake. Instead, the EXAFS spectra of uranium inside the receptacles show a different behavior with an important accumulation in the eggs (oogonium).

REFERENCES

1. Aleissa K., Shabana E-L., Al-Masoud F. *et al*, *J. Radioanal. Nucl. Chem.*, .., 683-687 (2004)
2. Silvaperumal P., Kumar P., Kamala K, *et al*, *Encyclop. Marin. Biotech.*, 2881-2894, (2020).
3. Chalkley R., Child F., Al-Thaqafi K. *et al*, *Ecotoxicol. Environ. Saf.* **182**, 1-10, (2019).
4. Reeves B., Beccia M.R., Solari P.L. *et al.*, *Environ. Sci. Technol*, 1-25 (2019).

Use of Metals in Microplastics to Track Microplastics during Digestion

N. Belkessa¹, C. Rivard^{1,2}, M.H. Ropers³, F. Jamme⁴

1 - LUCIA beamline, Synchrotron SOLEIL, 91192 Gif-sur-Yvette, France

2 - TRANSFORM, INRAE, 44300 Nantes, France

3 - BIA, INRAE, 44300 Nantes, France

4 – DISCO beamline, Synchrotron SOLEIL, 91192 Gif-sur-Yvette, France

ABSTRACT

Polyethylene (PE) is one of the most abundant microplastic contaminants found in marine species, with a concentration of 0.3 microparticles per gram of tissue (dry weight) measured in mussels for example¹. In the plastic industry, metallic compounds are added to plastics as additives or dyes, such as titanium dioxide (TiO₂) or barium sulfate (BaSO₄). As it is difficult to follow polyethylene in an organic matrix, we proposed to follow metals. The first objective of this study is to determine whether it is possible to use metal-enriched microspheres of PE to track the plastic during digestion process using *in vitro* simulated human digestion. The selected plastics were Ti or Ba-bearing PE microspheres. The second objective is to apply this procedure of PE detection using metals they contain to a succession of *in vivo* animal and *in vitro* human digestions.

In a first step, the starting PE microspheres were characterized by a combination of microscopy and micro-spectroscopy techniques: electron microscopies, UV and X-ray micro-spectroscopy (DISCO and LUCIA beamlines). The microspheres displayed a spherical structure with a filamentous and porous surface. Inter and intra-microspheres heterogeneities of metals distribution have been observed. Characterization by near structure X-ray absorption spectroscopy (XANES) showed the presence of TiO₂ in its rutile form and confirms the presence of Ba in the form of BaSO₄.

The PE microspheres were subjected to a standardized *in vitro* simulated human digestion process², including three main digestion steps: salivary, gastric and intestinal. All the results converge to consider Ti-bearing PE microspheres as a particularly good candidate for monitoring PE during digestion.

In the second step, mussels have been contaminated with Ti-bearing PE microspheres, a part of them were frozen, and another part was cooked before freezing. X-ray fluorescence (XRF) maps were collected on 80 µm cryo thin sections of raw and cooked mussels to display the spatial distribution of PE microspheres in the mussels.

The prospects are to further study PE/organic matter interface observed during the *in vitro* digestion by deep-UV micro spectroscopy in order to better understand the mechanisms of interaction between the PE and the digestive fluids. It is also planned to carry out real-time monitoring of the digestion process by UV spectroscopy in order to identify and understand the reaction mechanism at each step of the process.

REFERENCES

1. Hermabessiere, *et al.* Environmental Pollution 2019, 250, 807–819

2. Brodkorb A, *et al.* Nat Protoc 2019, 14 (4), 991–1014.

Brain Virtual Histology with X-ray Phase-contrast Tomography

M. Chourout¹, H. Rositi², M. Roux³, D. Legland⁴, I. Arganda-Carreras⁵,
A. Autret⁶, B. Fayard⁶, C. Olivier⁷, F. Perrin⁷, E. Brun⁸,
M. Wiart³, F. Chauveau¹

¹ Lyon Neuroscience Research Center (CRNL), 95 boulevard Pinel, 69675 Bron cedex, France

² Institut Pascal, 4 avenue Blaise Pascal TSA 60026 / CS 60026, 63178 Aubière cedex, France

³ Cardiology, Metabolism, Diabetology and Nutrition Lab (CarMeN), B13 building,
59 boulevard Pinel, 69500 Bron, France

⁴ INRAE Pays de la Loire, 3 Impasse Yvette Cauchois CS 71627, 44316 Nantes cedex 3, France

⁵ Department of Computer Science and Artificial Intelligence, Universidad del País Vasco, 1 paseo de Manuel
Lardizabal, 20018 Donostia-San Sebastian, Spain

⁶ NOVITOM, 3 avenue Doyen Louis Weil, 38000 Grenoble, France

⁷ Creatis, 21 avenue Jean Capelle O, 69100 Villeurbanne, France

⁸ Inserm UA7 Strobe, 2280 rue de la piscine, 38400 Saint Martin d'Hères, France

ABSTRACT

Virtual histology is the process of analyzing intact *ex vivo* organs or tissues through high-resolution 3D imaging, like synchrotron in-line x-ray phase-contrast tomography (XPCT). Unlike common absorption-sensitive x-ray imaging, XPCT is sensitive to small changes in refractive indices in the sample microstructure; thus, it is ideal for soft tissue imaging [1]. To date, dedicated tools to analyze these large datasets have been lacking. We propose efficient, neurobiologist-friendly tools to handle this data in two different pathologies: white matter (WM) injuries and Alzheimer's disease (AD).

Imaging was performed on excised, label-free, ethanol-dehydrated brains at the European Synchrotron Radiation Facility (ESRF). For WM injuries, we studied a model of multiple sclerosis (unilateral lysolecithin injection in the corpus callosum in 3 animals [2]). A dedicated algorithm was developed to detect fiber orientation and compute diffusion tensor imaging (DTI)-like parametric maps, such as Fractional Anisotropy (FA). For AD, we studied 3 transgenic mouse models: J20, APP/PS1 and 3xTg [3–5] (9 mice). A workflow was designed to segment amyloid- β (A β) plaques and analyze their 3D morphologies using open-source software for supervised machine learning (step-by-step tutorial available, doi: 10.5281/zenodo.4584753). This yielded an entirely new class of shape parameters, such as mean breadth.

DTI-like metrics in corpus callosum confirmed the ability of XPCT to quantitatively assess microstructural WM abnormalities, with an ipsilateral decrease in fractional anisotropy. New shape parameters—e.g. mean breadth—differentiated A β morphology in the 3 AD models. XPCT on excised organs has various advantages for neuroimaging studies: it is fast (3-min acquisition), isotropic with a microscopic resolution (6.5x6.5x6.5 μ m), it does not require tedious preparation, and it yields interesting contrasts on label-free samples. Though the availability of synchrotron sources with XPCT capacity is restricted to 20-30 sites in the world, several methods have been proposed to obtain phase-contrast images from a laboratory X-ray source [6–8].

XPCT is a powerful tool for investigating various brain diseases, such as white-matter injuries and amyloid seeding/spreading. Efficient post-processing tools will help XPCT expand its scope in neuroscience.

ACKNOWLEDGMENTS

We acknowledge the European Synchrotron Radiation Facility for allocation of beam time and we would like to thank the staff for assistance in using beamlines ID-17 and ID-19.

REFERENCES

1. Barbone, G.E., Bravin, A., et al. 2018, 'Micro-imaging of Brain Cancer Radiation Therapy Using Phase-contrast Computed Tomography', *International Journal of Radiation Oncology, Biology, Physics*, 101 (4), 965–984.
2. Nait-Oumesmar, B. et al. 1999, 'Progenitor cells of the adult mouse subventricular zone proliferate, migrate and differentiate into oligodendrocytes after demyelination: Oligodendrocyte differentiation in adult SVZ', *European Journal of Neuroscience*, 11(12), pp. 4357–4366.
3. Jankowsky, J.L., Fadale, D.J., et al. 2004, 'Mutant presenilins specifically elevate the levels of the 42 residue β -amyloid peptide in vivo: evidence for augmentation of a 42-specific γ secretase', *Human Molecular Genetics*, 13 (2), 159–170.
4. Mucke, L., Masliah, E., et al. 2000, 'High-Level Neuronal Expression of A β 1–42 in Wild-Type Human Amyloid Protein Precursor Transgenic Mice: Synaptotoxicity without Plaque Formation', *The Journal of Neuroscience*, 20 (11), 4050–4058.
5. Oddo, S., Caccamo, A., et al. 2003, 'Triple-Transgenic Model of Alzheimer's Disease with Plaques and Tangles', *Neuron*, 39 (3), 409–421.
6. Töpferwien, M., Krenkel, M., et al. 2017, 'Three-dimensional mouse brain cytoarchitecture revealed by laboratory-based x-ray phase-contrast tomography', *Scientific Reports*, 7 42847
7. Paganin, D.M., Labriet, H., et al. 2018, 'Single-image geometric-flow x-ray speckle tracking', *Physical Review A*, 98 (5), 053813.
8. Zdora, M.-C., Thibault, P., et al. 2020, 'X-ray phase tomography with near-field speckles for three-dimensional virtual histology', *Optica*, 7 (9), 1221.

Investigation of Magnetite/cobalt Interactions at Nanoscale

L. Fablet^{1,2}, M. Pedrot¹, R. Marsac¹ and F. Choueikani²

¹ Univ Rennes, CNRS, Géosciences Rennes – UMR 6118, F-35000 Rennes, France

² Synchrotron SOLEIL, l'Orme des Merisiers, Saint-Aubin – BP48, 91192 Gif-sur-Yvette, France

ABSTRACT

Magnetite nanoparticles (Fe_3O_4) are widely used in many fields due to their unique properties and high affinity with metals, which makes them all the more interesting for environmental and electronic applications. However, the mechanisms involved between magnetite and transition metals are still poorly understood and require further study to determine the interactions and the resulting chemical and magnetic properties. This study focused on the interactions between magnetite and cobalt, a metal of great interest due to its important presence in the environment and its magnetic properties. Magnetite nanoparticles were synthesized by coprecipitation and batch studies were performed with different Co concentrations. Adsorption isotherms were used to describe the behavior of cobalt in relation to magnetite. The models allow to differentiate three species according to the Co concentration, with Co^{2+} adsorption or incorporation at low Co concentration, Co polymer formation at intermediate concentrations, and Co precipitation from the magnetite surface for high Co concentrations. The electronic and magnetic properties of these particles were probed by soft X-ray absorption spectroscopy (XAS) and X-ray magnetic circular dichroism (XMCD), at the $L_{2,3}$ absorption edges. These measurements revealed the presence of Co^{2+} in the structure of the particles, with the formation of an antiferromagnetic $\text{Co}(\text{OH})_2$ phase for the highest Co concentrations. According to the literature, the magnetic signal for very low concentrations is similar to that obtained by cobalt ferrite (CoFe_2O_4). On the contrary, the particles with high Co concentrations show a hard magnet behavior. This study provides detailed knowledge of the sorption mechanisms that occur between cobalt and magnetite, as well as the chemical and magnetic properties of these particles. This understanding is necessary to determine the mechanisms that occur naturally in the environment, and to understand sorption effects for environmental applications and core-shell formation for electronic applications.

X-ray Microtomography of Non-small Cell Lung Cancer Tumours (NSCLC) Treated with Cold Atmospheric Plasma

K. Géraud^{a*}, M. Soulier^a, S. Marmier^b, J. Perrin^c,
I. Cremer^b, T. Dufour^a

^a LPP, Sorbonne Université, CNRS, Ecole Polytechnique, Paris, France

^b Centre de Recherche des Cordeliers (CRC), Sorbonne Université,
Université de Paris, INSERM, Paris, France

^c ANATOMIX beamline, Synchrotron SOLEIL, Saint-Aubin, France

* geraudkor@gmail.com

ABSTRACT

For the past twelve years, the scientific community has been interested in the therapeutic potential of Cold Atmospheric Plasmas (CAP) applied to oncology [1]. These represent an innovative technological alternative to conventional options (radiotherapy, chemotherapy).

In this context, LPP and CRC laboratories are developing new therapeutic approaches for the treatment of non-small cell lung cancer (NSCLC). NSCLC is asymptomatic in the early stages of its development and thus belatedly diagnosed. Its prognosis is therefore very poor, with a 5-year survival rate of about 20% in France [2]. Even if systemic therapies (e.g. surgery and chemotherapies) are well functioning on the first stages, non-responder patients constitute one of the main issue on the next stages (only 30% for immunotherapies).

The consortium has demonstrated that the Reactive Oxygen Species (ROS) generated by CAP activate cellular mechanisms such as oxidative stress, capable of initiating apoptosis of tumour cells but also of activating immune cells (macrophages, etc.). Experimental campaigns carried out on immunocompetent murine models have shown that tumours exposed to CAP were smaller in size compared to those in the control group. Understanding such differences requires to characterise tumour physiology as well as tumour inner morphology. For this, synchrotron radiation microtomography experiments have been performed on the Anatomix beamline at SOLEIL. Three groups of NSCLC tumours (resected from immunocompetent murine models) were analysed: control, "A" plasma treatment and "B" plasma treatment. Plasma treatments "A" and "B" correspond to a treatment with two different plasma sources, a plasma jet and a dielectric barrier discharge (DBD). The objective of the microtomography experiments is to highlight key morphological modifications that were induced by plasma, e.g. vascular network, cavities, fibrous regions, ...

The microtomography images have been processed with ImageJ and Dragonfly softwares. Preliminary analyses relying on the deep learning tools of Dragonfly highlight the existence of numerous cavities in the periphery of plasma-treated tumours.

REFERENCES

1. E. Robert *et al.*, *Clinical Plasma Medicine*, 2013, 1, 8-16
2. HAS, "Dépistage du cancer bronchopulmonaire par scanner thoracique faible dose sans injection : actualisation de l'avis de 2016", 2022

Unmasking the Otolith using Synchrotron-based Scanning X-ray Fluorescence

V. Haÿ¹, S. Berland¹, M.I. Mennesson¹, P. Keith¹, K. Medjoubi²,
A. Somogyi² and C. Lord¹

¹UMR 8067, Biologie des organismes et écosystèmes aquatiques (BOREA), Sorbonne Université, Muséum national d'histoire naturelle, Université des Antilles, CNRS, IRD, CP26, 43 rue Cuvier 75005 Paris, France.

²Synchrotron SOLEIL, Université Paris-Saclay, Saint-Aubin, 91190, France.

ABSTRACT

The application to otolithometry of high-resolution analytical microchemistry by synchrotron-based X-ray diffraction (coherent beam and nanometric spatial focusing) is making a major breakthrough in tracing fish life history events, especially fish migration pathways. Otoliths, three pairs located in the teleost's inner ear, have stato-acoustic functions. They are biocarbonate concretions, formed by a biologically controlled continuous accretion of crystalline matrix. Thus matrix, retains individual biogeochemical signatures of the environments encountered by elemental substitutions and also presents biological growth marks (1). Unfortunately, for many species, such as in Syngnathidae (seahorses, seadragons and pipefish), otoliths are highly challenging: small size (less than 400 µm in length), fragile and without raw discernible growth increments. The resolution on Nanoscopium beamline in the SOLEIL synchrotron, whose architecture allows simultaneous multi-detector acquisition during the two-dimensional scanning of a sample, offers the possibility to discriminate the zonation of these signatures at the sub-micrometric scale in such mute otolith.

We have applied synchrotron-based scanning XRF on otoliths from two tropical Indo-Pacific freshwater pipefish species: *Micropphis brachyurus* (Bleeker, 1854) and *Micropphis retzii* (Bleeker, 1856), which are of conservation concern (2). This method allows the mapping of elements on the entire otolith sagittal plane that runs through the lengthwise axis with 0.5 µm pixel size spatial resolution. With this approach, we confirm for the first time, by mapping the strontium element (correlated with water salinity) that the species studied are diadromous (transition freshwater/marine/freshwater). Trace element quantification at the ppm level allowed to conclude on different migratory routes. Another major breakthrough is that the growth increment counts were made by following up the sulfur signal pattern as this element is part of the organic paced-by-growth deposit and involved in the biomineralization process. This novel method circumvents reader bias issues and enables age estimation even for otoliths with seemingly untraceable increments otherwise.

Present innovative results on the temporalization and spatialization of the life cycle is one of the outcomes showing how far high spatial resolution of elemental mapping method can push back limits of the studies based on otoliths.

REFERENCES

1. K. Hüsey, K. E. Limburg, H. De Pontual, O. R. Thomas, P. K. Cook, Y. Heimbrand, M. Blass, A. M. Sturrock, *Journal of Fish Biology*, **97**(2), 552-565 (2020)
2. R.A. Pollom, G. M. Ralph, C. M. Pollock, A. C. Vincent, *Oryx*, **55**(4), 497-506 (2021).

Impact of the Polymer Degradation on the Metallic Additives Distribution in Microplastics

I. Khatib¹, M. Davranche¹, D. Vantelon², C. Catrouillet³,
J. Gigault⁴, R. Tucoulou⁵, C. Rivard^{2,6}

¹Laboratoire Géosciences Rennes, UMR6118, 263 Avenue Général Leclerc, 35042 Rennes, France

² Synchrotron SOLEIL, L'orme des Merisiers Départementale 128, 91190 Saint-Aubin, France

³Institut de Physique du Globe de Paris, 1 Rue Jussieu, 75005 Paris, France

⁴ Pavillon Alexandre-Vachon, local 2064. Université Laval, Québec, Canada

⁵ ESRF - European Radiation Synchrotron Facility, 71 Av. des Martyrs, 38000 Grenoble, France

⁶ UAR 1008 TRANSFORM, INRAE, Nantes, France

ABSTRACT

The increasing production of plastics combined with the mismanagement of the plastic waste contributes to the creation of an environmental and health threat at a planetary scale. In addition to the alteration of plastic waste, the release of their additives and their fate remains unexplored. Although many studies focused on organic additives such as endocrine disruptors, few information is available on inorganic additives, especially on metals. These metallic additives can be released into the environment by degradation of the polymer matrices, becoming a new source of toxicity.

To assess the impact of plastic degradation on the metallic additives' distribution and release, altered macroplastics (> 5 mm) were collected in the environment. By micro-XRF performed on a synchrotron line, colocalizations of metals were observed in the altered and unaltered layers of plastics. In the polyethylene plastics, metal additives are distributed as hotspot and large area as well as diffused elements. Statistical study analysis of the ratios between metals present in the non-altered and altered layers showed a preferential release of some metals. For a given additive some metals are released in greater quantity than the other. Plastics are therefore not only vectors, but also sources of metals in the environment.

Mouse Arterial Wall Analysis from Synchrotron Micro-CT Imaging

X. Liang^{1,2}, A. Ben Zemzem², S. Almagro², J-C. Boisson³,
L-A. Steffemel³, T. Weitkamp⁴, L. Debelle², N. Passat¹

¹ Université de Reims Champagne Ardenne, CRéSTIC EA 3804, 51100 Reims, France

² Université de Reims Champagne Ardenne, UMR CNRS 7369 MEDyC, 51100 Reims, France

³ Université de Reims Champagne Ardenne, LICIIS / LRC CEA DIGIT, 51100 Reims, France

⁴ Synchrotron SOLEIL, 91192 Gif-sur-Yvette, France

ABSTRACT

Age-related diseases can be precipitated by metabolic disorder such as diabetes [1]. In particular, vascular aging is characterized by profound modifications of large elastic arteries [2] and vascular diseases involve remodeling of elastic lamellae in vessel walls. Our study aims to investigate arterial alterations due to aging and age-related diseases. Some characteristics of these alterations may help find biomarkers to forecast vascular outcome. In this study, we use synchrotron X-ray microtomography to acquire arterial wall images of mice of different ages and different health status. We segment and classify various regions of interest to analyze their modifications.

We apply a methodological pipeline to extract the *tunica media* where elastic lamellae lie. We preprocess images to reduce noise. We further segment the lumen, which has a relatively clear boundary with the inner contour of the *tunica media*, by a co-occurrence texture analysis [3]. Then, we compute a normal field to define image patches and orient them homogeneously to build a dataset used to train a Siamese neural network [4] in order to find the outer contour of the *tunica media*. In this analysis, patches are labeled according to their similarities based on their spatial relations. We also propose a measure to evaluate the tortuosity of skeletonized elastic lamellae fragments to quantitatively compare their geometries in different health situations.

The proposed pipeline leads to a segmentation precision higher than 90% on 2D cross-sections and the proposed measure shows a significant difference between the geometries of elastic lamellae in healthy and diabetic mice. Our current and future works are the further segmentation and classification of the 5 medial lamellae by preprocessing and analyzing stacks of 2D images, extending segmentation methods to 3D, and finally analyzing how these structures are modified during aging and pathological processes.

REFERENCES

1. F.S. Vatner, J. Zhang, C. Vyzas, K. Mishra, R.M. Graham, and D.E. Vatner, "Vascular stiffness in aging and disease," in *Frontiers in Physiology*, vol. 12, pp. 762437, 2021.
2. M.F. O'Rourke, M.E. Safar, and V. Dzau, "The cardiovascular continuum extended: Aging effects on the aorta and microvasculature," in *Vascular Medicine*, vol. 15, no. 6, pp. 461–468, 2010.
3. R.M. Haralick, K. Shanmugam, and I. Dinstein, "Textural features for image classification," in *IEEE Transactions on Systems, Man, and Cybernetics*, vol. 3, pp. 610–621, 1973.
4. G. Koch, R. Zemel, and R. Salakhutdinov, "Siamese neural networks for one-shot image recognition," in *ICML Deep Learning Workshop*, Proceedings, 2015.

Surface Chemistry Engineering of Mercury Telluride Nanocrystals for Infrared LEDs

E. Bossavit¹, J. Qu¹, E. Izquierdo¹, A. Khalili¹, C. Greboval¹, T. Dang¹, S. Pierini¹, M. Cavallo¹, A. Chu¹, Y. Prado¹, V. Parahyba², X. Z. Xu³, A. Decamps-Mandine⁴, M. Silly⁵, S. Ithurria³, E. Lhuillier¹

¹ Sorbonne Université, CNRS, Institut des NanoSciences de Paris, INSP, F-75005 Paris, France.

² New Imaging Technologies SA, 1 impasse de la Noisette 91370 Verrières le Buisson, France.

³ Laboratoire de Physique et d'Etude des Matériaux, ESPCI-Paris, PSL Research University, Sorbonne Université Univ Paris 06, CNRS UMR 8213, 10 rue Vauquelin 75005 Paris, France.

⁴ Centre de MicroCaractérisation Raimond Castaing, UAR3623, CNRS, Université de Toulouse, 3 rue Caroline Aigle, 31400 Toulouse, France

⁵ Synchrotron-SOLEIL, Saint-Aubin, BP48, F91192 Gif sur Yvette Cedex, France.

ABSTRACT

Nanocrystals (NCs) of semiconductors are of particular interest for light emission. Thanks to quantum confinement, NCs present tunable and bright luminescence.

While, in the visible, NCs based light emitting diodes (LEDs) have reached a high degree of maturity, the infrared ranges remain under-researched. Targeted applications for this spectral range span from airfield lighting to organic molecule sensing.

To achieve these goals, we work on synthesizing Mercury Telluride (HgTe) NCs emitting at 1.3 μm and integrating them into infrared LEDs. Previous works have demonstrated that such HgTe-NCs-based devices have decent performances regarding electroluminescence (EL)^{1,2}. However, compared to the strong photoluminescence (PL) that colloidal HgTe NCs exhibit, their efficiency greatly decreases when integrated into devices, pointing towards a need for optimizations.

We focus on engineering the surface chemistry of HgTe NCs to improve their performances. We perform halide ligand exchange to improve PL quantum yields through surface passivation and show that this method can be made compatible with building complete devices. Finally, we show that implementing this halide treatment in HgTe-NCs-based LEDs leads to a 2-to-3-fold increase in the efficiency of the EL signal, while preserving high brightness and low turn-on voltages.³

REFERENCES

1. Qu, J. *et al.* Electroluminescence from HgTe Nanocrystals and Its Use for Active Imaging. *Nano Lett.* **20**, 6185–6190 (2020).
2. Qu, J. *et al.* Electroluminescence from nanocrystals above 2 μm . *Nat. Photonics* **16**, 38–44 (2022).
3. Bossavit, E. *et al.* Optimized Infrared LED and Its Use in an All-HgTe Nanocrystal-Based Active Imaging Setup. *Adv. Opt. Mater.* **10**, 2101755 (2022).

The Impact of Substitutions in Goethite on Rare Earth Element Adsorption

A. Buist^{1*}, C. Rivard^{1,2}, M. Davranche³, M. Bouhnik-Le Coz³,
F. Brisset⁴, E-A. Paineau⁵, S. Rouziere⁵, D. Vantelon¹

¹Synchrotron SOLEIL, L'orme des merisiers, Saint Aubin BP48, 91192 Gif-sur-Yvette, France

²INRAE, UAR 1008, TRANSFORM, 44316 Nantes, France

³Géosciences Rennes, UMR 6118, University of Rennes 1, Campus de Beaulieu, 35042 Rennes, France

⁴ICMMO, University Paris-Saclay, 91450 Orsay Cedex, France

⁵Laboratoire de Physique des Solides, University Paris-Saclay, 91400 Orsay, France

ABSTRACT

Since the 1980's the uses, and thus mining, of Rare Earth Elements (REE) have grown exponentially. This has led to questions about the impact of REE on the environment, and REE being designated emerging pollutants. Currently, knowledge about the behaviour of REE in the environment is still incomplete. For example, there are few studies on REE adsorption on iron (Fe) (oxy)hydroxides, which are considered key carriers of metal pollution, and on the other factors controlling this adsorption [1-4]. Knowing that in natural (oxy)hydroxides, Fe is frequently substituted by other elements in the environment in which they form, we were interested in the effect of these substitutions on the adsorption capacity of (oxy)hydroxides towards REE.

This study focusses on aluminium (Al, common in natural environments and easily substituted into Fe-oxyhydroxides) and gallium (Ga, chemical analogue to Al) substitutions in goethite (Goe), representative of commonly found Fe-(oxy)hydroxides whose well-defined structure allows for modelling of sorption and surface interactions. For this purpose, experiments of REE were conducted on pure and substituted goethites (Goe) with varying Al and Ga content.

A characterisation of these goethites, shows that the substitution does not affect the shape, size, and specific surface area significantly. The Neodymium (Nd) L₃-edge EXAFS experiments shows no modification of its binding mode to the Goe surfaces, forming corner sharing bidentate-binuclear complexes regardless of the substitution rate. However, TEM observations and Cerium (Ce) L₃-edge XANES experiments demonstrate that the Ga substitution favours a higher Ce(IV)O₂ adsorption, while the Al substitution favours Ce(III) adsorption compared to the pure Goe.

These results reveal there is an impact of substitutions on the reactivity of goethite towards REE.

REFERENCES

1. Davranche, M., Pourret, O., Gruau, G., & Dia, A. (2004). Impact of humate complexation on the adsorption of REE onto Fe oxyhydroxide. *Journal of Colloid and Interface Science*, 277(2), 271-279.
2. Quinn, K. A., Byrne, R. H., & Schijf, J. (2006). Sorption of yttrium and rare earth elements by amorphous ferric hydroxide: influence of pH and ionic strength. *Marine Chemistry*, 99(1-4), 128-150.
3. Koeppenkastrup, D., & De Carlo, E. H. (1993). Uptake of rare earth elements from solution by metal oxides. *Environmental science & technology*, 27(9), 1796-1802.
4. Ohta, A., & Kawabe, I. (2001). REE (III) adsorption onto Mn dioxide (δ -MnO₂) and Fe oxyhydroxide: Ce (III) oxidation by δ -MnO₂. *Geochimica et Cosmochimica Acta*, 65(5), 695-703.

Exploring the Application of Inelastic X-ray Scattering for Novel Spectral Imaging and Spectroscopy of Contemporary Art Materials

L. Dalecky^a, J-P. Rueff^b, L. Cazals^{a,c}, J. Ablett^b,
A. Chevalier, A. Desolneux^c, L. Bertrand^c

^aPPSM, CNRS, ENS Paris-Saclay, 4, avenue des Sciences, 91190 Gif-sur-Yvette, FR

^bSOLEIL Synchrotron, L'Orme des Merisiers, 91190 Saint-Aubin, FR

^cCentre Borelli, CNRS, ENS Paris-Saclay, 4, avenue des Sciences, 91190 Gif-sur-Yvette, FR

ABSTRACT

In recent years, synchrotron-based Inelastic X-ray Scattering (IXS), an in particular X-ray Raman Scattering (XRS), has been used as a spectroscopic and imaging method for cultural heritage materials, specifically by using hard X-rays (6–12 keV) for the organic speciation of art, archaeological and paleontological samples [1–4].

Recently, using the coupling of the novel high-resolution monochromator with the 40-crystal analyzer-based MATRIXS detector at the GALAXIES beamline of SOLEIL, we have explored the potential of this spectroscopy to identify and image the distribution of contemporary paints in real-to-life the sample. In particular, studying chemically heterogeneous inorganic-organic paints and preparation layers inspired by the practice of the contemporary painter Simon Hantaï (Budapest, 1922 - Paris, 2008), we have explored the information potential of low-energy-loss excitations.

We will discuss the promise shown by IXS as a novel spectroscopic technique for the discrimination and in-depth chemical characterization of pigment compositions. In particular, it brings potential to discriminate between crystal polymorphs in paints in the inelastic low-energy loss region (<20 eV) the spectra, relating to apparent color of pigments [5].

We acknowledge support from ENS Paris-Saclay. The MATRIXS4H is supported by the the DIM Matériaux anciens et patrimoniaux of the Région Île-de-France (project). The European Commission project GoGreen (Horizon Europe GA no. 101060768) supports developments by LC and LB.

REFERENCES

1. R. Georgiou, et al., *Science Advances*, **5**(8), 2019, eaaw5019.
2. P. Gueriau, et al., *Analytical Chemistry*, **89**(20), 2017, pp. 10819–10826.
3. R. Georgiou, et al., *Proc. Natl Acad. Sci. USA*, **119**(22):e2116021119, 2022.
4. R. Georgiou, et al., *Chemical Reviews*, **122**(15), 2022, pp. 12977–13005.
5. De Sauve, et al., *Angew. Chem. Int. Ed.*, 2020, **59**, pp. 9113 – 9119

Investigation of the crystal electric field in rare-earth titanate pyrochlores by resonant inelastic x-ray scattering

Octave Duros^{†,1,2}, Brouder C.², Delaunay R.¹, Elnaggar H.², Jarrier R.¹, Juhin A.², Chiuzbăian G. S.¹

¹ Sorbonne Université, CNRS, Laboratoire de Chimie Physique - Matière et Rayonnement, LCPMR, F-75005 Paris, France

² Sorbonne Université, Muséum National d'Histoire Naturelle, CNRS, Institut de Minéralogie, de Physique des Matériaux et de Cosmochimie, IMPMC, F-75005 Paris, France

Rare-earth titanate pyrochlores are defined by the general chemical formula $R_2Ti_2O_7$ (where R is a rare-earth metal) and a distinctive crystalline structure, made of two interpenetrating tetrahedral networks (see Fig.1). One of the most interesting aspect of the $R_2Ti_2O_7$ compounds is the presence of fascinating magnetic states, such as spin-liquid or quantum spin-ice states [1–5]. The key ingredient for the understanding of such behaviors is the characterization of the crystal electric field (CEF) acting on the R sites. Here, the CEF is created by the surrounding oxygen ligands and interacts with the rare-earths $4f$ orbitals. Considering the D_{3d} symmetry of the rare-earths in $R_2Ti_2O_7$ crystals, the CEF can be expressed as a function of six parameters in the Wybourne convention:

$$H_{\text{CEF}} = B_0^2 C_0^{(2)} + B_0^4 C_0^{(4)} + B_3^4 (C_{-3}^{(4)} - C_3^{(4)}) + B_0^6 C_0^{(6)} + B_3^6 (C_{-3}^{(6)} - C_3^{(6)}) + B_6^6 (C_{-6}^{(6)} - C_6^{(6)})$$

However, several definitions have been used in the literature and their variety has lead to many misunderstandings [6-9]. One can mention the definitions expressed with the Crystal Field operators $C_n^{(m)}$ expanded on spherical harmonics $Y_{l,m}$ or on tesseral harmonics $Z_{l,m}$, sometimes found as C_m^n , as well as the definitions expressed with the Stevens Operators O_n^m expanded on renormalized tesseral harmonics with an arbitrary prefactor, sometimes found as O_k^q . All those operators take single coefficients, called crystal field parameters, that are written either as A_m^n , A_n^m , B_m^n or B_n^m depending on the publications but regardless of the definition in use for the operators. Experimentally, CEF parameters can be determined with spectroscopic techniques such as resonant inelastic x-ray scattering (RIXS) [10], by probing the ff excitations at the rare-earths edges and confronting them with ligand field multiplet theory calculations [11]. A complete understanding of the CEF theory is thus mandatory. This poster aims at presenting the origin of the CEF in $R_2Ti_2O_7$ as well as a clear definition to describe and compute it in the ligand field multiplet theory.

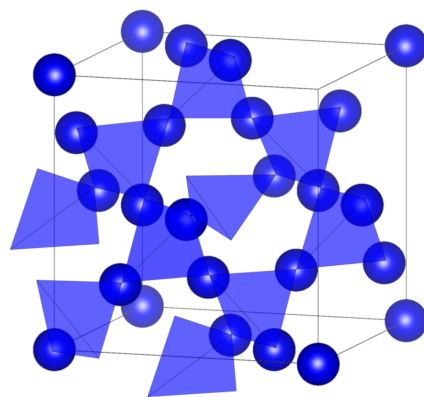


Figure 1: Tetrahedral network formed by rare-earth sites R in $R_2Ti_2O_7$

- [1] R.A. Borzi *et al.*, Nat. Comm. **7**, 12592 (2016). doi:10.1038/ncomms12592
- [2] S.T. Bramwell, Nat. Comm. **8**, 2088 (2017). doi:10.1038/s41467-017-02102-1
- [3] L. D. C. Jaubert *et al.*, Phys. Rev. Lett. **118**, 207206 (2017). doi:10.1103/PhysRevLett.118.207206
- [4] S.R. Giblin *et al.*, Phys. Rev. Lett. **121**, 067202 (2018). doi:10.1103/PhysRevLett.121.067202
- [5] A. M. Samarakoon *et al.*, Nat. Comm. **11**, 892 (2020). doi:10.1038/s41467-020-14660-y
- [6] B. Z. Malkin *et al.*, Phys. Rev. B **70**, 075112 (2004). doi:10.1103/PhysRevB.70.075112
- [7] A Bertin *et al.*, J. Phys.: Condens. Matter **24**, 256003 (2012). doi:10.1088/0953-8984/24/25/256003
- [8] M. Ruminy *et al.*, Phys. Rev. B **94**, 024430 (2016). doi:10.1103/PhysRevB.94.024430
- [9] C. Rudowicz and C. Y. Chung, J. Phys.: Condens. Matter **16**, 5825 (2004). doi:10.1088/0953-8984/16/32/018
- [10] Chiuzbăian, S.G., in: Beaurepaire, E. *et al.*, *Magnetism and Synchrotron Radiation: Towards the Fourth Generation Light Sources*, Springer, Cham., pp 185-210, doi:10.1007/978-3-319-03032-6_6
- [11] H. Elnaggar *et al.*, in Springer Proc. Phys. **262**, 83 (2021). doi:10.1007/978-3-030-64623-3_4

[†]Speaker

ARPES Investigations of the Topological States in TaTe₄ and NbTe₄

P. Gonçalves¹, M. Thees¹, R. Luca Bouwmeester², A. Antezak¹,
E. David¹, A.J. Thakur¹, P. Le Fèvre³, N. Olszowska⁴, M. Rosmus⁴,
E. Frantzeskakis¹, F. Fortuna¹, R. Paniago⁵, P. Giraldo-Gallo⁶,
A. Santander-Syro¹

¹ *Université Paris-Saclay, CNRS, Institut des Sciences Moléculaires d'Orsay, 91405, Orsay, France*

² *MESA+ Institute for Nanotechnology, University of Twente, 7500 AE Enschede, Netherlands*

³ *Synchrotron SOLEIL, L'Orme des Merisiers, Saint-Aubin-BP48, 91192 Gif-sur-Yvette, France*

⁴ *SOLARIS National Synchrotron Radiation Centre, Czerwone Maki 98, 30-392 Kraków, Poland*

⁵ *Federal University of Minas Gerais, Av. Pres. Antônio Carlos, 6627 - Pampulha,
Belo Horizonte - MG, 31270-901, Brazil*

⁶ *Department of Physics, Universidad de Los Andes, Bogota 111711, Colombia*

ABSTRACT

The research of topological materials has been an extensive source for prediction and observation of new and exotic phenomena in condensed matter physics. Over the last years, a variety of new topological phases of matter has emerged. The most prominent classes are the Topological Insulators, materials characterized by a bulk band gap with non-trivial metallic surface states showing, e.g., spontaneous spin polarization. However, the concept of topology in condensed matter can also be extended to non-insulating materials. Here, we present our recent findings on the study of the topological semimetal candidates TaTe₄ and NbTe₄. These compounds are an interesting subject for research, since they present two competing electronic ground states: a charge-density-wave at room temperature and superconductivity under mechanical pressure at low temperatures. Our angle-resolved photoemission (ARPES) experiments report a well-defined 3D metallic Fermi surface with the existence of topological states in the form of Dirac/Weyl cones.

Investigation of the Structure Evolution of Thermal Treated Imogolite Nanotubes

Y. Pan,^{1,*} S. Rouzière,¹ V. Baledent,¹ N. Trcera,²
D. Vantelon,² A. Beauvois,² P. Launois,¹ E. Paineau¹

¹Laboratoire de Physique des Solides, CNRS, Université Paris-Saclay, 91405 Orsay, France

²Synchrotron SOLEIL, L'Orme des Merisiers, 91192 Gif-sur-Yvette Cedex, France

[*yifan.pan@universite-paris-saclay.fr](mailto:yifan.pan@universite-paris-saclay.fr)

ABSTRACT

Thermal treatment is one of the most commonly applied processes to modify the structure, porosity, and surface reactivity properties of clay minerals. Imogolite nanotubes (INT), $(\text{OH})_3\text{Al}_2\text{O}_3\text{SiOH}$, are unique clays consisting of a curved octahedral $[\text{O}_3\text{Al}(\text{OH})_3]$ outer layer and of isolated $[\text{SiO}_3(\text{OH})]$ tetrahedron units in inner surface connected through three shared oxygen atoms [1]. The imogolite name can be enlarged to nanotubes where the silicon atoms are replaced by germaniums or the internal hydroxyl groups by methyl groups. A recent study by Monet et al. [2] showed that three different intermediate stages occur during the thermal annealing of $(\text{OH})_3\text{Al}_2\text{O}_3\text{GeOH}$ imogolite nanotubes. After dehydroxylation, the first stage is formed with six-fold and five-fold coordinated aluminums, which further reorganize at higher temperature until re-crystallization into a Ge-mullite compound beyond 950°C . However, a comprehensive investigation of thermal transformations in the whole imogolite family is lacking, as well as the in-situ observation of Al(V) species. The five-fold coordinated atoms were only observed by nuclear magnetic resonance, after heating the samples ex-situ.

Here, we investigated the thermal transformations of methyl-modified $(\text{OH}_3\text{Al}_2\text{O}_3(\text{Si,Ge})\text{CH}_3)$ and of hydrophilic aluminosilicate $(\text{OH}_3\text{Al}_2\text{O}_3\text{SiOH})$ imogolite nanotubes by performing ex-situ characterizations (FTIR and X-ray scattering) coupled with in-situ X-ray Absorption Spectroscopy (XAS) at aluminum and silicon K-edges up to 1000°C . Complex structural transformations are observed. We will present our ex-situ and in-situ experimental results and their first analyses. Combined with XAS results and quantitative analysis by MCR-ALS chemometrics [3], the Al coordination shows a strong evolution from an Al(VI) octahedral environment to a combination of Al(IV), Al(V) and Al(VI) sites. Moreover, different temperature behaviors are observed for hydroxylated and methylated nanotubes at the Si edge. The ab-initio simulation of the spectra is also in progress to unravel the mechanisms of structural modifications of these nanomaterials. It should represent a benchmark for further studies concerning the adsorption properties of these transformed INT-based compounds

REFERENCES

- [1] Cradwick P. D. G., Farmer V. C., Russell J. D., Masson C. R., Wada K. and Yoshinaga N. (1972), Nat. Phys. Sci., 240, 187-189.
[2] Monet G., Rouzière S., Vantelon D., Coelho Diogo C., Maurin D., Bantignies J. L., Launois P. and Paineau E. (2021), J. Phys. Chem. C, 125, 12414-12423.sics, Melville, NY, 2002, pp. 651-654.
[3] Vantelon D., Davranche M., Marsac R., Fontaine C. L., Guenet H., Jestin J., Campaore G., Beauvois A. and Briois V. (2019), Environ. Sci. : Nano, 6, 2641

Influence of the Crystal Structure and Nature of the Ligands on the Valence of Uranium in Binary Chalcogenides: A HERFD-XANES and RIXS Study

T. Stephant^{ab}, M. Hunault^b, M. Pasturel^a, C. Prestipino^a, P-L. Solari^b

^a Univ Rennes, CNRS, ISCR-UMR6226, F-35000, Rennes, France

^b Synchrotron SOLEIL, MARS beamline, F-91192, Gif sur Yvette cedex, France

ABSTRACT

Thanks to its $5f$ orbitals, uranium benefits from several valence states, from U^{3+} to U^{6+} , in inorganic compounds and possesses a wide crystal-chemistry. The radial expansion of these orbitals leads to energetically close crystal field (dominating in the case of $3d$ elements) and spin-orbit (dominating in the case of $4f$ rare earths) interactions, and subsequent rich and exotic physical properties¹ (e.g. coexistence of superconductivity and ferromagnetism).

Associated with a chalcogen element ($Q = S, Se, Te$), uranium forms inorganic compounds characterized by various crystallographic structures leading to unique uranium polyhedra² with e.g. the presence of $(S_2)^{2-}$ dimers. However, due to the limited number of known uranium chalcogenides, practically no experimental information on the nature of U-Q bond is available in the literature. As a consequence, understanding the localization of $5f$ electrons of actinides in solid-state, a great challenge for theoretical physicists, remain limited to the study of oxides³ and intermetallic materials.

To increase the field of investigation, some binary uranium chalcogenides (S, Se, Te) have been characterized and studied by HERFD-XANES and RIXS spectroscopies at the U M4 edge. These preliminary measurements enabled to determine the oxidation states of uranium for some binary compounds. The results will be presented and discussed towards the influence of crystal structure and ligands on this oxidation state.

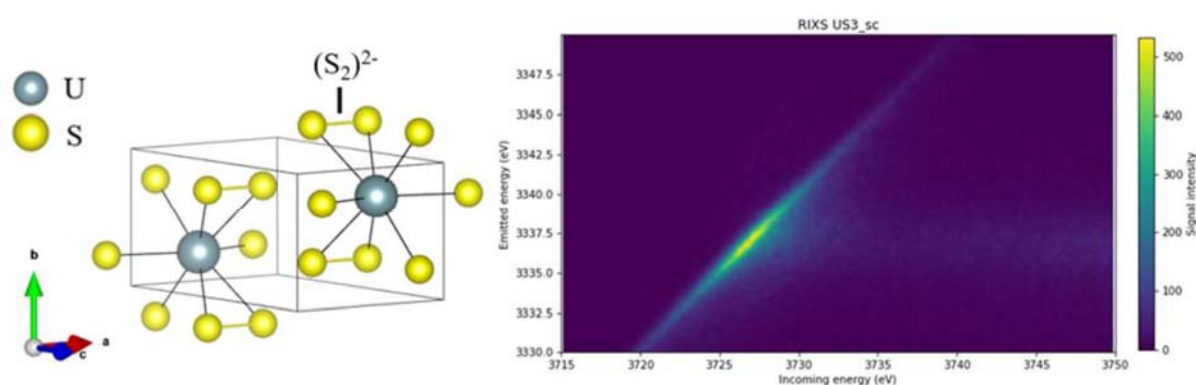


Figure 1: Crystal structure and U $4f$ RIXS map of US_3 ($P21/m$).

REFERENCES

1. Aoki, D., Ishida, K. & Flouquet, J. Review of U-based Ferromagnetic Superconductors: Comparison between UGe_2 , $URhGe$, and $UCoGe$. *J. Phys. Soc. Jpn.* **88**, 022001 (2019).
2. Mesbah, A., Prakash, J. & Ibers, James. A. Overview of the crystal chemistry of the actinide chalcogenides: incorporation of the alkaline-earth elements. *Dalton Trans.* **45**, 16067–16080 (2016).
3. Kvashnina, K. O. & Butorin, S. M. High-energy resolution X-ray spectroscopy at actinide M 4,5 and ligand K edges: what we know, what we want to know, and what we can know. *Chem. Commun.* **58**, 327–342 (2022).

List of Other Posters

- PO-01** Structural imaging and characterization of vascular wall and perivascular adipose tissue
S. Almagro
- PO-02** Gas phase XANES, core and Valence photoelectron spectroscopy of 1-methylbenzotriazole, 2-methylbenzotriazole and 1,2,3-benzotriazole
D. Batchelor
- PO-03** Structure of spin-crossover molecules ultra-thin films on Cu(110)
A. Bellec
- PO-04** Effect of freezing and storage on the crystallization of a porous food: 3D-characterization using Synchrotron X-rays microtomography
H. Benkhelifa
- PO-05** Understanding the surface dynamics of LaFeO₃-based perovskites by the means of GI-XAS and NAP-XPS
E. Berrier
- PO-06** Circular economy: Access to research facilities with EU project ReMade@ARI
H. Chevreau
- PO-07** Structural damage under electron irradiation of some lamellar hydrous minerals, analysed by XRD and spectroscopies (Infrared, Raman and NMR)
M-N. de Noirfontaine
- PO-08** Coherent X-ray scattering on the D2AM beamline at the ESRF
M. Dupraz
- PO-09** Structural analysis of HCV core protein associated with lipid droplets using SRCD and Synchrotron nanoIR
M. Froissard
- PO-10** Discovery of interstellar C₅ molecule
R. Hakalla
- PO-11** FT spectroscopy of ¹²C¹⁸O and deperturbation analysis of the A¹Π(v = 3) level
R. Hakalla
- PO-12** Spectroscopy of ¹³C¹⁸O and extended deperturbation analysis of the A¹Π(v = 2) level
R. Hakalla
- PO-13** Resolving the symmetry of the C₆₀⁺ cation: How high-resolution photoelectron spectroscopy meets astrophysics
H.R. Hrodmarsson
- PO-14** Electrostatic alignment for micro- and nanoARPES: First results
H. Karakachian
- PO-15** Spectral ptychography at the SWING beamline
A. Kulow

- PO-16** Fuzzy DNA recognition by the vibrio cholerae transcription factor HigBA2
R. Loris
- PO-17** Combien de photons ?
Y. Ménesguen
- PO-18** Reaction cells for operando studies of catalysts using Synchrotron radiation
A. Nassereddine
- PO-19** Structural properties of TbMgNi_{4-x}Cox compounds and their hydrides
V. Paul-Boncour
- PO-20** Structure and energetics of GTP-and GDP-tubulin isodesmic self-association
U. Raviv
- PO-21** Contribution de SOLEIL au PEPR DIADEM
J-P. Rueff
- PO-22** Deciphering the mechanism of formation of CoRu nanoalloys using in situ spectroscopy techniques
L. Sicard
- PO-23** Evidence of ion-migration in hybrid perovskite films under electrical bias: A STXM study
S. Swaraj
- PO-24** FT-VIS emission spectroscopy of the A1Π,v=0,1,2 levels of AlD: New data for the ExoMol line list
W. Szajna
- PO-25** FT-UV emission spectroscopy of the B2Σ⁺-X2Σ⁺ system of 12C17O⁺
W. Szajna
- PO-26** The training portal for photon and neutron data services
A. Valcarcel Orti
- PO-27** Studying catalytic reactions using ambient pressure X-ray photoelectron spectroscopy
T. Wätjen

Structural Imaging and Characterization of Vascular Wall and Perivascular Adipose Tissue

A. Ben Zemzem¹, L. Vanalderwier¹, X. Liang^{1,2}, S. Blaise¹,
T. Weitkamp³, M. Dauchez¹, N. Passat², L. Debelle¹ and S. Almagro¹

¹ UMR CNRS 7369 MEDyC, Université de Reims Champagne-Ardenne, France.

² CReSTIC EA 3804, Université de Reims Champagne Ardenne, France.

³ Soleil synchrotron Light Source, beamline Anatomix, Saclay, France.

ABSTRACT

Background. Perivascular adipose tissue (PVAT) is a crucial regulator of vascular homeostasis and implicated in vascular dysfunction during aging and pathology. Indeed, there are a crosstalk between the PVAT and vascular wall. Under pathophysiological conditions, such as type 2 diabetes and aging, they can cause PVAT dysfunction and distension, leads to endothelial and smooth muscle cell dysfunctions. During this process, the vascular extracellular matrix and the PVAT extracellular matrix, in particular elastin, are degraded. The aim of our study is to characterize PVAT and vascular wall extracellular matrix structures to understand how these alterations are set up in physiological and physiopathological conditions.

Materials & Methods. Aorta was harvested after euthanasia from diabetic and control mice 6 months old. Heparin was injected to avoid blood coagulation. Heart and aorta were flushed with phosphate buffered saline (PBS) using a syringe driver to remove residual blood. Then, the aorta was fixed in formalin and agarose low melting was injected. Afterwards, Heart and aorta were fixed in formalin for 24-48 hours. Then, they were dehydrated and embedded in paraffin. Each aorta was imaged using SOLEIL/ANATOMIX beam line with a 0.65 μm voxel resolution and images were reconstructed. We have developed an automatic algorithm which allows to segment images: first we extract the elastic lamellae from the arterial wall and measure them (thickness, number, distance between lamellae), second, we isolate PVAT network and we measure its density.

Results. We previously demonstrate that diabetes alters the aortic wall structure [1]. Our preliminary results on PVAT alterations show that there is a thickening of the elastic lamellae of the arterial wall of diabetic mice compared to controls. Also, the extracellular matrix of PVAT seems to degrade in diabetic mice and it rather dense in controlled mice. This matrix represents 17 to 26% of the total volume of perivascular adipose tissue in controls while in diabetic mice it ranges from 6 to 12%.

Conclusions. Our study shows that there is a structural difference between the vascular extracellular matrix and PVAT network in diabetic mice and control mice. Diabetes alters the three-dimensional architecture of the PVAT. This confirms that diabetes is an accelerated form of vascular aging.

REFERENCES

1. Ben Zemzem, A., et. al (2022). *Early Alterations of Intra-Mural Elastic Lamellae Revealed by Synchrotron X-ray Micro-CT Exploration of Diabetic Aortas*. Int J Mol Sci. 23. Doi: <https://doi.org/10.3390/ijms23063250>

Gas Phase XANES, Core and Valence Photoelectron Spectroscopy of 1-Methylbenzotriazole, 2-Methylbenzotriazole and 1,2,3-Benzotriazole

D. Batchelor^a, S. Bölke^b, K. Greulich^b, S. Klysch^b, L. Weinhardt^a,
C. Nicolas^c, J. Bozek^c, T. Chassé^a, H. Peisert^a

^a *Karlsruher Institut für Technologie, Institute for Photon Science and Synchrotron Radiation (IPS), Hermann-von-Helmholtz-Platz 1, D-76344 Eggenstein-Leopoldshafen, Germany*

^b *Institut für Physikalische und Theoretische Chemie, Eberhard Karls Universität Tübingen, Auf der Morgenstelle 18, 72076 Tübingen, Germany*

^c *Synchrotron SOLEIL, L'Orme des Merisiers, Départementale 128, 91190 Saint-Aubin*

ABSTRACT

1,2,3-Benzotriazole (BTAH) is a much-studied molecule that is interesting for a range of applications covering pharmaceuticals [1], synthetic chemistry [2] and corrosion protection [3]. Considerable work exists for BTAH adsorption showing both chemisorption, and/or physisorption with the latter showing a spectral signature similar to the gas phase. XANES calculations confirm physisorbed species on a gold substrate [4]. In an effort to better understand the bonding and electronic structure gas phase BTAH together with the methylated species 1-Methylbenzotriazole and 2-Methylbenzotriazole were measured using core level spectroscopies.

While previous experimental work concentrated on the UPS and Vibrational spectroscopy [5] we present Nitrogen edge XANES, N1s core level photoelectron spectroscopy, and valence region spectra for the three molecules and compare with calculations and the previous work. In particular the XANES calculations show good agreement which is a necessary step to confirm and understand the polymerization on the surface [4], the modelling, and calculations. Further work involving resonant Auger electron spectroscopy is planned.

REFERENCES

1. I. Brigugli, et. al., Eur. J. Med. Chem. 2015, 97, 612-645
2. A.R. Katritzky, et. al., Tetrahedron, 1991, 47, 2683-2732
3. V. Brusica et. al. J. Electrochem. Soc., 1991, 138, 2253
4. Federico Grillo, David Batchelor, Christian R. Larrea, Stephen M. Francis, Paolo Lacovig, Neville V. Richardson. Nanoscale, 11 (2019) 13017-13031; F. Grillo, J. A. Garrido Torres, M.-J. Treanor, C. R. Larrea, J. P. Götze, P. Lacovig, H. A. Früchtl, R. Schaub, N. V. Richardson, Nanoscale, 2016, 8, 9167
5. W. Roth, D. Spangenberg, et. al. Chem. Phys. 1999, 248, 17-25 and refs therein. I. Novak, T. Abu-Izneid, et. al. J. Phys. Chem. A 2009, 113, 9751-9756, P. Rademacher, K. Kowski, A.R. Katritzky et. al. J. Mol. Struct. 1999, 513,

Structure of Spin-crossover Molecules Ultra-thin Films on Cu(110)

A. Bellec¹, Y. Garreau^{1,2}, V. Repain¹, A. Coati²

¹Université Paris Cité, CNRS, Laboratoire Matériaux et Phénomènes Quantiques, F-75013, Paris, France

²Synchrotron SOLEIL, L'Orme des Merisiers, Saint-Aubin, 91192 Gif sur Yvette, France

ABSTRACT

Spin crossover (SCO) molecules present two spin states that can be controlled by external stimuli such as light or temperature^{1,2}. Their ability to switch makes them promising for incorporation in molecular spintronic devices. In this purpose, it is mandatory to understand how the properties of spin crossover molecules are modified when in direct contact with metallic substrates and how the growth of molecular films is governed by the substrate. Additionally, the bistability, i.e. the ability to reversibly switch between two stable states in the hysteretic temperature range, is an important property that needs to be controlled at the nanoscale.

Grazing incidence x-ray diffraction measurements on monolayer of Fe[HB(3,5-(CH₃)₂Pz)₃]₂ (Pz=pyrazolyl) adsorbed on Au(111) and Cu(111) substrates enable us to evidence that an epitaxial relationship between the molecular layer and the substrates exists [FOU19]. This has a direct consequence on the transition from one spin-state to the other either by using temperature^{3,4}, light⁵ or electric field⁶ as external stimuli. Here, we will discuss in detailed the molecular structure of Fe[HB(3,5-Me₂Pz)₃]₂ ultra-thin films adsorbed on Cu(110). For sub-monolayer coverage, the molecules arrange in a nearly hexagonal structure which is a reconstruction of the underlying Cu(110). For larger thicknesses, an additional molecular network appears which resemble the [100] plane of the bulk molecular crystal. By XAS measurements, we demonstrated that for a one-monolayer-high layer, the molecules are locked in the high spin state; while for a six-monolayer-high layer the molecules recovered their spin-crossover properties.

REFERENCES

1. A. Hauser, *Top. Curr. Chem.*, **234**, 155-198, (2004)
2. J. A. Real et al., *Dalton Trans.*, **12**, 2062 (2005)
3. K. Bairagi et al., *Nat. Comm.*, **7**, 12212 (2016)
4. M. Kelaï et al., *J. Phys. Chem. Lett.*, **12**, 6152-6158 (2021)
5. L. Zhang et al., *Angew. Chem.*, **59**, 13341-13346 (2020)
6. Y. Tong et al., *J. Phys. Chem. Lett.*, **12**, 11029-11034 (2021)

Effect of Freezing and Storage on the Crystallization of a Porous Food: 3D-characterization using Synchrotron X-rays Microtomography

H. Benkhelifa^{1,2}, A. Zennoune^{1,2}, P. Latil³, F. Flin³,
C. Geindreau⁴, F-T. Ndoye²

¹ Université Paris-Saclay, INRAE, AgroParisTech, 75005 Paris, France

² Université Paris-Saclay, INRAE, UR FRISE, F-92761 Antony, France;

³ Université Grenoble Alpes, Météo-France, CNRS, CNRM, Grenoble, France

⁴ Université Grenoble Alpes, Grenoble INP, 3SR, CNRS, Grenoble, France

ABSTRACT

Although porous foods such as foams, bread or pastries represent a significant part of frozen food products, they have so far been little studied. In such products, the initial microstructure is defined by the freezing process with the formation of ice crystals. This microstructure then evolves during storage by recrystallization and sublimation phenomena. The high porosity (>50%) of such foods makes them more difficult to investigate, especially due to water transfer coupled with heat transfer at the pore–matrix interface (evaporation-condensation phenomenon).

Non-destructive and low temperature synchrotron X-ray microtomography (ANATOMIX SOLEIL beamline) was applied to image and quantify 3D microstructural evolution of a porous model food (sponge cake) after freezing and storage. Samples were frozen at two different freezing rates (slow at 0,3 °C/min and fast at 17 °C/min) and stored during fourteen days at -20 °C. A specific thermostated cell was used to image the samples at frozen state [1]. One of the challenges in this work was to obtain 3D images with sufficient contrast within the sponge cake to differentiate pores, ice and starch with a spatial resolution ranging from the submicron scale to several hundreds of microns and an acceptable temporal resolution. The images were segmented using a global grey level threshold [2] to distinguish between the 3 phases (air in black, ice in grey, starch in white, Figure 1) followed by morphological and logical operations to differentiate the ice localized at the pores interface and the ice blended inside the starch phase. Volume fraction of each phase, ice location and local thickness were determined.

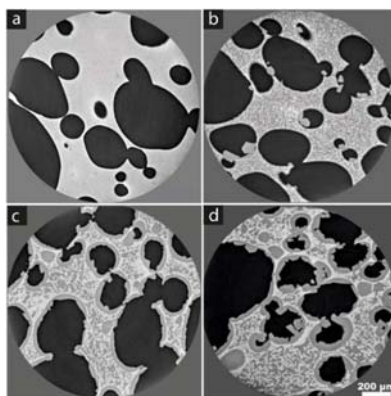


Figure 1: Synchrotron X-rays slices of sponge cake : (a) before freezing (b) after fast freezing (c) after slow freezing (d) after slow freezing and 7days of storage at -20 °C

The results show that both freezing rates and storage conditions significantly affect the microstructure of the sponge cake: ice was formed in the starch matrix but also at the interface between the matrix and the pores at a ratio depending on freezing and storage conditions. Recrystallization phenomena were observed: ice crystals grow and water redistribution occurs within the starch as well as water migration toward the pores. These differences will affect the quality attributes of this porous food. Even if the benefits of fast freezing are reduced after fourteen days of storage, the fast frozen sponge cakes still have a better quality than the slowlyfrozen samples.

REFERENCES

[1] N. Calonne, F. Flin, C. Geindreau, B. Lesaffre, S. Rolland du Roscoat, *The Cryosphere* **8**(6): 2255-2274 (2014).

[2] A. Zennoune, P. Latil, F.-T. Ndoye, F. Flin, J. Perrin, C. Geindreau, H. Benkhelifa, *Foods* **10**(12): 2915 (2021).

<https://doi.org/10.3390/foods10122915>

Understanding the Surface Dynamics of LaFeO₃-based Perovskites by the Means of GI-XAS and NAP-XPS

S. Nandi¹, P. Simon¹, N. Nuns², A. Tougerti¹, M. Trentesaux¹, J.-S. Girardon¹, J.-F. Paul¹, E. Fonda³, A.-S. Mamede¹ and E. Berrier¹

¹ Univ. Lille, CNRS, Centrale Lille, Univ. Artois, UMR 8181 – UCCS – Unité de Catalyse et Chimie du Solide, F-59000 Lille, France.

² Univ. Lille, CNRS, Centrale Lille, ENSCL, Univ. Artois, IMEC-Institut Michel-Eugène Chevreul F-59000 Lille, France

³ Synchrotron SOLEIL, L'Orme des Merisiers, BP48 Saint Aubin 91192 Gif-Sur-Yvette, France.

ABSTRACT

The versatility of ABO₃ perovskite oxide surface plays a central role in key materials such as fuel cell electrodes or air-remediation catalysts. In three-way catalytic process (TWC), this aspect however translates into significant lanthanum surface enrichment as La oxo-hydroxides or carbonates, having a negative impact on the catalytic activity. On the other hand, surface re-organization dynamics can be profitably used to assist the regeneration of the active phase or fine-tune the ionic mobility at seldedge. Targeting the rational design of functional perovskite surfaces, we show here a genuine surface-resolved investigation of LaFeO₃ relevant to both real-life materials and proper operating conditions. To this end, poly-crystalline thin films of LaFeO₃ and La_{0.67}FeO₃ have been specially made for being used as models, representative of both the surface and the sub-surface of LaFeO₃ and its La-deficient counterpart.

We present here a study of the electronic and structural properties of Fe under use-relevant conditions by the means of *in situ* X-Ray absorption in grazing incidence mode (GI-XAS) and near-ambient pressure XPS, run at SAMBA and TEMPO beamlines, respectively.

Especially, in the case of La-deficient perovskite, we have observed the speciation of iron in surface and bulk by varying the incidence angle upon a temperature-programmed reaction under carbon monoxide (CO).

Under CO at high temperature, majority of surface iron species are involved in the mixed (II, III) valence phase Fe₃O₄ (magnetite) while mostly remain as Fe³⁺ as B-site of LaFeO₃ in bulk, as shown in Figure 1.

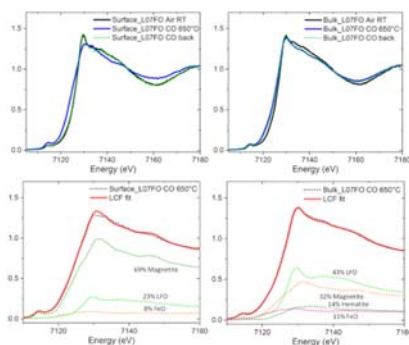


Figure 1: Top: Surface (left) and bulk (right) Fe K-edge GI-XANES spectra of La_{0.67}FeO₃ in air at room temperature (black), under CO at 650°C (blue) and return spectrum under CO at room temperature (green). Bottom: decomposition of spectra recorded at 650°C under CO using XANES spectra of reference Fe oxides.

Together with the NAP-XPS analysis of the same system, this study has allowed to draw a scenario of the structural and electronic evolution of La_{0.67}FeO₃ surfaces under CO.

REFERENCES

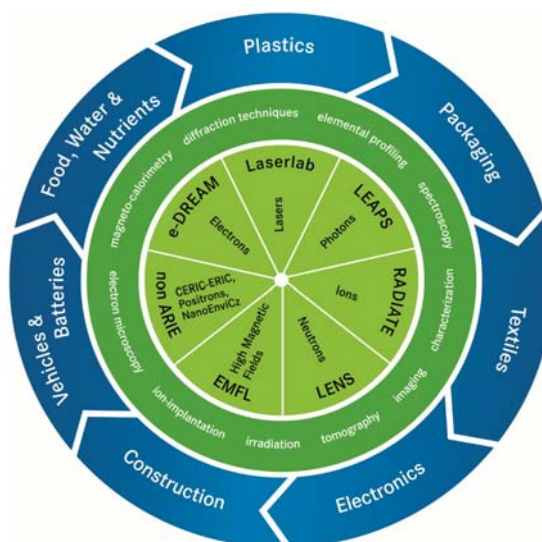
1. H. Tanaka, M. Taniguchi, M. Uenishi, N. Kajita, I. Tan, Y. Nishihata, J. Mizuki, K. Narita, M. Kimura and K. Kaneko, *Angew. Chem. Int. Ed.* **45**, pp. 5998–6002 (2006)
2. M. B. Katz, G. W. Graham, Y. Duan, H. Liu, C. Adamo, D. G. Schlom and X. Pan, *J. Am. Chem. Soc.*, **133**, pp. 18090–18093 (2011).
3. S. Nandi, D. Blanck, T. Carlier, M.-H. Chambrier, A.-S. Mamede, M. Trentesaux, P. Simon, N. Nuns, P. Roussel, A. Ferri and E. Berrier, *Surf. Interf. Anal.*, **50**, 1018–1024 (2018).

Circular Economy: Access to Research Facilities with EU Project ReMade@ARI

H. Chevreau,¹ A. Valcarel Orti,¹ C. Albert,¹ F. Fraissard,¹
B. Schramm,² S. Facsko,² A. Taleb¹

1. Synchrotron SOLEIL, L'Orme des Merisiers, 91190 Saint Aubin. France.
2. Helmholtz-Zentrum Dresden-Rossendorf, Bautzner Landstrasse 400, 01328 Dresden. Germany.

ABSTRACT



In ReMade@ARI,¹ the most significant European analytical research infrastructures join forces to pioneer a support hub for materials research facilitating a step change to the Circular Economy.

ReMade@ARI offers coordinated access to more than 50 European analytical research infrastructures, comprising most of the facilities that constitute the Analytical Research Infrastructures in Europe (ARIE) network. ReMade@ARI offers comprehensive services suiting any research focusing on the development of new materials for the Circular Economy in the key areas highlighted in the CEAP and plays an important role in the preparation of the common technology roadmap for circular industries.

The project is coordinated by HZDR² and SOLEIL³ is one of the project partners offering access to European users.

REFERENCES

1. <https://remade-project.eu/>
2. <https://www.hzdr.de>
3. <https://www.synchrotron-soleil.fr>

Structural Damage under Electron Irradiation of some Lamellar Hydrous Minerals, Analysed by XRD and Spectroscopies (Infrared, Raman and NMR)

M.-N. de Noirfontaine¹, E. Garcia-Caurel², M. Courtial^{1,3},
C. Cau Dit Coumes⁴, L. Acher^{1,4}, J. Jdaini^{1,4}, S. Tusseau-Nenez⁵,
O. Cavani¹, F. Borondics⁶, C. Sandt⁶, D. Gorse-Pomonti¹

¹Laboratoire des Solides Irradiés, CEA-DRF-IRAMIS, CNRS, Ecole Polytechnique, Institut Polytechnique de Paris, 91120, Palaiseau, France

²Laboratoire de Physique des Interfaces et des Couches Minces, CNRS, Ecole polytechnique, Institut Polytechnique de Paris, 91120 Palaiseau, France

³Université d'Artois, 1230 rue de l'Université, CS 20819, 62408 Béthune, France

⁴CEA, DES, ISEC, DE2D, SEAD, LCBC, Univ Montpellier, Marcoule, France

⁵Laboratoire de Physique de la Matière Condensée, CNRS, Ecole Polytechnique, Institut Polytechnique de Paris, 91120, Palaiseau, France

⁶Synchrotron SOLEIL, 91190, Gif - sur - Yvette Cedex, France

ABSTRACT

Electron irradiation with the SIRIUS electron accelerator at LSI allows the study of defects created by irradiation and the resulting changes in properties. The context of the present study is the optimization of cementitious matrices for the conditioning of nuclear waste. These cementitious matrices are composed of hydrated minerals, some of which are lamellar, characterized by structural layers (portlandite, gibbsite, gypsum, brushite,...).

Very few data exist in the literature on the structural damage of these hydrated lamellar minerals. X-ray diffraction and spectroscopic methods are very complementary methods to reveal the structural modifications induced by irradiation (dimensional variations of the crystal unit cell, appearance of disorder until amorphization, phase transformation,...).

We discuss here the behavior of so-called analogous structures, portlandite $\text{Ca}(\text{OH})_2$ & brucite $\text{Mg}(\text{OH})_2$, gypsum $\text{CaSO}_4 \cdot 2\text{H}_2\text{O}$ & brushite $\text{CaHPO}_4 \cdot 2\text{H}_2\text{O}$, irradiated under similar conditions, with 2.5 MeV electrons at room temperature and with high doses up to GGy. We observe on these minerals an extremely different sensitivity to irradiation. Portlandite and brucite keep their structure up to very high doses 10 GGy [1], while gypsum and brushite, for which phase transformations are observed, are much less resistant. Brushite is the most sensitive compound to irradiation, with progressive amorphization with dose to near-total amorphization at 5.5 GGy [2]. Coupled analysis by X-ray diffraction and spectroscopies (IR, Raman and NMR) revealed the progressive transformation of brushite into amorphous calcium pyrophosphate. In conclusion, the nature of the inter- and intra-sheet bond strengths under irradiation in these hydrated lamellar minerals will be discussed, as a first step to progress in the understanding of the damage mechanisms of these compounds under irradiation.

REFERENCES

1. M.-N. de Noirfontaine, L. Acher, M. Courtial, F. Dunstetter, D. Gorse - Pomonti, *Journal of Nuclear Materials*, **509**, 78-93, (2018).
2. M.-N. de Noirfontaine, E. Garcia-Caurel, D. Funes-Hernando, M. Courtial, S. Tusseau-Nenez, O. Cavani, J. Jdaini, C. Cau-dit-Coumes, F. Dunstetter, D. Gorse-Pomonti, *Journal of Nuclear Materials*, **545**, 152751, (2021).

Coherent X-ray Scattering on the D2AM Beamline at the ESRF

M. Dupraz¹, G. Stoclet, G. Chahine², N. Blanc¹, S. Arnaud¹, F. Livet¹,
JC. da Silva¹, A. Kulow¹

¹*Institut Néel, CNRS, Université Grenoble Alpes, 38000 Grenoble, France*

²*SIMaP, Grenoble INP, CNRS, Université Grenoble Alpes, 38000 Grenoble, France*

ABSTRACT

Coherent x-ray beams are typically obtained from synchrotron sources, whose high brilliance and small source size allows to obtain coherent x-ray beams of reasonable intensity and of nearly macroscopic spatial extension. The intensity available from a source in a coherent scattering experiment is connected to the average source brilliance. Typically, the brilliance achieved by Bending Magnet (BM) sources is significantly lower (typically 2 orders of magnitude) than the brilliance offered by undulator sources¹. However, the large reduction of the source size after the EBS upgrade opens new avenues for the use of coherence on BM beamlines.

Recently we explored the use of coherence on the D2AM beamline. In Bragg geometry, we used Platinum nanoparticles (NPs, 100 nm to 1 μ m in size) on a Yttria-stabilized zirconia (YSZ), obtained by solid-state dewetting to evaluate the feasibility of Bragg Coherent Diffraction Imaging. We managed to reconstruct 5 NPs using two Bragg reflections, clearly demonstrating the potential of the beamline for such measurements. This is the first demonstration of BCDI on a bending magnet (BM) beamline, opening new avenues for the use of coherence on this type of beamlines.

In transmission geometry we carried promising X-ray Photon Correlation Spectroscopy (XPCS) measurements on filled polymers. In particular we investigated crystallization dynamics in polyactide by combining XPCS and WAXS measurement. In parallel, to optimize the experimental setup for future experiments, we performed an in-depth analysis of the coherent properties of the beam using different approaches, *i.e.*, diffraction from a 5 microns pinhole, XPCS on a series of aerogel samples, and ptychography on a Siemens star sample to reconstruct both the sample and the incoming X-ray beam.

REFERENCES

1. Livet, F. Diffraction with a coherent X-ray beam: dynamics and imaging. *Acta Crystallographica Section A Foundations of Crystallography* 63, 87–107 (2007).

Structural Analysis of HCV Core Protein Associated with Lipid Droplets using SRCD and Synchrotron NanoIR

D. Rapoport¹, S. Hentati-Mansouri¹, T. Disparti¹, F. Wien²,
C. Sandt², Y. Gohon¹, M. Froissard¹

¹Université Paris-Saclay, INRAE, AgroParisTech, IJPB, F-78026, Versailles

²SOLEIL synchrotron, F-91190, Saint-Aubin

ABSTRACT

The hepatitis C virus (HCV) controls the lipid metabolic pathways of the host cell to carry out its viral cycle. The virus highjacks cell lipid droplets (LDs), the cellular structures for lipid storage. LDs serve as source of energy and lipids, but also as an assembly platform for the viral particle [1]. LD and its metabolism are therefore new targets for the development of antiviral strategies. LDs have an original organization with a neutral lipid core, surrounded by a monolayer of phospholipids and various proteins. We focus our research in a particular class of LD proteins, the class I proteins, which includes the HCV core [2] whose main function is to form the viral capsid to surround and protect the genomic RNA. LD class I proteins exhibit structural convergence with a hairpin folding. Very few structural data exist on these proteins. They are very difficult to handle due to their high hydrophobicity. Scientists bypass this bottleneck using recombinant proteins without hydrophobic domains, for RMN, crystallography, and in artificial protein/lipid reconstituted systems for CD.

Our previous work reveals that oleosin, the class I protein of LD oilseeds, can adopt various folding, depending on the detergent use for maintaining in solution, from mainly alpha to mainly beta [3,4]. These contradictory results prompted us to develop a strategy to obtain oleosin biologically folded and targeted to cellular LDs for structural studies using heterologous expression in yeast. We revealed that oleosin is mainly beta-folded when biologically inserted in LDs using SRCD on purified LDs [4]. We also shown that FTIR microspectroscopy was able to detect oleosins in LDs and evaluate their conformation on clusters of thousands LDs at spatial resolutions of 5 μm using synchrotron FTIR. We confirmed the folding of LD class I proteins observed using SRCD.

Thanks to this expertise, we propose an original structural study of HCV core protein in lipid droplets using SRCD-synchrotron nanoIR coupled approach.

REFERENCES

1. Welte, M. A. and A. P. Gould (2017). *Biochim Biophys Acta* 1862(10 Pt B): 1260-1272.
2. Kory, N., et al. (2016). *Trends Cell Biol* 26(7): 535-546.
3. Gohon, Y., et al. (2011). *Biochim Biophys Acta* 1808(3): 706-716.
4. Jamme, F., et al. (2013). *PLoS One* 8(9): e74421.

Discovery of Interstellar C₅ Molecule

J. Krelowski, W. Szajna and R. Hakalla

Materials Spectroscopy Laboratory, Institute of Physics, University of Rzeszów, Poland,
jacek@umk.edu.pl, rhakalla@ur.edu.pl

ABSTRACT

The current work demonstrates the presence of the carbon chain C₅ molecule in translucent interstellar HI clouds. This species, the only five atom interstellar molecule, observable in dark, translucent clouds, seems to be observable in reasonably dense clouds, causing also rather high reddening. The poster shows two discovered spectral features of C₅: near 4975 and 5109 Å. The attempt to discover the 3789 Å C₄ feature gave the negative result.

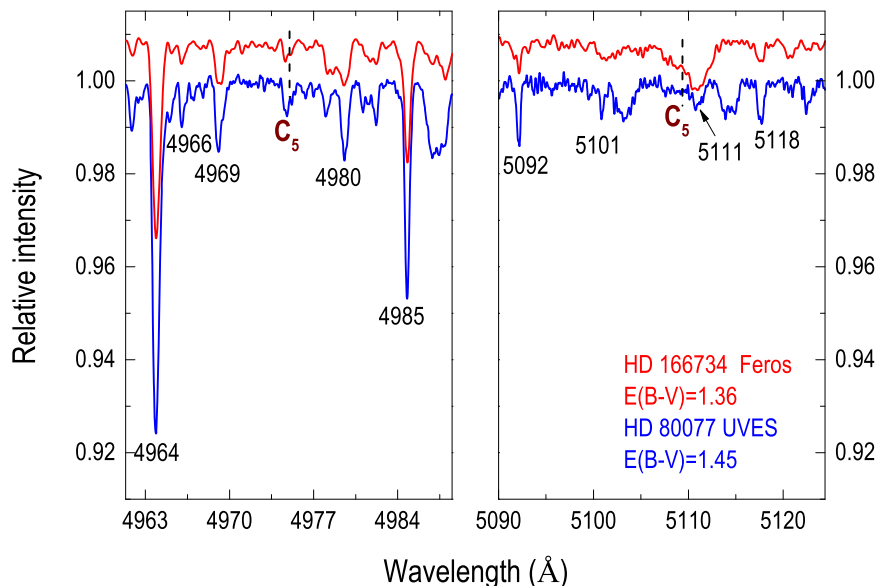


Fig. 1: The blown-up narrow ranges including the expected C₅ features. Note the presence of many DIBs^{1,2} and differences in stellar spectra. The 5109/5111 DIB is very likely a composition of two profiles. The first one coincides with the expected 5109 C₅ feature.

ACKNOWLEDGMENTS

The authors acknowledge the financial support of the National Science Centre, Poland (grant No. 2017/25/B/ ST9/01524) for the period 2018–2023. This research has made use of the services of the ESO Science Archive Facility and the SIMBAD database, operated at CDS, Strasbourg, France (Wanger et al. 2000).

REFERENCES

1. J. Krelowski, G. A. Galazutdinov, P. Gnaciński, R. Hakalla, W. Szajna, R. Siebenmorgen, *Monthly Notices of the Royal Astronomical Society*, 2021, **508**, pp. 4241 - 4248.
2. G. Galazutdinov, A. Bondar, Byeong-Cheol Lee, R. Hakalla, W. Szajna, J. Krelowski, *The Astronomical Journal*, 2020, **159**, pp. 113.

FT Spectroscopy of $^{12}\text{C}^{18}\text{O}$ and Deperturbation Analysis of the $\text{A}^1\Pi(\nu = 3)$ Level

M.I. Malicka¹, S. Ryzner², A.N. Heays³, N. de Oliveira⁴, R.W. Field⁵,
W. Ubachs⁶, W. Szajna², A. Stasik², A. Para², I. Piotrowska²,
R. Kępa² and R. Hakalla²

¹ The Faculty of Mathematics and Applied Physics, Rzeszów University of Technology, Poland.

² Materials Spectroscopy Laboratory, Institute of Physics, University of Rzeszów, Poland.

³ J. Heyrovský Institute of Physical Chemistry, Prague, Czech Republic.

⁴ Synchrotron SOLEIL, Orme de Merisiers, St. Aubin, France.

⁵ Department of Chemistry, Massachusetts Institute of Technology, Cambridge, USA.

⁶ Department of Physics and Astronomy, and LaserLaB, Vrije Universiteit, Amsterdam, Netherlands.

m.malicka@prz.edu.pl, rhakalla@ur.edu.pl

ABSTRACT

This research was carried out using two complementary methods: (i) emission VIS-FT spectroscopy with the accuracy of about 0.005 cm^{-1} by means of the Bruker IFS 125HR spectrometer (University of Rzeszów) and (ii) absorption VUV-FT spectroscopy with the accuracy ca. 0.01 cm^{-1} using the wave-front-division spectrometer working as the end station on the DESIRS beamline (SOLEIL synchrotron). An effective Hamiltonian and the *term-value fitting method* were implemented. The precise deperturbation analysis of the $\text{A}^1\Pi(\nu = 3)$ level was performed by means of the PGOPHER program [1]. The data set was consisted of more than 400 spectral lines belonging to 5 bands: $\text{B}^1\Sigma^+ - \text{A}^1\Pi(0, 3)$, $\text{C}^1\Sigma^+ - \text{A}^1\Pi(0, 3)$, $\text{A}^1\Pi - \text{X}^1\Sigma^+(3, 0)$, $\text{B}^1\Sigma^+ - \text{X}^1\Sigma^+(0, 0)$ and $\text{C}^1\Sigma^+ - \text{X}^1\Sigma^+(0, 0)$. As the results, the improved deperturbed molecular constants of the $\text{A}^1\Pi(\nu = 3)$ level and their perturbers, spin-orbit and rotation-electronic (*L*-uncoupling) interaction parameters as well as their ro-vibronic terms were obtained. The current work is a continuation of the studies on the $\text{A}^1\Pi$ state in the CO isotopologues, made by our team [1-5].

ACKNOWLEDGMENTS

RH thanks LASERLAB-EUROPE for support of this research [grants: EUH2020-RIP-654148 and EC's-SPF-284464]. AH acknowledges grant funding from the CAAS ERDF/ESF "Centre of Advanced Applied Sciences" (No. CZ.02.1.01/0.0/0.0/16_019/0000778). RWF thanks the US National Science Foundation (grant number CHE-1800410) for support of his research, which includes substantial collaborations. The authors are grateful to the general and technical staff of SOLEIL synchrotron for running the facility and providing beam time under project numbers 20120653 and 20160118.

REFERENCES

1. C. M. Western, *Journal of Quantitative Spectroscopy and Radiative Transfer*, 2017, **186**, pp. 221–242.
2. M.I. Malicka, S. Ryzner, A.N. Heays, N. de Oliveira, R.W. Field, W. Ubachs, R. Hakalla, *Journal of Quantitative Spectroscopy and Radiative Transfer*, 2021, **273**, pp. 107837.
3. R. Hakalla, M. Niu, R.W. Field, E. Salumbides, A. Heays, G. Stark, J. Lyons, M. Eidelsberg, J.L. Lemaire, S. Federman, M. Zachwieja, W. Szajna, P. Kolek, I. Piotrowska, M. Ostrowska-Kopec, R. Kępa, N. De Oliveira, W. Ubachs, *Royal Society of Chemistry Advances*, 2016, **6**, pp. 31588 – 31606.
4. S. Ryzner, M.I. Malicka, A.N. Heays, R.W. Field, N. de Oliveira, W. Szajna, W. Ubachs, R. Hakalla, *Spectrochimica Acta Part A*, 2022, **279**, pp.121367.
5. R. Hakalla, M.L. Niu, R.W. Field, A.N. Heays, E.J. Salumbides, G. Stark, J.R. Lyons, M. Eidelsberg, J.L. Lemaire, S.R. Federman, N. de Oliveira, W. Ubachs, *Journal of Quantitative Spectroscopy and Radiative Transfer*, 2017, **189**, pp. 312 – 328.

Spectroscopy of $^{13}\text{C}^{18}\text{O}$ and Extended Deperturbation Analysis of the $\text{A}^1\Pi(v = 2)$ Level

S. Ryzner¹, M.I. Malicka², A.N. Heays³, W. Ubachs⁴, R.W. Field⁵,
N. de Oliveira⁶, W. Szajna¹, A. Stasik¹, A. Para¹, I. Piotrowska¹, R. Kępa¹
and R. Hakalla¹

¹ Materials Spectroscopy Laboratory, Institute of Physics, University of Rzeszów, Poland.

² The Faculty of Mathematics and Applied Physics, Rzeszów University of Technology, Poland.

³ J. Heyrovský Institute of Physical Chemistry, Prague, Czech Republic.

⁴ Department of Physics and Astronomy, and LaserLaB, Vrije Universiteit, Amsterdam, Netherlands.

⁵ Department of Chemistry, Massachusetts Institute of Technology, Cambridge, USA.

⁶ Synchrotron SOLEIL, Orme de Merisiers, St. Aubin, France.

sryzner@ur.edu.pl, rhakalla@ur.edu.pl

ABSTRACT

The aim of this work was a thorough reinvestigate of the $\text{A}^1\Pi(v = 2)$ level in the $^{13}\text{C}^{18}\text{O}$ isotopologue. For this purpose, two complementary Fourier-transform techniques was used to obtain the spectra: (i) the emission spectroscopy in the visible region using Bruker IFS 125HR FT-spectrometer (University of Rzeszów) and (ii) the vacuum-ultraviolet absorption spectroscopy using the wave-front-division spectrometer working as the end station on the DESIRS beamline (SOLEIL synchrotron).

A deperturbation analysis of the $\text{A}^1\Pi(v = 2)$ level in the $^{13}\text{C}^{18}\text{O}$ isotopologue was conducted on the basis of obtained data using the PGOPHER program [1]. In the analysis, an effective Hamiltonian and the term-value fitting approach were applied. As a result, precise molecular parameters of the $^{13}\text{C}^{18}\text{O}$ investigated levels were obtained, including: molecular constants, interaction parameters as well as ro-vibronic terms of the $\text{B}^1\Sigma^+(v = 0)$, $\text{B}^1\Sigma^+(v = 1)$ and $\text{C}^1\Sigma^+(v = 0)$ levels.

The new results provide a significantly improved (compare to the previous one [2]) description of the complex set of intra-molecular interactions within the $^{13}\text{C}^{18}\text{O}$ $\text{A}^1\Pi(v = 2)$ level. This research is a continuation of the studies on the $\text{A}^1\Pi$ state and its numerous perturbers in the CO isotopologues made by our team [3 - 7].

ACKNOWLEDGMENTS

RH thanks LASERLAB-EUROPE for support of this research [grants: EUH2020-RIP-654148 and EC's-SPF-284464]. AH acknowledges grant funding from the CAAS ERDF/ESF "Centre of Advanced Applied Sciences" (No. CZ.02.1.01/0.0/0.0/16_019/0000778). RWF thanks the US National Science Foundation (grant number CHE-1800410) for support of his research, which includes substantial collaborations. The authors are grateful to the general and technical staff of SOLEIL synchrotron for running the facility and providing beam time under project numbers 20120653 and 20160118.

REFERENCES

1. C. M. Western, *Journal of Quantitative Spectroscopy and Radiative Transfer*, 2017, **186**, pp. 221–242.
2. C. Haridass, S. P. Reddy, A. C. Le Floch, *Journal of Molecular Spectroscopy*, 1994, **167**, pp. 334–352.
3. S. Ryzner, M.I. Malicka, A.N. Heays, R.W. Field, et al., *Spectrochimica Acta Part A*, 2022, **279**, pp.121367.
4. R. Hakalla, M. L. Niu, R. W. Field, E. J. Salumbides, et al., *Royal Society of Chemistry Advances*, 2016, **6**, pp. 31588–31606.
5. R. Hakalla, T.M. Trivikram, A.N. Heays, E.J. Salumbides, et al., *Molecular Physics*, 2019, **117**, pp. 79–96.
6. R. Hakalla, M. L. Niu, R. W. Field, et al., *Journal of Quantitative Spectroscopy and Radiative Transfer*, 2017, **189**, 312–328.
7. M. I. Malicka, S. Ryzner, A. N. Heays, et al., *Journal of Quantitative Spectroscopy and Radiative Transfer*, 2021, **273**, pp. 107837.

Resolving the Symmetry of the C_{60}^+ Cation: How High-resolution Photoelectron Spectroscopy meets Astrophysics

H.R. Hrodmarsson

LISA UMR CNRS 7583, Université Paris Est Créteil and Université Paris Diderot, Institut Pierre Simon Laplace, 61 Avenue du Général de Gaulle, 94010 Créteil, France

ABSTRACT

Despite C_{60}^+ being the first molecular carrier of the diffuse interstellar bands (DIBs) to be identified, there is still ambiguity in the literature concerning its photophysics.¹ There have been studies that favor D_{3d} symmetry² whilst *ab initio* theoretical calculations seem to favor D_{5d} symmetry.³ To resolve this issue, we recorded the first high-resolution threshold photoelectron spectrum (TPES) of C_{60} and in combination with molecular dynamics DFTB calculations, we show that when our results are compared to an *ab initio* photoelectron spectrum (PES), a D_{5d} symmetric ground state interpretation is irrefutable.⁴ This allows us to further elucidate the photoexcitation mechanisms of the transitions that have been assigned to several DIBs in diffuse interstellar space.

REFERENCES

1. H. R. Hrodmarsson, G. A. Garcia, H. Linnartz, L. Nahon, *Phys. Chem. Chem. Phys.* 2020, **22**, 13880.
2. S. Canton, A. Yench, E. Kukk, J. Bozek, M. Lopes, G. Snell, N. Berrah. *Phys. Rev. Lett.* 2002, **89**(4), 045502.
3. N. Manini, P. Gattari, E. Tosatti. *Phys. Rev. Lett.* 2003, **91**(19), 196402.
4. H. R. Hrodmarsson, M. Rapacioli, F. Spiegelman, G. A. Garcia, J. Bouwman, L. Nahon, H. Linnartz, *in preparation*

Electrostatic Alignment for Micro- and NanoARPES: First Results

T. Wätjen¹, H. Karakachian¹, C. Polley², K. Ali²,
T. Hashimoto¹, P. Karlsson¹

¹ Scienta Omicron AB, Danmarksгатan 22, 75323 Uppsala, Sweden

² MAX IV Laboratory, Fotogatan 2, 225 94 Lund, Sweden

Author Email: h.karakachian@scientaomicron.com

ABSTRACT

High quality ARPES measurements, particularly micro/nanoARPES, require optimised alignment. Without optimal alignment, deflection mode measurement performance is reduced. The required iterative alignment of sample position and light source to match the analyser focal point is a time-consuming process. We present groundbreaking Electrostatic 3D Focus Adjustment technology for DFS30 analysers, replacing the imprecise mechanical movements of samples and beamline optics with electronic precision. This significantly improves workflow, speed, and reproducibility when optimizing experimental conditions. The DFS30 analyser introduces dynamic lens tables that enable real time electronic shifting of the analyser focal point in three dimensions for transmission, angular, and deflection modes. We will show how the alignment of focal point and emission spot is particularly important in micro/nanoARPES and how the electronic alignment achieves this without mechanical movements. ARPES spectra of graphene measured at the Bloch beamline at MAX IV are presented to showcase this groundbreaking technology

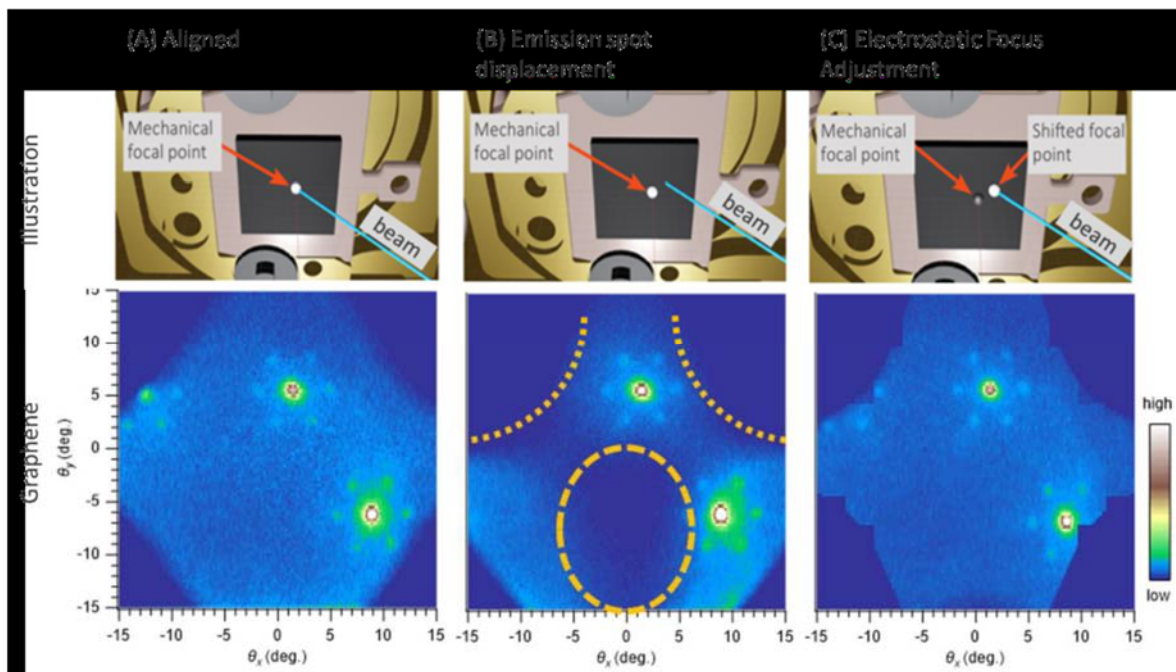


Fig. 1: (A) shows a well-aligned situation with the analyser focal point and photoelectron emission spot overlapping and a uniform background intensity. (B) The 15 μm emission spot is misaligned by 200 μm . The corresponding measurement now shows shadowing and asymmetry. (C) Using Electrostatic 3D Focus Adjustment, the analyser focal point is easily shifted to the displaced emission spot, recovering the uniform background intensity without shadows as in (A) for the well aligned situation.

Spectral Ptychography at the SWING Beamline

A. Kulow¹, R. Boudjehem¹, J.-L. Hazemann¹, S. Ould-Chickh²,
J. Perez³, J. C. da Silva¹

¹ Univ. Grenoble Alpes, CNRS, Grenoble INP, Institut Néel, 38000 Grenoble, France

² King Abdullah University of Science and Technology, KAUST Catalysis Center,
Advanced Functional Materials, Thuwal 23955, Saudi Arabia R.

³ Synchrotron SOLEIL, 91190 St Aubin, France

ABSTRACT

The nanoprobe endstation at the SWING beamline allows for 2D nano ptychography and 3D nano tomo ptychography [1]. Ptychography is a scanning coherent diffractive imaging technique [2]. A probe with size in the micrometer range is used to scan a sample, with an overlap between adjacent scan positions. The complex-valued object function is iteratively retrieved, using the diffraction patterns measured at each scan position. The resolution is not limited by X-ray optics, the probe size, or the scanning step width, but only by the maximum angle at which speckles can be recorded with a reasonable signal-to-noise-ratio. A further advantage of ptychography is that both phase and absorption contrast can be exploited, thus allowing the investigation of only weakly absorbing samples. In 3D-nano-tomo-ptychography, ptychographic projections are recorded at different angles in a range of 180°. From these projections, a 3D tomogram of the δ and β values can be reconstructed, with δ and β being the components of the complex refractive index, which is related to the complex scattering factor :

$$n = 1 - \delta + i\beta = 1 - \frac{r_e}{4\pi} \lambda^2 \cdot \sum_k n_{at}^k [(f_{0k} + f'_{0k} + if''_{0k})] \quad (1)$$

with r_e the classical electron radius, λ the wavelength of the incoming X-rays, n_{at} the atomic density, $f = f_0 + f' + if''$ the atomic scattering factor, and the sum goes over all components of the sample. This offers the possibility to get quantitative information of the sample, as δ is directly proportional to the electron density [3].

Performing ptychographic measurements at different incident energies including the energy of the absorption edge of an element of interest (resonant or spectral ptychography) adds spectral information. As the scattering factor varies only slowly with energy far from absorption edges, the differences between the tomograms recorded at resonant energy and off resonant energy can be attributed to the element of interest [4].

Here, we will show measurements on a Ni wire (Fig. 1A) performed at SWING to show the principle of 2D spectral ptychography and 3D resonant ptychographic X-ray computed tomography and the performance of the nanoprobe endstation. We can extract an absorption and a δ spectrum (Fig. 1B and 1C) from the measured ptychographic projections, and determine the electron and atomic density from the reconstructed tomogram.

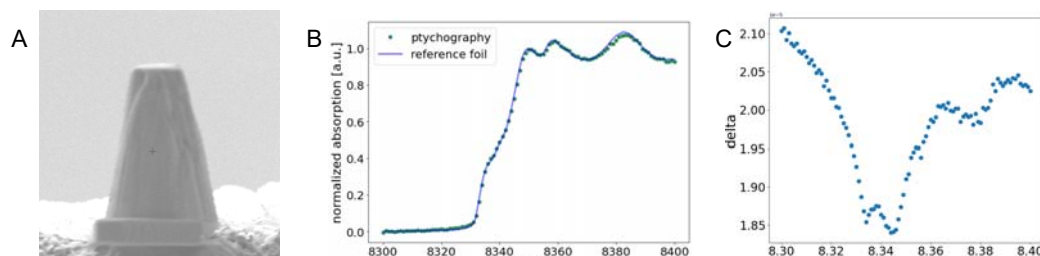


Figure 1: A) The Ni wire sample as prepared by focused ion beam (FIB) milling. B) The absorption spectrum of the Ni wire found by 2D spectral ptychography (dots) compared to a classical XANES spectrum of a Ni reference foil (line). C) δ -spectrum of the Ni wire calculated from 2D spectral ptychography measurements.

REFERENCES

1. C. Engblom et al., 17th Int. Conf. on Acc. and Large Exp. Physics Control Systems ICALPECS2019, New York, NY, USA
2. J.M. Rodenburg and H.M.L. Faulkner, *Appl. Phys. Letters* **85**, 4795-4797 (2004).
3. A. Diaz et al., *Physical Review B* **85**, 020104 (R) (2012).
4. C. Donnelly et al., *Physical Review Letters*, PRL **114**, 115501 (2015).

Fuzzy DNA Recognition by the *Vibrio cholerae* Transcription Factor HigBA2

R. Loris¹, Z. Živič², M. Kovačič³, U. Zavrtnik², S. Haesaerts¹,
J. Plavec³, D. Charlier⁴, A. Volkov¹, J. Lah² and S. Hadži²

1. Structural Biology Brussels, VIB and VUB, Pleinlaan 2, B-1050 Brussels, Belgium

2. Department of Physical Chemistry, Faculty of Chemistry and Chemical Technology,
University of Ljubljana, Večna pot 113, 1000 Ljubljana, Slovenia

3. Slovenian NMR Center, National Institute of Chemistry, Hajdrihova, 19, Ljubljana SI-1000, Slovenia

4. Laboratory for Genetics and Microbiology, Department of Biotechnology, Vrije Universiteit Brussel,
Pleinlaan 2, B-1050 Brussels, Belgium

ABSTRACT

Fuzzy binding of macromolecules is a poorly understood phenomenon where at least one of the partners in an otherwise specific macromolecular interaction remains unfolded. Such fuzzy recognition entails a high degree of specificity and can occur with high affinity, thus defying the classical structure-function paradigm. It is best known for its importance for the formation of membrane-less organelles in Eukaryotes through liquid-liquid phase separation. However, fuzzy recognition also occurs commonly outside the context of LLPS and can occur in a large variety of flavors¹.

Toxin-antitoxin (TA) systems are small bacterial operons that encode a protein that inhibits a part of the basic cellular metabolism (the "toxin" acting on translation, transcription, cell wall synthesis, ...) and a corresponding regulator (the "antitoxin") that inhibits the action of the toxin during normal growth. TA antitoxins typically are composed of a folded DNA binding domain combined with an intrinsically disordered toxin neutralizing domain that folds upon binding the toxin².

Here we present the fuzzy interaction between the antitoxin HigA2 from the *Vibrio cholerae* higBA2 toxin-antitoxin operon and its operator. HigA2 controls repression via the interplay between a classic helix-turn-helix motif and fuzzy recognition via its intrinsically disordered domain. The folded domain confers specificity towards a single 5'-TGACGC(N)5GCGTACA-3' operator sequence while the IDP region enhances affinity without folding. Upon binding, the IDP region remains disordered, but its conformational ensemble is reduced and a subset of residues show changes in their NMR chemical shifts. Removal of the IDP or its sequestration by the HigB2 toxin reduces DNA binding and increases transcription *in vitro* and *in vivo*. Alanine scanning mutagenesis as well as sequence scrambling show a large degree of specificity at the individual amino acid level, with both charges and hydrophobicity contributing to affinity. Together, this results in ratio-dependent regulation of transcription through a mechanism that differs from the classic conditional cooperativity³ mechanism that is observed in transcription regulation of many TA systems.

REFERENCES

1. P. Tompa and M. Fuxreiter, *The New Physique, Trends Biochem. Sci.* **33**, 2-8 (2008).
2. D. Jurenas, Fraikin N., Goormaghtigh F. and Van Melderen L. *Nat. Rev. Microbiol.* **20**, 335-350 (2022).
3. A. Garcia-Pino et al. *Cell* **142**, 110-111 (2010).

Combien de Photons ?

Y. Ménesguen¹, V. Hernandez-Elvira¹, M-C. Lépy¹

¹Université Paris-Saclay, CEA, LIST, Laboratoire National Henri Becquerel (LNE-LNHB),
F 91120 Palaiseau, France.

ABSTRACT

La caractérisation absolue en rendement des détecteurs permet de connaître la puissance optique incidente sur l'échantillon étudié et s'avère indispensable pour les applications à caractère métrologique et pour des analyses quantitatives précises. L'utilisation d'un radiomètre cryogénique à substitution électrique est une technique largement utilisée par les laboratoires de métrologie nationaux, particulièrement dans le domaine des rayonnements visibles (1,2). La technique est basée sur l'équivalence entre la puissance fournie par le rayonnement photonique et la puissance produite par un courant électrique.

L'application aux rayonnements X a été initialement développée par le CEA/DAM (3) et remis récemment en service par le CEA/LNE-LNHB : le bolomètre (BOLUX : BOLomètre pour l'Utilisation dans le domaine des rayons X) utilise un cristal de germanium refroidi à 4 K comme élément de détection de l'élévation de température. Pour une sensibilité accrue aux puissances optiques faibles (jusqu'à quelques nW), il est possible de refroidir à 1,3 K le cristal, mais l'expérience a montré que la sensibilité maximale ainsi obtenue n'est pas nécessaire quand la puissance est supérieure au μW , et qu'on pouvait se contenter d'un refroidissement à 4 K. La mesure de la puissance optique d'un rayonnement X monochromatique s'effectue en deux temps : le bolomètre est soumis au rayonnement photonique, puis le faisceau est occulté et le bolomètre est chauffé par un courant électrique d'intensité telle que l'élévation de température soit identique à celle obtenue avec les photons. Les grandeurs électriques sont mesurées de manière absolue grâce à des électromètres étalonnés et la puissance obtenue peut être déterminée avec une très faible incertitude.

Grâce au bolomètre BOLUX, nous avons pu caractériser en puissance le faisceau monochromatique des lignes METROLOGIE et PUMA afin d'étalonner la réponse en rendement (A.W^{-1}) de photodiodes du marché avec une incertitude de l'ordre de 1 % sur la gamme 1-60 keV en utilisant les gammes d'énergies combinées des lignes de lumière METROLOGIE (branches XDURS et XUV) et PUMA. Pour appuyer ces étalonnages qui dépassent la gamme originelle du bolomètre, des simulations de Monte-Carlo viennent quantifier la perte de rendement dû à l'échappement des photons de fluorescence pour une énergie de photons incidents supérieure à l'énergie de liaison K du germanium ainsi qu'à la transmission du faisceau incident à travers le cristal de germanium. Les résultats ont été comparés avec les valeurs de rendement fournies par le constructeur pour une diode de la même gamme et montrent un très bon accord avec les mesures.

REFERENCES

1. O. Touayar, J.-M. Coutin, J. Bastie, « Le radiomètre cryogénique : référence primaire du BNM-INM pour les mesures de rayonnements optiques », Bulletin du BNM N° 177, Volume 1999-3, 35-44.
2. M. Gerlach, M. Krumrey, L. Cibik, P. Müller, G. Ulm, "A cryogenic electrical substitution for hard X-rays", Nuclear Instruments and Methods in Physics Research A 580 (2007) 218-221.
3. P. Troussel, N. Coron, "BOLUX : a cryogenic electrical-substitution radiometer as high accuracy detector in the 150-11000 eV range", Nuclear Instruments and Methods in Physics Research A 614 (2010) 260-270.
4. V. H.-Elvira, M.-C. Lépy, Y. Ménesguen, "Primary calibration of photodiodes with monochromatic X-ray beams using an electrical-substitution radiometer", X-ray Spectrometry, doi : 10.1002/xrs.3318

Reaction Cells for Operando Studies of Catalysts using Synchrotron Radiation

A. Nassereddine¹, A. Aguilar Tapia¹, S. Ould-Chikh², A. Prat¹,
E. Lahera³, O. Proux³, I. Kieffer³, S. Min³, D. Testemale¹,
M. Rovezzi³, I. Maurin¹, J. Gascon² and J-L. Hazemann¹

¹ Institut Néel, Univ. Grenoble Alpes, CNRS, Grenoble INP, 38000 Grenoble, France

² King Abdullah University of Science and Technology (KAUST), KAUST Catalysis Center (KCC) and Physical Sciences and Engineering Division (PSE), 4700 KAUST, Thuwal, 23955-6900, Saudi Arabia

³ OSUG, UMS 832 CNRS - Université Grenoble Alpes, F-38041 Grenoble, France

ABSTRACT

Heterogeneous catalysis plays an essential role in many industrial processes and holds a great potential to address current global challenges [1]. However, while the potential of heterogeneous catalysts is undeniable, our ability to design more active catalysts is hampered by the lack of detailed understanding of the catalyst during reaction. This lack of information is detrimental to the determination of the structure-catalytic reactivity relationships of catalysts and identification of their active sites, which is necessary for a better understanding of catalytic mechanisms. It is therefore essential to study heterogeneous catalysts under "operando" conditions, by experimental techniques allowing, in parallel, the monitoring of the possible evolution of the catalyst structure under gas, and the evaluation of its catalytic activity.

X-ray absorption spectroscopy (XAS) using synchrotron radiation is well adapted to study catalytic materials in working conditions. This technique enables an adequate analysis of the electronic and geometric structure of an element, in particular the active phase of a catalyst [2]. In this contribution, we present several examples of operando XAS studies of catalysts during different reactions, using different experimental set-ups. Our first reactor (Fig.1.A) can operate at high temperatures (up to 1000 °C) and atmospheric pressure [3], i.e. under conditions commonly applied in heterogeneous catalysis of industrial and environmental interest. The design offers the capability to use fluorescence and transmission detection modes and includes a plug-flow reactor made from glassy carbon, which allows the majority of the X-rays to be transmitted to the sample. In contrast, our second reactor (Fig. 1.B) can operate at high pressures (up to 1000 bar) [4], which makes it ideal for the characterization of catalysts in reactions requiring high-pressure conditions. The reaction cells have been successfully used in different experiments (Fig. 1.C) and they are available for users of the BM30 and BM16 beamlines at the ESRF.

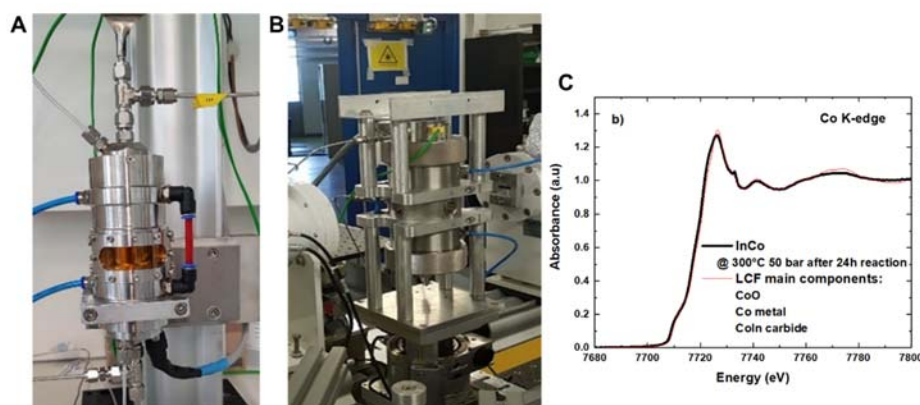


Figure 1. operando catalytic set-up available in the BM-30 (FAME) and BM-16 (FAME-UHD) beamline at ESRF using (A) High temperature reaction cell (up to 1000 °C) and (B) High temperature/pressure reaction cell (1000°C/1000 bar). (C) Co K-edge spectrum of an InCo catalyst under reaction conditions at 50 bar and 300 °C.

REFERENCES

1. Fecheté, I.; Wang, Y.; Védrine, J. C., *Catal. Today* 189, 2–27 (2012)
2. Nachtegaal, M., Müller, O., König, C. and Frahm, R., 2016. *X-Ray Absorption and X-Ray Emission Spectroscopy: Theory and Applications*, 155-183 (2016).
3. Aguilar-Tapia, A., Ould-Chikh, S., Lahera, E., Prat, A., Delnet, W., Proux, O., Kieffer, I., Basset, J.-M., Takanabe, K., & Hazemann, J.-L., *Review of Scientific Instruments* 89, 035109 (2018).
4. Testemale, D., Argoud, R., Geaymond, O., & Hazemann, J.-L., *Review of Scientific Instruments* 76, 043905 (2005).

Structural Properties of TbMgNi_{4-x}Co_x Compounds and their Hydrides

V. Paul-Boncour¹, F. Couturas¹, H. Bénet¹, F. Cuevas¹,
J. Zhang¹, E. Elkaim³, V.V. Shtender^{1,2}

¹Université Paris-Est, ICMPE (UMR7182), CNRS, UPEC, F-94320 Thiais, France

²Department of Chemistry – Ångström Laboratory, Uppsala University, Box 538,
Uppsala 75121, Sweden

³Synchrotron SOLEIL, L'Orme des Merisiers, Saint-Aubin, BP 48, 91192 Gif-sur-Yvette, France

ABSTRACT

Magnesium metal is a very attractive materials for hydrogen storage with high gravimetric hydrogen capacity (7.6 wt. % H₂). However, due to some drawbacks as slow kinetics and high hydride stability, its use as a medium for energy storage and transportation is limited. To improve both thermodynamic and kinetic properties, Mg-based binary and ternary intermetallic compounds have been extensively investigated [1]. The *R*-Mg-*T* (*R* = rare earth, *T* = Ni, Co, Cu) ternary alloys have attracted interest as hydrogen absorbing materials with reversible hydrogen capacity in ambient conditions. Many studies have been conducted on the hydrogenation properties of *RMgNi*₄ compounds (preferably with *R* = light rare earth) [2,3]. We have systematically investigated *RMgNi*_{4-x}Co_x compounds [4, 5], where a 50 % increase of the hydrogen capacity was found upon Co for Ni substitution.

TbMgNi_{4-x}Co_x alloys crystallize in a cubic SnMgCu₄ structure type and form a solid solution with a linear cell volume increase versus Co content [6]. TbMgNi₄ can absorb 3.8 H/f.u forming an orthorhombic hydride (*Pmn*2₁ S.G). Upon Co for Ni substitution, the first plateau pressure decreases whereas a second plateau is observed at higher pressure for *x* ≥ 2 with a maximum capacity of 6.5 H/f.u. for *x* = 4. Two hydrides with different structures are observed for *x* ≥ 2. For *x* = 2-3, the hydrides, with capacity of 3.8-4.1 H/f.u., are orthorhombic (*Pmn*2₁ S.G). For *x* = 4, TbMgCo₄H_{3.9} is monoclinic (*Pm* S.G.), while for higher concentration of hydrogen the cubic structure is preferred. The structural properties of the TbMgCo₄ alloy and deuterides have been studied versus temperature by X-ray diffraction with synchrotron radiation (CRISTAL BL @ SOLEIL, Saint Aubin) and neutron diffraction (D2B and D20 @ ILL, Grenoble). Their structural evolution will be presented and discussed considering magnetostrictive effects for the alloy.

REFERENCES

1. J.-C. Crivello, R.V. Denys, M. Dornheim, M. Felderhoff, D.M. Grant, J. Huot, T. R. Jensen, P. de Jong, M. Latroche, G. S. Walker, C. J. Webb and V.A. Yartys, *Appl. Phys. A*, **122**, 85 (2016).
2. H. Oesterreicher and H. Bittner, *J. Less-Common Met.*, **73**, 339–344, (1980)
3. J.-L. Bobet, E. Gaudin and S. Couillaud, In: F. Souza and E. Leite (eds) *Nanoenergy*. Springer, Cham, (2018).
4. V.V. Shtender, R.V. Denys, V. Paul-Boncour, A.B. Riabov and I.Yu. Zavaliy, *J. Alloys Compds*, **603**, 7–13. (2014).
5. V.V. Shtender, R.V. Denys, V. Paul-Boncour, Yu.V. Verbovytsky and I.Yu. Zavaliy, *J. Alloys Compds*. **639**, 526–532 (2015).
6. V.V. Shtender, V. Paul-Boncour, R.V. Denys, J.-C. Crivello and I.Y. Zavaliy, *J. Phys. Chem. C*, **124**, 196-204, (2020).

Structure and Energetics of GTP- and GDP-tubulin Isodesmic Self-association

A. Shemesh, A. Ginsburg, R. Dharan,
Y. Levi-Kalishman, I. Ringel and U. Raviv

*Institute of Chemistry, The Hebrew University of Jerusalem,
Edmond J. Safra Campus, Givat Ram, Jerusalem 9190401, Israel*

ABSTRACT

Tubulin self-association is a critical process in microtubule dynamics. The early intermediate structures, energetics, and their regulation by fluxes of chemical energy, associated with guanosine triphosphate (GTP) hydrolysis, are poorly understood. We reconstituted an in vitro minimal model system, mimicking the key elements of the nontemplated tubulin assembly. To resolve the distribution of GTP- and guanosine diphosphate (GDP)-tubulin structures, at low temperatures (~ 10 °C) and below the critical concentration for the microtubule assembly, we analyzed in-line size-exclusion chromatography–small-angle X-ray scattering (SEC-SAXS) chromatograms of GTP- and GDP-tubulin solutions. Both solutions rapidly attained steady state. The SEC-SAXS data were consistent with an isodesmic thermodynamic model of longitudinal tubulin self-association into 1D oligomers, terminated by the formation of tubulin single rings. The analysis showed that free dimers coexisted with tetramers and hexamers. Tubulin monomers and lateral association between dimers were not detected. The dimer–dimer longitudinal self-association standard Helmholtz free energies were $-14.2 \pm 0.4 k_B T$ (-8.0 ± 0.2 kcal mol $^{-1}$) and $-13.1 \pm 0.5 k_B T$ (-7.4 ± 0.3 kcal mol $^{-1}$) for GDP- and GTP-tubulin, respectively. We then determined the mass fractions of dimers, tetramers, and hexamers as a function of the total tubulin concentration. A small fraction of stable tubulin single rings, with a radius of 19.2 ± 0.2 nm, was detected in the GDP-tubulin solution. In the GTP-tubulin solution, this fraction was significantly lower. Cryo-TEM images and SEC-multiangle light-scattering analysis corroborated these findings. Our analyses provide an accurate structure–stability description of cold tubulin solutions.

REFERENCES

1. A Shemesh, A Ginsburg, R Dharan, Y Levi-Kalishman, I Ringel, U Raviv ACS Chemical Biology 16 (11), 2212-2227

Contribution de SOLEIL au PEPR DIADEM

J-P. Rueff¹

¹. *Synchrotron SOLEIL, L'Orme des Merisier, Départementale 128, 91190 Saint-Aubin*

ABSTRACT

DIADEM est un projet ANR PEPR exploratoire lancé en juin 2022 à l'initiative du CNRS et du CEA. Le projet rassemble de nombreux groupes de recherche français travaillant dans le domaine des matériaux en mettant l'accent sur la découverte accélérée notamment guidée par l'IA, le design numérique, et la caractérisation haut débit. Les thématiques de DIADEM sont larges qui couvrent la métallurgie, les problèmes de corrosion, les céramiques, les nanomatériaux, les polymères et matériaux hybrides, les MOF, les matériaux architecturés, les voies de synthèse par chimie combinatoire, l'impression 4D, etc. SOLEIL fait partie des plateformes de caractérisation retenues dans DIADEM. Le poster donne un bref aperçu de la contribution de SOLEIL au sein de DIADEM et des futures étapes du projet.

Deciphering the Mechanism of Formation of CoRu Nanoalloys using *in situ* Spectroscopy Techniques

L. Sicard,¹ B. Azeredo,¹ N. Huang,¹ L. Barthe,² M. Giraud,¹
J. Peron,¹ J.-Y. Piquemal,¹ V. Briois²

¹ Université de Paris, ITODYS, CNRS, UMR 7086, 15 rue J-A de Baïf, F-75013 Paris, France

² Synchrotron SOLEIL, L'Orme des Merisiers, BP48, Saint-Aubin, 91192 Gif-sur Yvette, France

ABSTRACT

Bimetallic nanoparticles (NPs) display tunable properties and synergetic effects for different catalytic reactions.¹ Recently, we reported the high activity and selectivity of unsupported Ru-decorated Co NPs for the acceptorless dehydrogenation of alcohols.² These results were an incentive to prepare Co-Ru nanoalloys.

Bimetallic nanoplatelets were prepared by reducing Ru(III) and Co(II) acetylacetonate (acac) salts under reflux in octan-1-ol playing the role of both the solvent and the reducing agent.³ The key parameter to obtain homogeneously distributed Co and Ru atoms was to choose metal precursors and a solvent permitting a concomitant reduction of Ru(III) and Co(II). The reduction kinetics of the two metal salts were studied by UV-visible and X-ray absorption (XAS) spectroscopies. The first one revealed a quick reduction at ca. 170 °C of Ru(III) species for pure Ru(acac)₃ as well as for a mixture with Co(acac)₂. *In situ* XAS experiments were carried out using a cell designed on purpose for this experiment on the Rock Soleil beamline. The spectra were processed using Principal Component Analysis (PCA) and Multivariate Curve Resolution with Alternating Least Squares (MCR-ALS).^{4,5} The analysis at the Ru-K edge confirmed the UV-visible results. The Co K-edge analysis showed, on the contrary, a clear influence of the presence of Ru(III) on the reduction of Co(II) species which occurs at an early stage when adding Ru. Moreover, for the Co monometallic system, a CoO-like intermediate species was evidenced at the boiling temperature and its reduction to Co(0) necessitates to remain under reflux for a sufficient time. On the contrary, CoO was not observed for bimetallic systems for which Co(II) reduction occurs concomitantly with that of Ru(III) when reaching the boiling temperature. This is in agreement with the fact that Ru is known as a promoter for the reduction of Co in Fischer Tropsch catalysis:⁶ the Ru(0) would form first and activate hydrogen, allowing the complete reduction of Ru(III) and Co(II) species by an autocatalytic process, followed by solid state diffusion.⁷ This was experimentally observed by *in situ* monitoring the volume of H₂ produced during the synthesis. The nanoalloys were tested for the acceptorless dehydrogenation of octan-2-ol. A clear synergetic effect was evidenced. The Co₅₀Ru₅₀ composition exhibits the best performances, with turnover numbers surpassing pure Co NPs with the same morphology and structure.

REFERENCES

1. K.D. Gilroy, A. Ruditskiv, H.-C. Peng, D. Qin and Y. Xia, *Chem. Rev.* **116**, 10414-10472 (2016).
2. A. Viola, J. Peron, K. Kazmierczak, M. Giraud, C. Michel, L. Sicard, N. Perret, P. Beaunier, M. Sicard, M. Besson and J.-Y. Piquemal, *Catal. Sci. Technol.* **8**, 562-572 (2018).
3. B. Azeredo, T. Ben Ghzaïel, N. Huang, K. Kazmierczak, W. Shen, G. Wang, D. Schaming, P. Beaunier, P. Decorse, N. Perret, J. Peron, M. Giraud, C. Michel, L. Sicard and J.-Y. Piquemal, *ACS Applied Nano Materials* **5**, 5733-5744 (2022).
4. A. De Juan, J. Jaumot and R. Tauler, *Anal. Methods* **6**, 4964-4976 (2014).
5. J. Jaumot, R. Gargallo, A. De Juan and R. Tauler *Chemom. Intell. Lab. Syst.* **76**, 101-110 (2005).
6. E. Iglesia, S. L. Soled, R. A. Fiato and G. H. Via, *J. Catal.* **143**, 345-368 (1993).
7. J. Hong, E. Marceau, A. Y. Khodakov, L. Gaberová, A. Griboval-Constant, J. S. Girardon, C. La Fontaine and V. Briois, *ACS Catal.* **5**, 1273-1282 (2015).

Evidence of Ion-migration in Hybrid Perovskite Films under Electrical Bias: A STXM Study

H. Jun^{1,3}, D. Tondelier³, B. Geffroy^{2,3}, P. Schulz⁴, J-E Bouree³,
Y. Bonnassieux³ & S. Swaraj¹

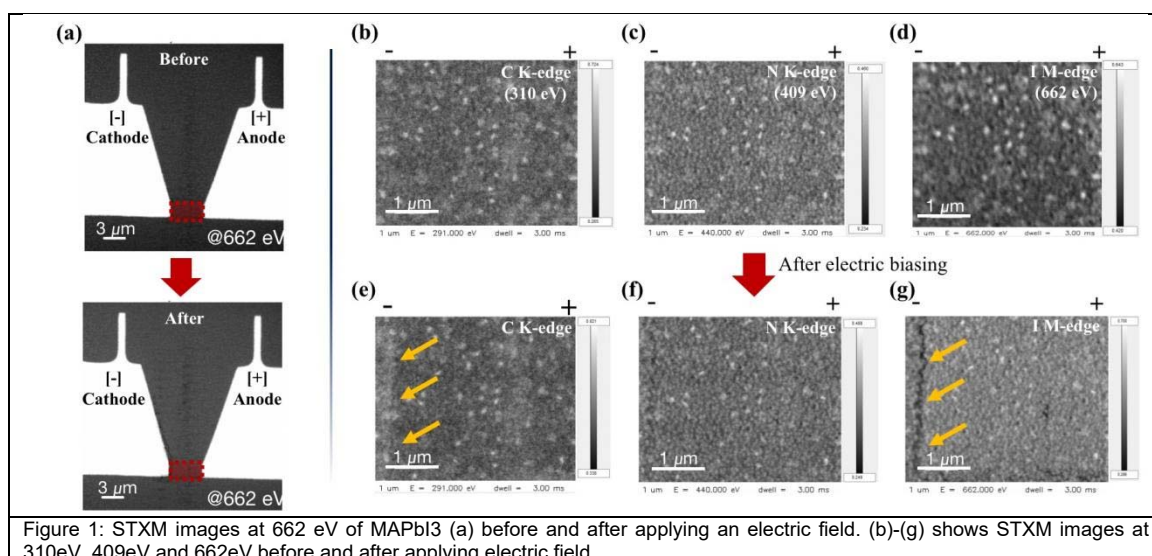
¹Synchrotron SOLEIL, L'Orme Des Merisiers Saint-Aubin, BP 48, 91192 Gif-sur-Yvette Cedex, France.

²CEA, CNRS, NIMBE, LICSEN, Université Paris-Saclay, 91191 Gif-sur-Yvette, France. ³LPICM, CNRS, Ecole Polytechnique, Institut Polytechnique de Paris, Route de Saclay, 91128 Palaiseau, France. ⁴CNRS, Institut Photovoltaïque d'Ile de France (IPVF), UMR 9006, 18, Boulevard Thomas Gobert, 91120 Palaiseau, France

ABSTRACT

Considering the relevance of alternative energy solutions in today's world, the research in the field of perovskite solar cells is highly significant. One of the factors that influence the stability and efficiency degradation of these solar cells is the electrical field in operation conditions. These effects need to be investigated at nano- and microscale such that the degradation mechanism can be understood and possibly mitigated. Scanning Transmission X-ray Microscopy (STXM) has been shown to be highly sensitive to various chemical components of these materials and provides spatially resolved spectra at the nanoscale¹⁻³.

In this study, we present the evidence of halide and organic ion migrations in $\text{CH}_3\text{NH}_3\text{PbI}_3$ (MAPbI₃) films caused by an applied electrical field (in-situ & ex-situ) using STXM. Change in optical density (figure 1) in STXM images as well changes in spectral features were observed after electrical biasing.



REFERENCES

1. Jun H. et al., Sci. Rep. 12, 4520 (2022).
2. Dindault C. et al. RSC Adv., vol. 12, pp. 25570-25577, Sep. 2022.
3. Jun H. Phd Ecole Polytechnique (2022) "Study of Degradation Mechanisms in Halide Perovskite Films and Perovskite Solar cells"

FT-VIS Emission Spectroscopy of the $A1\Pi, v=0,1,2$ Levels of AID: New Data for the ExoMol Line List

W. Szajna¹, R. Hakalla¹, I. Piotrowska¹, S. Ryzner¹, A. Stasik¹,
P. Kolek¹, A. Para¹, M.I. Malicka², R. Kępa¹,
S.N. Yurchenko³, J. Tennyson³

¹*Materials Spectroscopy Laboratory, Institute of Physics, University of Rzeszów,
Pigonia 1 Street, 35-310 Rzeszów, Poland*

²*The Faculty of Mathematics and Applied Physics, Rzeszow University of Technology,
Powstańców Warszawy 8 Street, 35-959 Rzeszów, Poland*

³*University College London, Department of Physics and Astronomy, London WC1E 6BT, UK*

ABSTRACT

High-resolution emission spectra of the AID, $A1\Pi-X1\Sigma^+$ system have been observed with a Fourier transform spectrometer. The $0-0, 1, 2, 1-0, 1, 2, 3, 4$ and $2-1, 2$ bands were recorded with an instrumental resolution of 0.03 cm^{-1} and the best signal-to-noise ratio ca. 4000:1 for the $0-0$ band. The $2-1$ and $2-2$ band were observed for the first time since 1934, when work of Holst and Hulthén was published [1]. The $A1\Pi, v=2$ vibronic level is a quasi-bound, predissociative state. Over, 400 ro-vibronic frequencies were measured with an absolute accuracy of about 0.0020 cm^{-1} . The present data were fitted using program PGOPHER [2] and molecular constants for the $X1\Sigma^+, v=0-4$ and $A1\Pi, v=0, 1, 2$ levels [3] was obtained. Furthermore, the values of the rotational term of the $A1\Pi, v=0, 1, 2$ levels were improved [4]. The current data were combined with the ground state results of White et al. [5] and the Dunham parameters Y_{kl} for the $A1\Pi$ state of AID were determined.

The new line positions of AID reported here were used to improve the WYLLoT ExoMol line list for AID [6]. The line list was computed using an empirical spectroscopic model based on literature data involving $v'=0$ and $v'=1$ ($A1\Pi$) only and did not predict any bound or even quasi-bound states for AID above $v'=1$. Very recently, WYLLoT for AIH, built using a similar model, was used to identify AIH in the spectra of cool star Proxima Centauri [7]. This study showed the limitations of WYLLoT at high rotational excitations and for the $A1\Pi, v=2$ state. We present an improved spectroscopic model for AID together with a new high-temperature line list for AID covering $A1\Pi, v=0, 1, 2$ computed using the Duo program suite [8].

This work illustrates the importance of experimental data for characterising complex potential energy curves, especially those with low dissociation limits or barriers, where extrapolations of the model can lead to inadequate or incorrect results.

Acknowledgments

Authors thank European Regional Development Fund and the Polish state budget within the framework of the Carpathian Regional Operational Programme (RPPK.01.03.00-18-001/10) through the funding of the Center for Innovation and Transfer of Natural Sciences and Engineering Knowledge of the University of Rzeszów.

REFERENCES

- [1] V.W. Holst, E. Hulthén, Z. Phys. **90**, 712, 1934.
- [2] C. Western, J. Quant. Spectrosc. Radiat Transfer. **186**, 221, 2017.
- [3] W. Szajna, K. Moore, J.C. Lane, J. Quant. Spectrosc. Radiat Transfer. **196**, 103, 2017.
- [4] W. Szajna, M. Zachwieja, R. Hakalla, J. Mol. Spectrosc. **318**, 78, 2015.
- [5] J.B. White, M. Dulick, P.F. Bernath, J. Chem. Phys. **99**, 8371, 1993.
- [6] S.N. Yurchenko, H. Williams, P.C. Leyland, L. Lodi, and J. Tennyson, Mon. Not. R. Astron. Soc. **479**, 1401, 2018.
- [7] Y. Pavlenko et al., Mon. Not. R. Astron. Soc. **516**, 5655, 2022.

FT-UV Emission Spectroscopy of the $B2\Sigma^+-X2\Sigma^+$ System of $^{12}C^{17}O^+$

W. Szajna¹, R. Hakallal¹, I. Piotrowska¹, S. Ryzner¹, A. Stasik¹,
P. Kolek¹, A. Para¹, M.I. Malicka², R. Kępa¹

¹*Materials Spectroscopy Laboratory, Institute of Physics, University of Rzeszów,
Pigonia 1 Street, 35-310 Rzeszów, Poland*

²*The Faculty of Mathematics and Applied Physics, Rzeszow University of Technology,
Powstańców Warszawy 8 Street, 35-959 Rzeszów, Poland*

ABSTRACT

The $B2\Sigma^+(v=0)$ level of $^{12}C^{17}O^+$ was investigated using the high-resolution, emission spectra obtained via Fourier transform spectroscopy of the (0-0), (0-1), (0-2) and (0-3) bands of the First Negative ($B2\Sigma^+-X2\Sigma^+$) system. The (0-0) band was recorded for the first time [1,2,3]. The bands were recorded with an instrumental resolution of 0.05 cm^{-1} and the best signal-to-noise ratio ca. 100:1 for the (0-1) band. For obtaining spectra of the $^{12}C^{17}O^+$ isotopologue an air-cooled hollow-cathode lamp was used. The cathode was equipped with a cylinder made of graphite. Isotopically enriched molecular oxygen $^{17}O_2$ (Sigma-Aldrich, 98.1% of ^{17}O) was admitted to the lamp at about 0.2 Torr. The present data were elaborated with the PGOPHER program [4] and wide set of molecular constants for the $X2\Sigma^+, v=0-3$ [5] and $B2\Sigma^+, v=0$ levels was obtained.

Acknowledgments

Authors thank European Regional Development Fund and the Polish state budget within the framework of the Carpathian Regional Operational Programme (RPPK.01.03.00-18-001/10) through the funding of the Center for Innovation and Transfer of Natural Sciences and Engineering Knowledge of the University of Rzeszów.

REFERENCES

- [1] W. Szajna, R. Kępa, *Spectrochim. Acta A*. **65**, 1014 (2006).
- [2] W. Szajna, R. Kępa, R. Hakalla, M. Zachwieja, *J. Mol. Spectrosc.* **240**, 75, 2006
- [3] W. Szajna, R. Kępa, R. Hakalla, M. Zachwieja, *Spectrosc. Lett.* **40**, 667, 2007
- [4] C. Western, *J. Quant. Spectrosc. Radiat Transfer.* **186**, 221, 2017
- [5] I. Piotrowska, R. Hakalla, W. Szajna, R. Kępa, *J. Quant. Spectrosc. Radiat Transfer.* **289**, 108268, 2022

The Training Portal for Photon and Neutron Data Services

O. Knodel^a, A. Padovani^b, M. Gutierrez^c, C. Albert^b, G. LaRocca^c,
A. Valcarcel Orti^b and U. Konrad^a and the PaNOSC project partners^d

- a. *Helmholtz-Zentrum Dresden-Rossendorf, 01328 Dresden, Germany. ExPaNDS partner*
- b. *Synchrotron SOLEIL, 91190 Saint-Aubin, France. ExPaNDS partner*
- c. *EGI Foundation, 1098 XG Amsterdam, the Netherlands. ExPaNDS partner*
- d. *The PaNOSC partners ESRF, ESS, ELI, CERIC and ILL*

ABSTRACT

Education is becoming an increasingly important topic to help scientists work on Photon and Neutron (PaN) sources. The pan-training.eu¹ portal is a result of the two H2020 projects ExPaNDS² and PaNOSC³.

From a technical perspective, the pan-training.eu portal consists of:

- A catalogue for the registration of third-party training materials such as tutorials, videos, or repositories
- A calendar of events related to the PaN community (listing training and community events) entered into the catalogue by users from our PaN community and beyond, as well as automatically compiled from various sources
- A tightly coupled e-learning system with PaN-specific blended learning courses with Jupyter notebook support

With the catalogue, ExPaNDS is strengthening the role of EOSC services for the PaN scientific field, with a focus on providing a sustainable training, learning and documentation platform for the PaN community as a whole including also initiatives such as LEAPS⁴, LENS⁵ and Laserlab Europe⁶. The catalogue is based on an established solution developed by the ELIXIR community⁷.

REFERENCES

1. [HTTPS://PAN-TRAINING.EU/](https://pan-training.eu/)
2. [HTTPS://EXPANDS.EU/](https://expands.eu/)
3. [HTTPS://WWW.PANOSC.EU/](https://www.panosoc.eu/)
4. [HTTPS://LEAPS-INITIATIVE.EU/](https://leaps-initiative.eu/)
5. [HTTPS://LENS-INITIATIVE.ORG/](https://lens-initiative.org/)
6. [HTTPS://WWW.LASERLAB-EUROPE.EU/](https://www.laserlab-europe.eu/)
7. [HTTPS://ELIXIR-EUROPE.ORG/COMMUNITIES](https://elixir-europe.org/communities)

Studying Catalytic Reactions using Ambient Pressure X-ray Photoelectron Spectroscopy

T. Wätjen¹, P. Amann^{1,2}, H. Karakachian², S. Eriksson¹

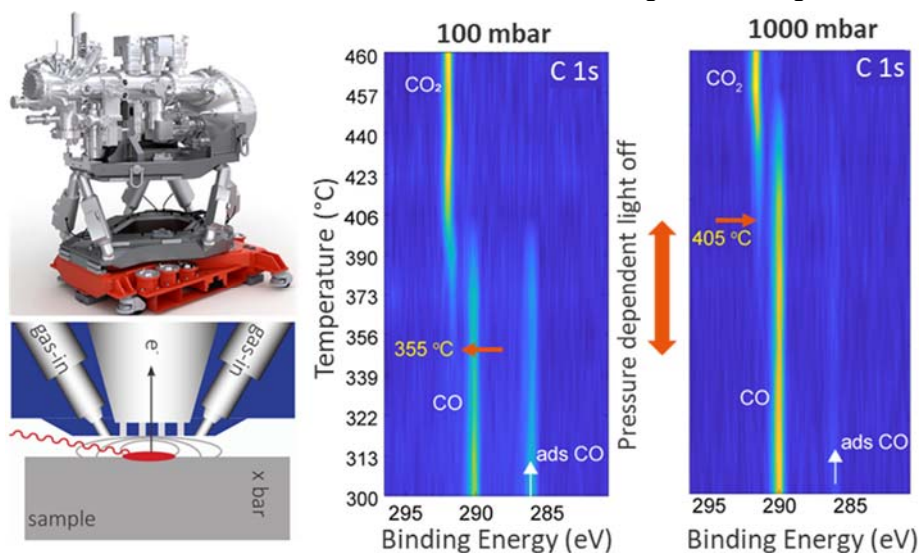
¹ Scienta Omicron AB, Danmarksgratan 22, 75323 Uppsala, Sweden

² Scienta Omicron GmbH, Limburger Strasse 75, 65232 Taunusstein, Germany

ABSTRACT

Investigating reaction intermediates, oxidation states, solid-liquid interfaces and buried interfaces under near ambient pressure conditions is highly desired in materials science applications. This is mainly driven by a need to understand how molecular bonds are broken and formed during a chemical reaction. In the last years a substantial effort in instrument development has taken place, mostly with the idea of studying the surface chemical reactions under well-controlled UHV or mbar environments. In typical industrial reactors, however, related processes take place at pressures of several bar and temperatures exceeding 100 °C, which makes it difficult to examine the involved reactions from a mechanistic point of view.

We report on a state of the art ambient-pressure x-ray photoelectron spectroscopy setup capable of investigating catalytic reactions under relevant conditions and exemplify this by CO oxidation on a Pd(100) surface [2]. At 100 mbar oxidation starts to occur from 355 °C. At a pressure of 1 bar, the surface remains CO poisoned. Only by increasing the temperature further to 405 °C, the CO starts to react and the light-off for the oxidation is reached. Bridging this pressure gap is critical for some reactions and only possible with a specially designed front cone with integrated gas supply. By decreasing the working distance to 30 µm a local sample pressure of 1 bar is reached. With a small volume, sub second gas exchange is achieved.



REFERENCES

- 1 Amann et al., Review of Scientific Instruments, 90 103102, (2019)
- 2 Blomberg et al., ACS Catalysis, 11 (15), 9128-9135, (2021)

TUTORIALS

TUTORIALS

Wednesday, January 18th

TU-01

SOLEIL Auditorium - Main Building

14:00 - 17:00

Use of the FASTOSH software for the XAS data treatment—Part. I

Gautier Landrot

Friday, January 20th

TU-01

SOLEIL Auditorium - Main Building

14:00 - 17:00

Use of the FASTOSH software for the XAS data treatment—Part. II

Gautier Landrot

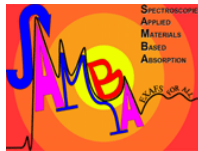
TU-02

Libra & Phenix Rooms –SOLEIL Main Building

14:00 - 17:00

PROXIMA 2A Training Tutorial: Using μ -Focused X-rays for Cryo-Crystallography and Plate Screening

William Shepard



TUTORIAL

Use of the Fastosh software for the XAS data treatment



Fastosh is a free standalone program that provides unique functionalities to process X-ray Absorption Fine Structure (XAFS) spectroscopy data. This program was created for Users of SAMBA beamline, SOLEIL Synchrotron, but can be employed to process data generated at any XAFS beamline since it can open data files in ASCII format. The program indeed allows users to easily and rapidly perform a number of operations such as chunking and averaging a large number of scans, auto-deglitching, 2D filtering, 3D plotting, data processing using chemometric methods, and assessing the progress in data acquisition using a fully automatic data viewer tool. Additionally, functions specifically compatible with SAMBA data notably allow to average HDF files and extract new fluorescence spectra from MCA patterns processed to minimize acquisitions artefacts, such as diffraction peaks.

Location : SOLEIL

Organizers : Gautier LANDROT (SAMBA), Amélie BORDAGE (ORGUES)

Number of participants : No limit

Part I : January 18th 14:00 – 17:00

The fundamentals of XAS data treatment will be presented: calibration & alignment, merging, normalization, background subtraction, Fourier Transform & Reverse Fourier Transform. Basic functionalities will be covered in this session, with an emphasis on those that are unique to the program, such as 3D data visualization, merging by sub-groups, 2D filtering, & auto deglitching.

All the users who want to discover XAS data treatment and / or the software developed by the SAMBA beamline can attend this part.

Part II : January 20th 14:00-17:00

The chemometric functionalities of the software will be presented: PCA, Target Transformation (TT), & Multivariate Curve Resolution Alternating Least Squares (MCR-ALS) method. The first part of this session will be dedicated to review the Singular Value Decomposition step of the PCA analysis, including the effects of data centering and scaling, which may subsequently affect the results obtained by TT and MCR-ALS methods that are employed after PCA. The basic functionalities of the Jaumot et al.'s MCR-ALS toolbox included in Fastosh will be covered during a step-by-step tutorial. By the end of this session, any attendee should be able to apply the TT or MCA-ALS procedure using personal computer and XAFS datasets generated at SAMBA or elsewhere.

All users (beginners as well as confirmed) can attend this session. For the beginners who want to attend this part, it is highly recommended to attend also the first part on Wednesday.

Requirement : It is mandatory to download the software prior to the tutorial, and check if it is starting properly on your laptop : <https://www.synchrotron-soleil.fr/fr/lignes-de-lumiere/samba>
The software can be installed on Linux, Mac and Windows machines.



PROXIMA 2A Training Tutorial: Using μ -Focused X-rays for Cryo-Crystallography and Plate Screening

Where: SOLEIL & Video Conference

When: Friday 14h – 17h, 20th January 2023

Number of Participants: No Limit

Requirements: None

Target Audience: Beginners to Experts

Format: Interactive Seminar

Organisers: Serena SIRIGU, Martin SAVKO, Damien JEANGERARD & William (Bill) SHEPARD

Quizzes & Prizes: Chocolate fish from Aotearoa

The PROXIMA 2A team proposes a training tutorial to illustrate tips, tricks and the best practices to use when collecting diffraction data with intense micro-focused X-rays in crystallographic experiments. We will present the beamline along with a variety of case studies and demonstrate many practical aspects on how to design your experiments specifically for your crystals. We will also explain how to circumvent common issues such as icing on crystals, the centering of micro-crystals, handling robot collisions and limiting radiation damage. Many functionalities have been implemented on the beamline to help users obtain the best diffraction from their crystals.

This tutorial is particularly aimed at novice structural biologists and chemists who intend to collect data on PROXIMA 2A as well as those who are more experienced and even experts. As such the tutorial will be very “interactive” and will allow the audience to not only ask questions, but also to test themselves with quizzes and even win prizes. For those who have specific questions, we have set up an [on-line survey to submit your burning questions](#) (see the link below). Participants may also practice on the beamline in sessions without X-rays.

The case studies available for discussion will include:

- Methods of centering crystals
- Data Collection methods and selecting parameters
- Radiation damage
- Finding sweet spots
- Helical scans
- Ultra-high resolution data collection
- Multiple-sweep data collection
- Using the kappa goniometer
- Anomalous phasing experiments (ANODE, SAD & MAD)
- Small molecule crystallography
- Any other topics from the survey

We will also present our in-house plate screener named the CRIBLEUR. This optional setup is available every 2-3 weeks during beamtime runs and can adapt to virtually any crystallisation format. It allows users to test crystals in-situ in their native crystallization drops and circumvents the need for manipulation and cryo-cooling of the sample that could potentially result in the loss of diffraction power. The CRIBLEUR is particularly valuable for very delicate, small or thin crystals such as amyloid-like peptides or *in-meso* grown membrane protein crystals that don't react well to the standard handling required for classical cryo-crystallography. The user can efficiently discriminate between protein and salt crystals as well as collecting merged X-ray data sets from multiple crystals for structure determination. During the tutorial we will present the main functionalities of the CRIBLEUR along with various study cases of crystallographic structures determined from data collected in-situ.

Link to the Burning Questions Survey, <https://forms.gle/H Cp8RU ndfPFU1D3m9>.

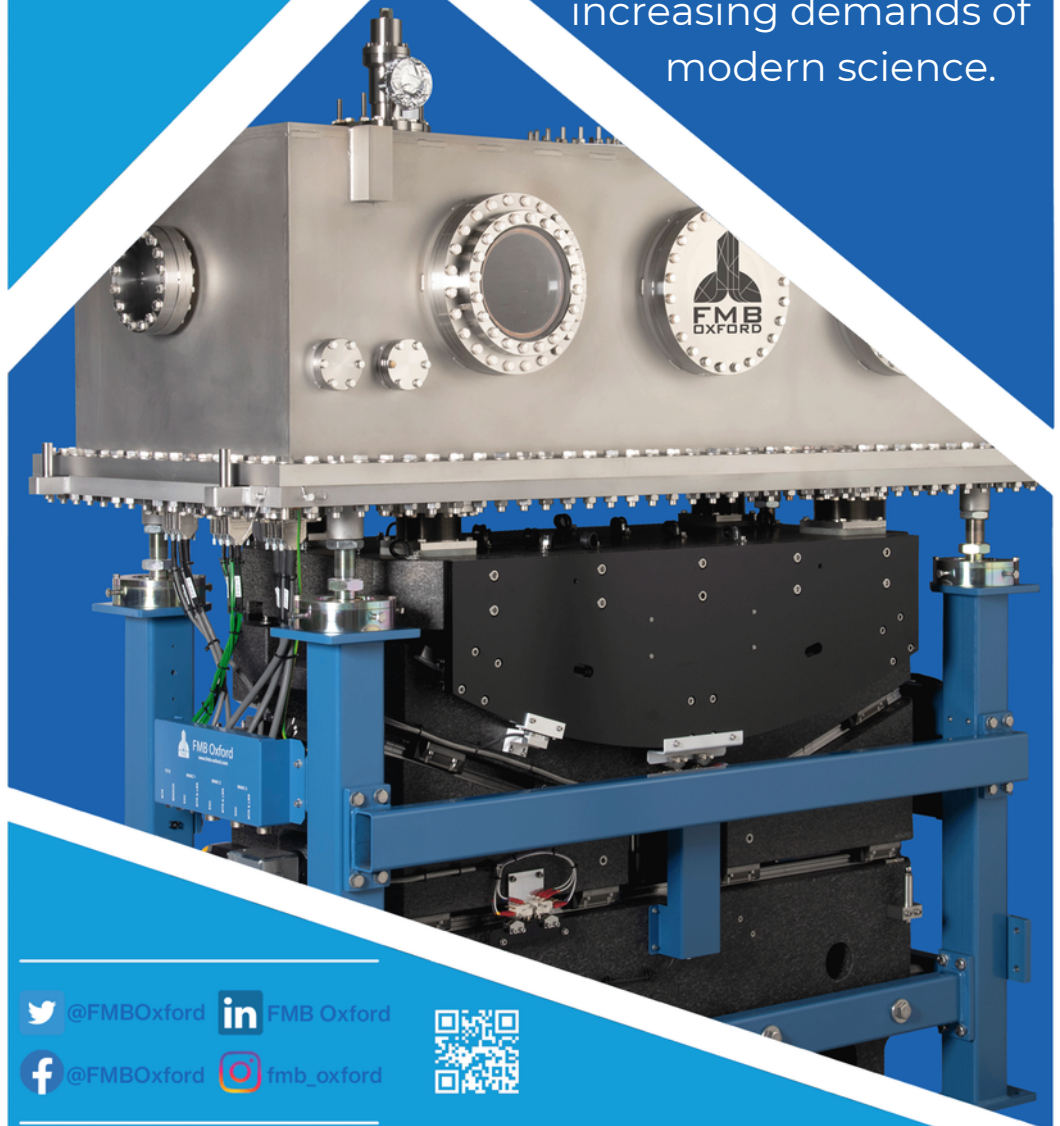
COMPANIES ADVERTISEMENTS



ENGINEERING SCIENCE FOR A BRIGHTER TOMORROW

FMB Oxford is a recognised and established leader in the supply of Beamlines and Beamline Components to the scientific community. Specialising in the design, assembly, testing, installation and commissioning of the high value systems.

With over 25 years' experience in the global synchrotron industry, FMB Oxford has built an extensive product range and continues to work with its customers and other experts in the community to expand and develop this range to provide new solutions capable of supporting the increasing demands of modern science.



 @FMBOxford  FMB Oxford
 @FMBOxford  fmb_oxford

